THE ELECTRO-OPTIC EFFECT IN SOLUTIONS OF RIGID MACROMOLECULES

By

DAVID IVAN BOWLING

Bachelor of Arts
University of California, Los Angeles
Los Angeles, California
1962

Master of Science
San Diego State College
San Diego, California
1964

Submitted to the Faculty of the Graduate College
of the Oklahoma State University
in partial fulfillment of the requirements
for the Degree of
DOCTOR OF PHILOSOPHY
July, 1968

THE ELECTRO-OPTIC EFFECT IN SOLUTIONS OF

RIGID MACROMOLECULES

Thesis Approved:

G B Thurston

Thesis Adviser

Franklin R. Leach

D D Dunham

Dean of the Graduate College

ACKNOWLEDGEMENTS

The author would like to express his appreciation to those who have assisted him during the course of this investigation; to Dr. G. B. Thurston for his helpful suggestions and guidance; to his wife, Janice, for her encouragement and assistance with the manuscript; to Mr. and Mrs. John Wyhof for their assistance in preparation of the manuscript; to Dr. Elton Kohnke and Dr. F. R. Leach for their critical reading of the manuscript; to the U.S. Army Research Office, Durham, for grants awarded to Dr. G. B. Thurston for the financial support of this work; and to the Physics Shop personnel for their expert construction of the apparatus.

TABLE OF CONTENTS

Chapter Page

LIST OF TABLES

LIST OF FIGURES

Figure Page

CHAPTER I

INTRODUCTION

A number of materials exhibit birefringence, the property whereby the index of refraction depends upon the directions of propagation and polarization of light transversing the material. This property is attributed to an assymetry in matter of the distribution of charge and mobility of that charge in the basic unit of the material. The structure of crystals in their normal state provides the assymetry. In amorphous solids this assymetry can be induced by stresses or may be present due to natural internal stresses in the material. In pure liquids, magnetic fields, electric fields or sustained shearing stress can produce an ordering of the molecules of the liquid to produce the assymetry. In the liquid crystals such ordering may occur spontaneously. Even gases may be ordered by electric or magnetic fields to produce birefringence. Finally, in the specific case to be considered here, a rigid particle suspended in a liquid may be electrically oriented to produce birefringence, even if the liquid itself is not birefringent.

Electrically induced birefringence is called the Kerr effect after its discoverer. Kerr first observed the effect in 1875 in glass, rosin, carbon bisulfide, benzol, parafin oil, kerosine, turpentine, olive oil and castor oil (32,33). Recently the effect has been more often called the electro-optic effect, even though there are other electro-optic effects. Since 1875 others have measured such effects in solids,

liquids and gases. Most recently Le Fevre (38) has used the electro-optic effect extensively to measure physical constants of pure liquids. This work has extended over two decades until the present time, and has been used in a very sophisticated manner.

In the specific application of the electro-optic effect to macromolecules one may conveniently break down the more significant work into that which is theoretical and the more recent experimental work. The work from which we draw for theory of electrical orientation birefringence is mainly by Peterlin and Stuart (57,58,59). Work done on flow orientation birefringence is useful because a great deal of the theory is independent of the mechanism of orientation. Thus, the reviews of flow birefringence by Cerf and Scheraga (11) and Jerrard (31) have provided a great deal of useful information in the interpretation of results.

The experimental work done to verify and make use of the theory developed has been restricted to relatively few workers. Benoit and his co-workers (4,6) have used the effect to measure the length and other physical constants of both tobacco mosaic virus (TMV) and Poly-γ-benzyl-L-glutamate (PBLG). Although Benoit presents the results of the theory for a rectangular pulse and for alternating fields, the measurements he presents are for an alternating field applied to the material. Benoit and his co-workers have also done work on light scattering in PBLG under electrical orientation (88,89,90).

The rectangular pulse method of measuring the E-O effect has been favored by some workers because it allows the measurement of conductive materials while avoiding the heating problem encountered when the field is applied for longer periods of time. Shaw and some of his co-workers

(66,67,68,69) have used this method in measuring Bentonite, a clay which will form stable suspensions in water.

O'Konski and his co-workers (44,45,46,51) have used the pulse method to measure deoxyribonucleic acid (DNA) and TMV. One of his students, Pytkowicz, (61) did a doctoral dissertation in which he measured TMV of various strains, Helix Pomatia Hemocyanin, Gum Arabic, PBLG and RNA using a pulse technique. O'Konski did some work using alternating fields and reported a fall off in birefringence in TMV far above the expected frequency for dispersion due to physical relaxation of the particle. Tsvetkov (85,87) has used the alternating field method to measure some of the physical properties of PBLG.

Some workers have used the electro-optic effect to observe some other processes. For example Ingram and Jerrard (27) have used the pulse method to measure the kinetics of enzymes acting on DNA. Tinoco (80) also has used the pulse method to observe the conversion of fibrinogen to fibrin.

The theory for the electro-optic effect in solutions of macromolecules is basically an orientation theory; that is, the birefringence is related directly to the orientation of the macromolecules by the electric field. Electrical orientation of macromolecules is also of primary importance in the treatment of effects such as light scattering, optical activity, dielectric response and dichroism. Thus the orientation theory as developed should apply to these other effects and likewise theoretical work on these other effects might be applicable to the electro-optic effect. Specifically, a number of polarization mechanisms have been suggested to explain certain results of dielectric measurements which bear directly on the measurements which are made here.

These mechanisms are best summarized and generalized in a paper by O'Konski (44) and are made use of in the development of the theory of the electro-optic effect.

In addition, the work of Schwan (64,65) and Takashima (76) provides information about the problems of electrode polarization. Although the problem is not as grave in electro-optic measurements as it is in dielectric measurements, it must be dealt with to make accurate measurements at the lowest frequencies.

This thesis covers the following material. A theory of the electro-optic effect for rigid particles is developed. The results of measurements are presented for four materials to test the adequacy of the theory. The materials are tobacco mosaic virus (TMV), Avicel, bentonite and Baymal. The test of theoretical adequacy is based on showing that the response of the four materials generally fits the character of response expected on the basis of the theory, on illustrating in one case possible ways in which the fit between theory and results might be made more exact, and in all cases examining the high frequency response for clues as to the manner in which the theory could explain the response in that region. In all cases measured values of physical constants of the materials are tabulated.

In previous work (4,47) the extent of verification of the theory has been limited to the matching of the general character of experiment with theory, noting that it is possible for polydispersity of the sample to explain the greater dispersion with respect to frequency of the results actually obtained. In this work, a general method for determining the polydispersity of a sample is presented and the method applied to one of the more difficult cases encountered. In addition,

the possibility of concurrent variations of some of the constants of the theory with molecular size is considered, although a formal procedure for determining such variation is not presented.

In previous work (4,6,47,66,etc.) on the electro-optic effect no mechanism or formalism was introduced to explain the induced moment contribution to the response. It was merely assumed that there was a fixed polarizability associated with the particle and the matter was not pursued. In this work, consideration is given to work which has been done to explain dielectric response of macromolecules and a mathematical method of introducing frequency dependency of the induced moment into the equations for the electro-optic response is developed. The formulation used is more general than is required for the theories which are applied to it, but it would allow the use of more complete and detailed theories should they ever be developed.

The findings presented in this thesis may be summarized as follows. (1) The orientation theory as presented along with considerations of polydispersity and the variation of the ratio of the induced to permanent moment with polydispersity adequately describes the low frequency electro-optic effect. (2) Theories developed to date (44) to account for the high frequency dispersion of the steady component of the electro-optic effect do not adequately describe the effect. (3) An adequate theory for the polarization of large molecules is needed. (4) Measurements of the electro-optic effect in conjunction with dielectric and flow birefringence measurements could provide a means of calculating physical constants of macromolecules that could not be calculated from any single type of measurement.

The measurements made were used to obtain some of the physical

constants of the materials measured and these values are tabulated. These determinations are, however, subordinate in importance to the demonstration that alternating field electro-optic measurements can be made in materials previously considered too conductive for such measurements and that the theory as developed is adequate to describe the results. At high frequencies the important finding is that existing theory does not adequately describe that which is observed.

CHAPTER II

THEORY

The theory of orientation of rigid particles in an electric field and the manifestation of the orientation in the optical properties of the solution of rigid particles will be developed in this chapter. First the theory of orientation is developed, then the results of the theory are used to determine the response in terms of the optical properties of the material. Finally some other theories will be added to these results which might better describe some of the experimental observations.

Rotary Diffusion Equation

The general rotary diffusion equation is developed here in a manner similar to that in which it was presented in seminar (78). Consider the area on the surface of a unit sphere and assume there are a large number of points moving about the surface of the sphere. The motion of these points at any small area on the sphere may be represented by a current vector $\vec{J}$. If the area is made vanishingly small, the vector becomes a vector function of the location on the sphere and the equation

$$\nabla \cdot \vec{J} = \frac{\partial \rho}{\partial t} \qquad \text{(II-1)}$$

known as the continuity equation is applicable. ρ is the density function of the points.

If the points on the sphere represent the projection onto the sphere of some axis attached to a molecule in solution, then the current due to Brownian motion is given by Einstein (15) to be

$$\vec{J}_B = -D\nabla\rho \quad , \tag{II-2}$$

where D is the rotary diffusion constant. If in addition all the molecules oriented in a certain direction are acted upon by a torque $\vec{M}$, then assuming that inertial effects are negligible, the particles will respond by turning with an angular velocity which may be represented by a velocity vector

$$\vec{\omega} = \frac{\vec{M}}{\mathcal{L}} \times \hat{r} \quad , \tag{II-3}$$

where $\mathcal{L}$ is a frictional factor and $\hat{r}$ is the unit vector perpendicular to the surface of the sphere. Also at that point the current will be given by the density times the velocity or

$$\vec{J}_m = \rho\vec{\omega} \quad . \tag{II-4}$$

The total current is therefore given by

$$\vec{J} = \vec{J}_B + \vec{J}_m = -D\nabla\rho + \rho\vec{\omega} \quad . \tag{II-5}$$

When this is placed in equation (II-1), one obtains

$$D\nabla^2\rho - \nabla\cdot(\rho\vec{\omega}) = \frac{\partial\rho}{\partial t} \quad . \tag{II-6}$$

According to Rozart (62) the frictional factor is given by

$$\mathcal{L} = \frac{kT}{D} \quad , \tag{II-7}$$

where k is Boltzmann's constant and T is the absolute temperature.

Electrical Orientation Theory

The case of electrically induced orientation is obtained when $\vec{M}$ is due to an electric field acting upon an electric dipole on the particle. The axis described in the definition of ρ may be conveniently assigned at this point to the direction of the electric dipole, and thus the torque is

$$\vec{M} = \vec{\mu} \times \vec{E} \quad , \tag{II-8}$$

where $\vec{\mu}$ is the moment and $\vec{E}$ the electric field. The moment can be broken into a permanent and induced moment

$$\vec{\mu} = \vec{\mu}^* + \vec{\mu}' \quad , \tag{II-9}$$

where $\vec{\mu}^*$ is a permanent dipole moment and $\vec{\mu}'$ is the induced dipole moment. For convenience in the solution of this problem it is further assumed that the $\vec{\mu}^*$ and $\vec{\mu}'$ are in the same direction and thus equation (II-9) reduces to

$$\mu = \mu^* + \mu' \quad . \tag{II-10}$$

In some cases the μ^* and μ' may not be in the same direction but the resulting torque may be the same as if there were a μ^* and an equivalent μ' in the same direction.

For example, Stratton (72) treats the case of a dielectric ellipsoid of revolution in an electric field and obtains an expression for a torque about an axis perpendicular to both the field direction and the major axis of the ellipsoid. The form of this result is

$$\vec{M} = f E_0^2 \cos\sigma \sin\sigma \hat{m}_1 \quad , \tag{II-11}$$

where $\hat{m}_1$ is a unit vector along the axis described above. σ is the angle between the electric field direction (the field strength is given by E_0) and the major axis of the ellipsoid. f is some function of the shape of the particle and the dielectric constants of the ellipsoid and the surrounding medium. This same moment could be obtained by having a μ directed along the major axis of the ellipsoid having a value

$$\mu = f E_0 \cos\sigma \quad . \tag{II-12}$$

It can be further shown that

$$f = g_{1e} - g_{2e} \quad , \tag{II-13}$$

where g_{1e} is the electrical polarizability of the ellipsoid in the direction of the major axis and g_{2e} is the electrical polarizability of the particle in the transverse direction. In the case of a dielectric particle in a dielectric solvent this torque may be due to the Maxwell-Wagner effect (21). However this result can be generalized to any polarization mechanism with major axes in the same direction.

The expression used in the rest of this derivation is

$$\mu = \mu^* + E(g_{1e} - g_{2e})\cos\sigma \quad . \tag{II-14}$$

This assumes that the μ^* axis is the one which has the polarizability g_{1e}.

The angle σ has been introduced but a complete coordinate system needs to be defined to solve the equation (II-6). The polar and Cartesian coordinate systems to be used are illustrated in Figure 1. The rectangular coordinate system will be used to determine vector products. In this coordinate system

$$\vec{M} = \vec{\mu} \times \vec{E} = \begin{vmatrix} \hat{i} & \hat{j} & \hat{k} \\ \mu_x & \mu_y & \mu_z \\ E & 0 & 0 \end{vmatrix} = \hat{j}\mu_z E + \hat{k}(-\mu_y)E \tag{II-15}$$

and

Figure 1: Cartesian and Polar Coordinate Systems as Used In The Theory of the Electro-Optic Effect.

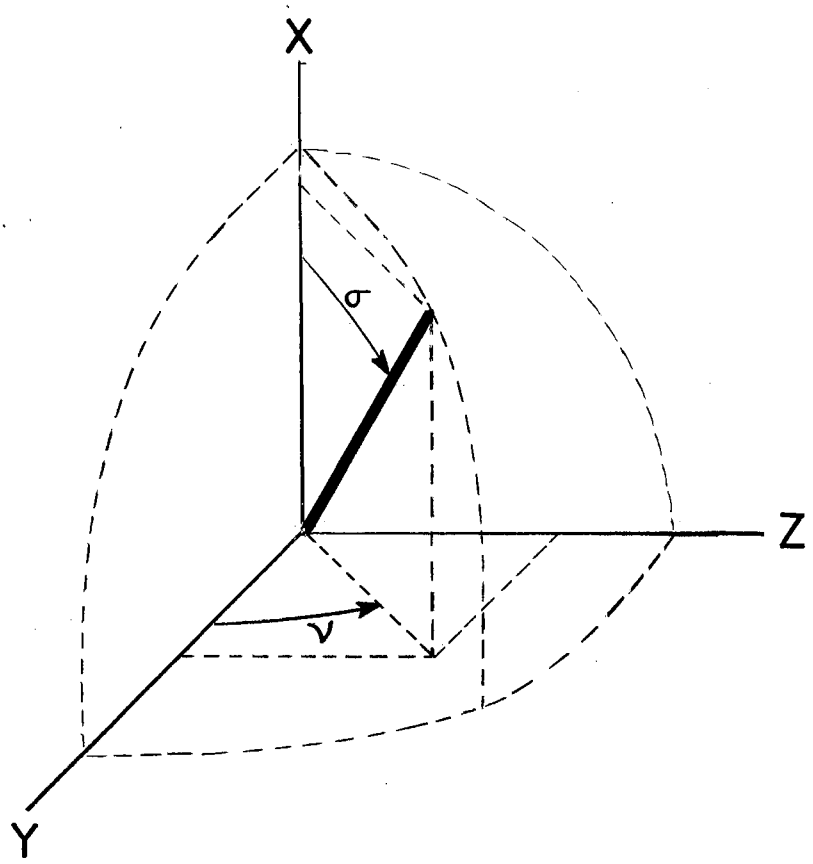
X
σ
Z
ν
Y

$$\vec{\omega} = \frac{D}{kT}\vec{M}\times\vec{r} = \begin{vmatrix} \hat{i} & \hat{j} & \hat{k} \\ 0 & \mu_z & -\mu_y \\ r_x & r_y & r_z \end{vmatrix} E$$

$$= \frac{DE}{kT}\left[\hat{i}(\mu_z r_z + \mu_y r_y) + \hat{j}(-\mu_y r_x) + \hat{k}(-\mu_z r_x)\right] , \quad \text{(II-16)}$$

where

$$\mu_x = \mu \cos\sigma ,$$

$$\mu_y = \mu \sin\sigma \cos\nu ,$$

$$\mu_z = \mu \sin\sigma \sin\nu , \quad \text{(II-17)}$$

and

$$r_x = \cos\sigma ,$$

$$r_y = \sin\sigma \cos\nu ,$$

$$r_z = \sin\sigma \sin\nu . \quad \text{(II-18)}$$

Thus

$$\vec{\omega} = \frac{DE}{kT}\,\mu\left[\hat{\imath}\,\sin^2\sigma + \hat{\jmath}\,(-\sin\sigma\cos\sigma\cos\nu) + \hat{k}\,(-\sin\sigma\cos\sigma\sin\nu)\right] . \qquad \text{(II-19)}$$

The following operator is used to transform a vector in the Cartesian system to the coordinate system used here.

$$\begin{vmatrix} -\sin\sigma & \cos\sigma\cos\nu & \cos\sigma\sin\nu \\ 0 & -\sin\nu & \cos\nu \\ \cos\sigma & \sin\sigma\cos\nu & \sin\sigma\sin\nu \end{vmatrix} . \qquad \text{(II-20)}$$

This operator produces a vector of the form

$$\begin{vmatrix} \sigma \\ r \\ \nu \end{vmatrix} , \qquad \text{(II-21)}$$

where σ, r and ν are the $\hat{\sigma}$, $\hat{r}$ and $\hat{\nu}$ components of a vector in the spherical coordinate system when it operates on the column vector

$$\begin{vmatrix} x \\ y \\ z \end{vmatrix} , \qquad \text{(II-22)}$$

where X, Y and Z are the $\hat{i}$, $\hat{j}$ and $\hat{k}$ components of the vector in question. Thus

$$\vec{\omega} = \frac{DE}{kT}\mu(-\sin\sigma)\hat{\sigma_1} \quad . \tag{II-23}$$

If equation (II-23) is substituted into equation (II-19) one obtains

$$\vec{\omega} = D\left[\beta(-\sin\sigma) + \gamma^2(-\sin\sigma\cos\sigma)\right]\hat{\sigma_1}, \tag{II-24}$$

where

$$\beta = \frac{\mu^* E}{kT} \quad , \tag{II-25}$$

and

$$\gamma^2 = \frac{(g_{1e} - g_{2e})}{kT} E^2 \quad . \tag{II-26}$$

In the polar coordinate system used

$$\nabla \cdot \vec{F} = \frac{1}{\sin\sigma}\frac{\partial}{\partial\sigma}(\sin F_\sigma) + \frac{1}{\sin\sigma}\frac{\partial F_v}{\partial v} \quad . \tag{II-27}$$

Thus

$$\nabla\cdot(\rho\vec{\omega}) = D\left[\beta\frac{1}{\sin\sigma}\frac{\partial}{\partial\sigma}(-\sin^2\sigma\rho)\right.$$

$$\left.+\gamma^2\frac{1}{\sin\sigma}\frac{\partial}{\partial\sigma}(-\sin^2\sigma\cos\sigma\rho)\right] = D\left[\beta\left(-\sin\sigma\frac{\partial\rho}{\partial\sigma}\right.\right.$$

$$\left.-2\rho\cos\sigma\right)+\gamma^2\left(-\sin\sigma\cos\sigma\frac{\partial\rho}{\partial\sigma}\right.$$

$$\left.\left.+\rho(-2\cos^2\sigma+\sin^2\sigma)\right)\right]. \qquad \text{(II-28)}$$

Equation (II-5) becomes

$$\frac{1}{\sin\sigma}\frac{\partial}{\partial\sigma}\left(\sin\sigma\frac{\partial\rho}{\partial\sigma}\right)+\frac{1}{\sin^2\sigma}\frac{\partial^2\rho}{\partial V^2}+\beta\left[-\sin\sigma\frac{\partial\rho}{\partial\sigma}\right.$$

$$\left.-2\rho\cos\sigma\right]+\gamma^2\left[\sin\sigma\cos\sigma\frac{\partial\rho}{\partial\sigma}+\rho(-2\cos^2\sigma\right.$$

$$\left.+\sin^2\sigma)\right] = \frac{1}{D}\frac{\partial\rho}{\partial t}. \qquad \text{(II-29)}$$

Equation (II-29) is separable. If the solution

$$\rho = \bar{\rho}(\sigma,t)V(V) \qquad \text{(II-30)}$$

is tried in equation (II-29) and the variables are separated one obtains

$$\left\{ \frac{1}{\bar{\rho}} \frac{1}{\sin\sigma} \frac{\partial}{\partial\sigma} \left(\sin \frac{\partial \bar{\rho}}{\partial \sigma} \right) + \frac{1}{\bar{\rho}} \beta \left[-\sin\sigma \frac{\partial \bar{\rho}}{\partial \sigma} - 2\bar{\rho}\cos\sigma \right] + \frac{1}{\bar{\rho}} \gamma^2 \left[\sin\sigma\cos\sigma \frac{\partial \bar{\rho}}{\partial \sigma} + \bar{\rho}\left(-2\cos^2\sigma + \sin^2\sigma \right) \right] - \frac{1}{D} \frac{\partial \bar{\rho}}{\partial t} \frac{1}{\bar{\rho}} \right\} \sin^2\sigma = \frac{1}{V} \frac{\partial^2 V}{\partial \nu^2} = k^2 , \tag{II-31}$$

where k^2 is the separation constant.

The equation in the variable ν is

$$V = C_k e^{k\nu} . \tag{II-32}$$

This equation has the solution

$$V = \text{Constant} . \tag{II-33}$$

Since V is not dependent upon time, if a boundary condition exists such that $\rho = \bar{\rho} V$ is independent of ν at any time, then V is independent of ν. Thus k is restricted to the value $k = 0$ and

$$\rho = \bar{\rho}(\sigma, t) . \tag{II-34}$$

Thus a solution to the original equation is

$$\rho = \rho(\sigma, t) . \tag{II-35}$$

That is, the solution is independent of the variable ν. Therefore

the only equation that needs to be solved is

$$\frac{1}{\sin\sigma}\frac{\partial}{\partial\sigma}\left(\sin\sigma\frac{\partial\rho}{\partial\sigma}\right)+\beta\left[-\sin\sigma\frac{\partial\rho}{\partial\sigma}-2\rho\cos\sigma\right]$$

$$+\gamma^2\left[\sin\sigma\cos\sigma\frac{\partial\rho}{\partial\sigma}+\rho\left(-2\cos^2\sigma+\sin^2\sigma\right)\right]=\frac{1}{D}\frac{\partial\rho}{\partial t}\,. \qquad \text{(II-36)}$$

This equation is solved in detail in Appendix A, where the solution is found to be

$$\rho=\frac{1}{4\pi}\left\{1+\beta u\frac{\cos(\omega t-\delta_1)}{1+(\omega/2D)^2}+\beta^2(3u^2-1)\frac{1}{12}\right.$$

$$\cdot\left[\frac{1}{1+(\omega/2D)^2}+\frac{\cos(2\omega t-\delta_1-\delta_2)}{\left[(1+(\omega/2D)^2)(1+(\omega/3D)^2)\right]^{1/2}}\right]$$

$$\left.+\gamma^2(3u^2-1)\frac{1}{12}\left[1+\frac{\cos(2\omega t-\delta_2)}{\left[1+(\omega/2D)^2\right]^{1/2}}\right]+\ldots\right\}\,. \qquad \text{(II-37)}$$

In terms of Legendre polynomials this is

$$\rho=\frac{1}{4\pi}\left\{P_0+P_1\beta\frac{\cos(\omega t-\delta_1)}{1+(\omega/2D)^2}+P_2\beta^2\frac{1}{6}\right.$$

$$\cdot\left[\frac{1}{1+(\omega/2D)^2}+\frac{\cos(2\omega t-\delta_1-\delta_2)}{\left[(1+(\omega/2D)^2)(1+(\omega/3D)^2)\right]^{1/2}}\right]$$

$$\left.+P_2\gamma^2\frac{1}{6}\left[1+\frac{\cos(2\omega t-\delta_2)}{\left[1+(\omega/3D)^2\right]^{1/2}}\right]+\ldots\right\}\,. \qquad \text{(II-38)}$$

Electro-Optic Effect

In dilute solutions it may be assumed that the physical characteristics of the solvent are unchanged by the presence of the large particles. Specifically, the polarization of the solvent in an electric field is unchanged by the presence of the solute particles, if there are relatively few solute particles. The total polarization of the solution is then simply the sum of the solvent polarization and the polarization of the solute particles. If there are N solute particles per unit volume then the polarization of the solution is given by

$$\vec{P} = \vec{P}_s + \sum_{n=1}^{N} \vec{p}_n \quad , \tag{II-39}$$

where P_s is the polarization per unit volume of solvent and $\vec{p}_n$ is the polarization of the n^{th} solute particle.

If the N particles are identical and the number of particles pointing in such a direction that their principle axes fall within $d\Omega$ on the unit sphere is $N\rho\, d\Omega$, then

$$\sum_{n=1}^{N} \vec{p}_n = \sum_{n=1}^{N} \vec{p}_n N\rho_n\, d\Omega_n = \int_{\Omega} \vec{p}\, N\rho\, d\Omega \quad , \tag{II-40}$$

where ρ is the distribution function of the particles in solution. $\vec{p}$ may be broken down into components.

$$\vec{p}_x = p_1 \cos(1x) + p_2 \cos(2x) + p_3 \cos(3x) \quad , \tag{II-41a}$$

$$p_y = p_1 \cos(1y) + p_2 \cos(2y) + p_3 \cos(3y) \quad , \qquad \text{(II-41b)}$$

$$p_z = p_1 \cos(1z) + p_2 \cos(2z) + p_3 \cos(3z) \quad , \qquad \text{(II-41c)}$$

where $(1x)$ is the angle between the major axis 1 of the particle and the x direction. The 2 and 3 directions refer to the two minor axis directions of the particle. If the electric field is in the x direction only, then

$$p_i = g_i E_x \cos(ix) \quad , \qquad \text{(II-42)}$$

where i = 1, 2, or 3 and g_i is the polarizability in the i^{th} direction.

Combining (II-39), (II-40), (II-41a,b,c) and (II-42),

$$P_x = P_{sx} + N E_x \int_\Omega \{ g_1 \cos^2(1x) + g_2 \cos^2(2x) + g_3 \cos^2(3x) \} \rho \, d\Omega \quad , \qquad \text{(II-43a)}$$

$$P_y = P_{sy} + N E_x \int_\Omega \{ g_1 \cos^2(1y) + g_2 \cos^2(2y) + g_3 \cos^2(3y) \} \rho \, d\Omega \quad , \qquad \text{(II-43b)}$$

$$P_z = P_{sz} + NE_x \int_{\Omega} \{g_1 \cos^2(1z) + g_2 \cos^2(2z) + g_3 \cos^2(3z)\} \rho d\Omega \quad .$$

(II-43c)

When written out in the σ, ν coordinate system each of the terms of equations (II-43b) and (II-43c) is of the form $f_1(\sigma)\sqrt{f_2(\sigma) + \sin^2\nu}$ or can easily be reduced to that form. If ρ is independent of ν then

$$\int_0^{2\pi} f_1(\sigma)\sqrt{f_2(\sigma) + \sin^2\nu}\,\rho d\nu = 0 \quad , \qquad \text{(II-44)}$$

and P_y and P_z are equal to zero.

The theory as developed can be used for the electric field of a light wave if a wave front with an area large enough such that the volume described by this area times a small increment of the wavelength is large enough to include a large total number of particles. It may be that most particles are not wholly within this volume, but the sum of all the parts of particles within this volume represents a large number of particles. The increment of wavelength is chosen in such a manner that the electric field in the volume described can be treated as constant over the volume. Thus the theory up to equation (II-44) is proper for a light wave polarized in the x direction and traveling in a direction perpendicular to x. If this direction is taken to be the z direction, an equation similar to (II-43a) may be written for light polarized in the y direction.

$$P_y = P_{sy} + N E_y \int_{\Omega} \{ g_1 \cos^2(1y) + g_2 \cos^2(2y) + g_3 \cos^2(3y) \} \rho \, d\Omega \quad . \qquad \text{(II-45)}$$

Birefringence is defined by

$$\Delta n = n_x - n_y = \frac{n_x^2 - n_y^2}{n_x + n_y} = \frac{n_x^2 - n_y^2}{2n} \quad , \qquad \text{(II-46)}$$

where n is the average index of refraction of the material. From electromagnetic theory

$$\vec{D} = n^2 \vec{E} = \vec{E} + 4\pi \vec{P} \quad . \qquad \text{(II-47)}$$

Writing (II-47) in component form and rearranging terms,

$$n_x^2 = 1 + \frac{4\pi P_x}{E_x} \quad , \qquad \text{(II-48a)}$$

$$n_y^2 = 1 + \frac{4\pi P_y}{E_y} \quad , \qquad \text{(II-48b)}$$

so

$$\Delta n = \frac{4\pi}{2n} \left[\frac{P_x}{E_x} - \frac{P_y}{E_y} \right] \quad , \qquad \text{(II-49a)}$$

or

$$\Delta n = \frac{2\pi}{n}\left[\frac{P_{sx}}{E_x} - \frac{P_{sy}}{E_y} + N\int_{\Omega}\left\{g_1\left[\cos^2(1x) - \cos^2(1y)\right]\right.\right.$$

$$\left.\left. + g_2\left[\cos^2(2x) - \cos^2(2y)\right] + g_3\left[\cos^2(3x) - \cos^2(3y)\right]\right\}\rho\, d\Omega\right] . \quad \text{(II-49b)}$$

But

$$\frac{P_{sx}}{E_x} + \frac{P_{sy}}{E_y} = \frac{n_s^2 - 1}{4\pi} - \frac{n_s^2 - 1}{4\pi} = 0 , \quad \text{(II-50)}$$

so that

$$\Delta n = \frac{2\pi}{n} N \int_{\Omega}\left\{g_1\left[\cos^2(1x) - \cos^2(1y)\right] + g_2\left[\cos^2(2x) - \cos^2(2y)\right]\right.$$

$$\left. + g_3\left[\cos^2(3x) - \cos^2(3y)\right]\right\}\rho\, d\Omega . \quad \text{(II-51)}$$

In the coordinate system of Figure 1 if $g_2 = g_3$, equation (II-51) becomes

$$\Delta n = \frac{2\pi}{n} N \int_{\sigma=0}^{\pi}\int_{\nu=0}^{2\pi}\left\{g_1\left[\cos^2\sigma - \sin^2\sigma \sin^2\nu\right]\right.$$

$$\left. + g_2\left[\sin^2\sigma - \cos^2\sigma \sin^2(\nu+180^\circ) - \sin^2(\nu-90^\circ)\right]\right\}$$

$$\cdot \rho \sin\sigma\, d\sigma\, d\nu . \quad \text{(II-52a)}$$

This may be reduced to

$$\Delta n = \frac{2\pi}{n} N \int_{\sigma=0}^{\pi} \int_{\nu=0}^{2\pi} (g_1 - g_2)(\cos^2\sigma - \sin^2\sigma \sin^2\nu) \cdot \rho \sin\sigma \, d\sigma \, d\nu \, . \qquad \text{(II-52b)}$$

If ρ is independent of ν then integration over ν yields

$$\Delta n = \frac{4\pi^2}{n} N (g_1 - g_2) \int_0^{\pi} \frac{1}{2} (3\cos^2\sigma - 1) \rho \sin\sigma \, d\sigma \, . \qquad \text{(II-53)}$$

If ρ is expanded in terms of Legendre polynomials

$$\rho = \sum_{n=0}^{\infty} C_n P_n(\cos\sigma) \, , \qquad \text{(II-54)}$$

final integration yields

$$\Delta n = \frac{4\pi^2}{n} N (g_1 - g_2) C_2 \frac{2}{5} \, . \qquad \text{(II-55)}$$

From equations (II-55) and (II-38), the birefringence is given by

$$\Delta n = \frac{4\pi}{n} N (g_1 - g_2) \frac{1}{15} \left\{ \beta^2 \left[\frac{1}{1 + (\omega/2D)^2} + \frac{\cos(2\omega t - \delta_1 - \delta_2)}{[(1 + (\omega/2D)^2)(1 + (\omega/3D)^2)]^{1/2}} \right] + \gamma^2 \left[1 + \frac{\cos(2\omega t - \delta_1)}{[1 + (\omega/3D)^2]^{1/2}} \right] \right\} \, . \qquad \text{(II-56)}$$

This may also be written in the form

$$\Delta n = \frac{N}{n}\frac{\pi}{15}(g_1-g_2)\left(\frac{\mu E}{kT}\right)^2\left\{P+\frac{1}{1+9(\omega/6D)^2}+\sqrt{\frac{P^2+\frac{1+2P}{1+9(\omega/6D)^2}}{1+4(\omega/6D)^2}}\cos(2\omega t-\delta)\right\},$$

(II-57)

where

$$\tan\delta = 3\frac{\omega}{6D}\left[\frac{2P+5+18P(\omega/6D)^2}{3(1+P)+(3P-2)9(\omega/6D)^2}\right], \quad \text{(II-58)}$$

and

$$P = \frac{\gamma^2}{\beta^2} \quad \text{(II-59)}$$

If the peak values of the alternating component and steady component of the birefringence are written out separately one obtains

$$\Delta n_{alt} = \frac{N}{n}\frac{\pi}{15}(g_1-g_2)\left(\frac{\mu E}{kT}\right)^2\sqrt{\frac{P^2\,\frac{1+2P}{1+9(\omega/6D)^2}}{1+4(\omega/6D)^2}}, \quad \text{(II-60)}$$

and

$$\Delta n_{st} = \frac{N}{n}\frac{\pi}{15}(g_1-g_2)\left(\frac{\mu E}{kT}\right)^2 \left\{P + \frac{1}{1+9(\omega/6D)^2}\right\}. \quad \text{(II-61)}$$

In both equation (II-60) and (II-61) the low frequency limit is

$$\Delta n_o = \frac{N}{n}\frac{\pi}{15}(g_1-g_2)\left(\frac{\mu E}{kT}\right)^2 (P+1) \quad . \quad \text{(II-62)}$$

Thus

$$\frac{\Delta n_{alt}}{\Delta n_o} = \sqrt{\frac{P^2 + \frac{1+2P}{1+9(\omega/6D)^2}}{1+4(\omega/6D)^2}} \Big/ (P+1) \quad , \quad \text{(II-63)}$$

and

$$\frac{\Delta n_{st}}{\Delta n_o} = \left(P + \frac{1}{1+9(\omega/6D)^2}\right) / (P+1) \quad . \quad \text{(II-64)}$$

This is a convenient form in which to present the frequency dependent character of the electro-optic equations. In all of the above the term $\omega/6D$ was chosen since many of the references in the literature refer to a relaxation time equal to $1/6D$.

The types of response curves expected for different values of P are shown in Figures 2, 3, 4, and 5. The curves for the steady component between the values of $P = 0$ and $P = -1$ are curves which would change sign if plotted on a linear scale.

Figure 2: Theoretical Steady Component of the Electro-Optic Effect as a Function of $\omega/6D$ for Varying Values of P From -1 to $-\infty$ and From $+\infty$ to 0 (A).

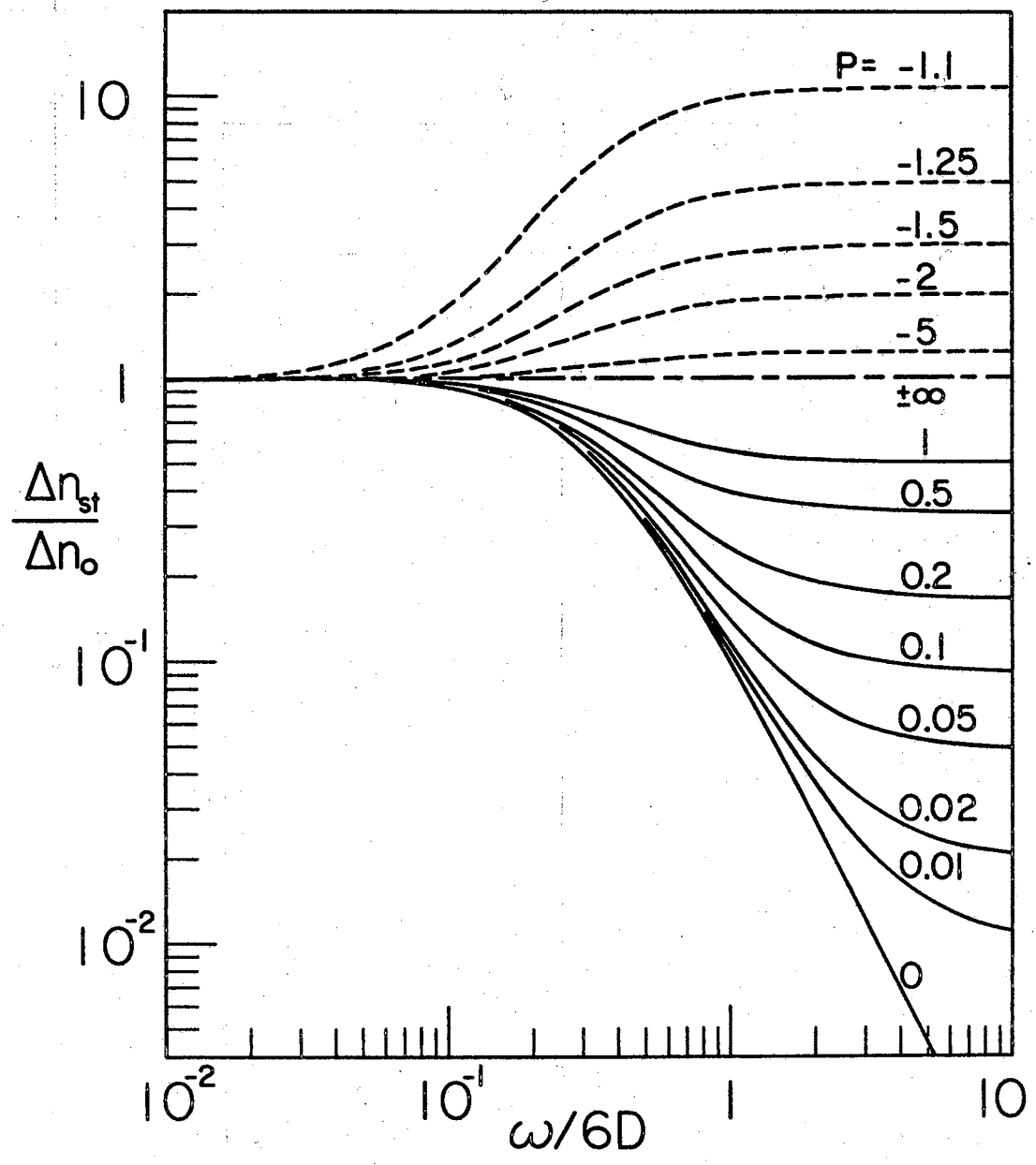
P= -1.1
-1.25
-1.5
-2
-5
±∞
1
0.5
0.2
0.1
0.05
0.02
0.01
0
10
1
10^-1
10^-2
Δn_st / Δn_o
10^-2
10^-1
1
10
ω/6D

Figure 3: Theoretical Steady Component of the Electro-Optic Effect as a Function of $\omega/6D$ for Varying Values of P From 0 to -1 (B).

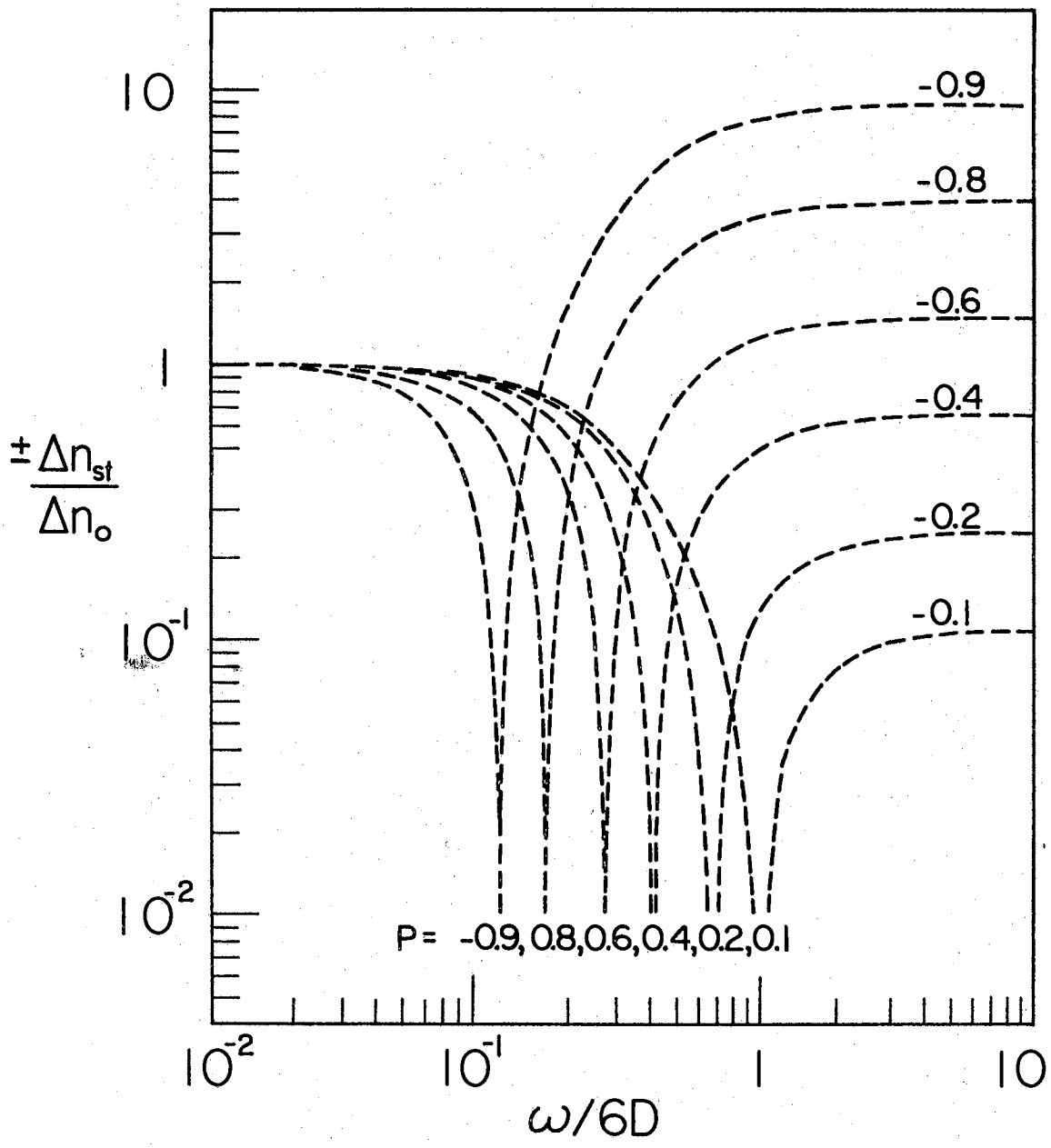
10
1
10^{-1}
10^{-2}
$\pm \frac{\Delta n_{st}}{\Delta n_o}$
-0.9
-0.8
-0.6
-0.4
-0.2
-0.1
P= -0.9, 0.8, 0.6, 0.4, 0.2, 0.1
10^{-2}
10^{-1}
1
10
$\omega/6D$

Figure 4: Theoretical Alternating Component of the Electro-Optic Effect as a Function of $\omega/6D$ for Varying Values of P .

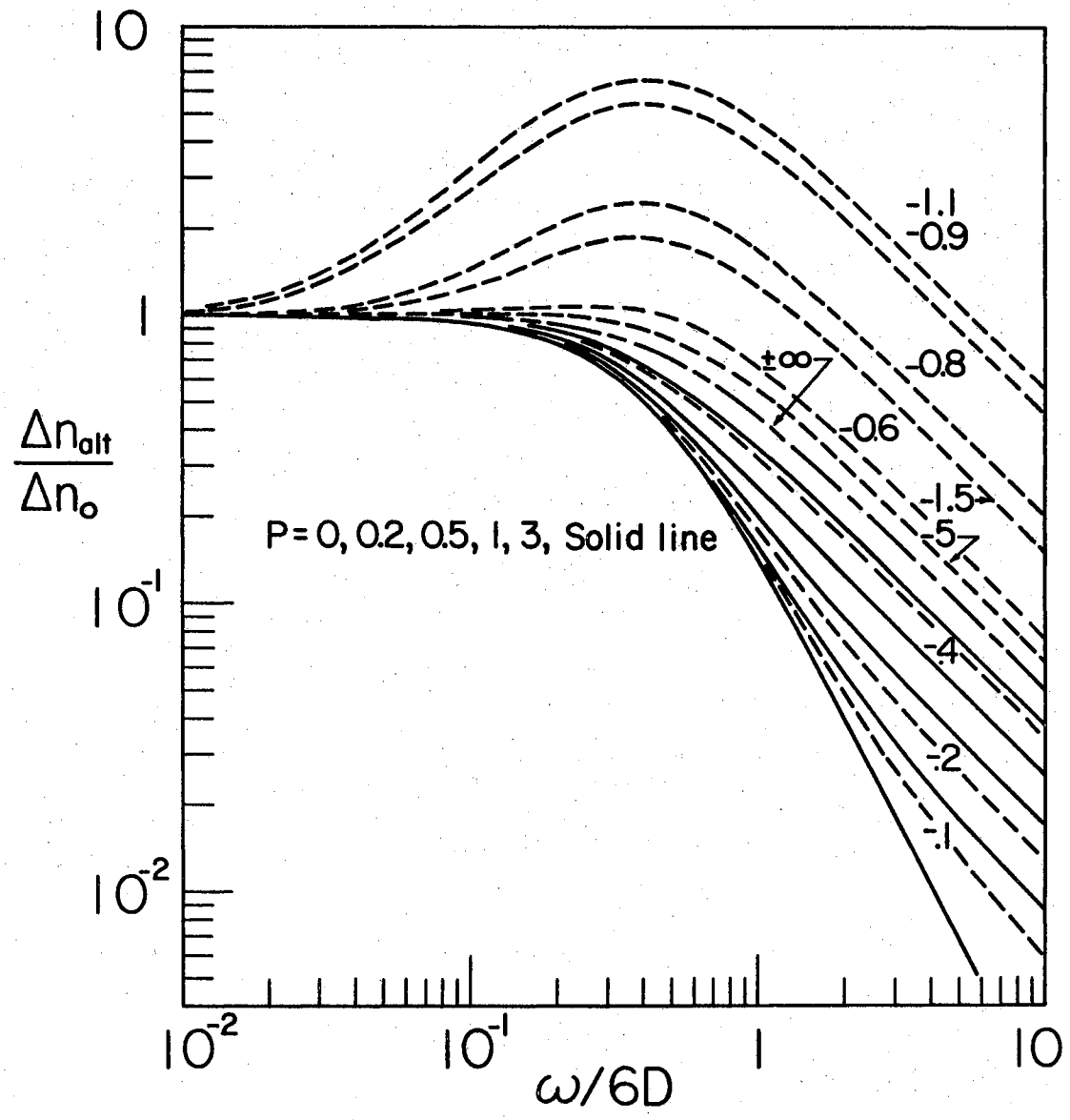
10
1
10^{-1}
10^{-2}
$\frac{\Delta n_{alt}}{\Delta n_o}$
P = 0, 0.2, 0.5, 1, 3, Solid line
±∞
-1.1
-0.9
-0.8
-0.6
-1.5
-5
-4
-2
-1
10^{-2}
10^{-1}
1
10
ω/6D

Figure 5: Theoretical Phase Angle of the Electro Optic Effect as a Function of $\omega/6D$ for Varying Values of P.

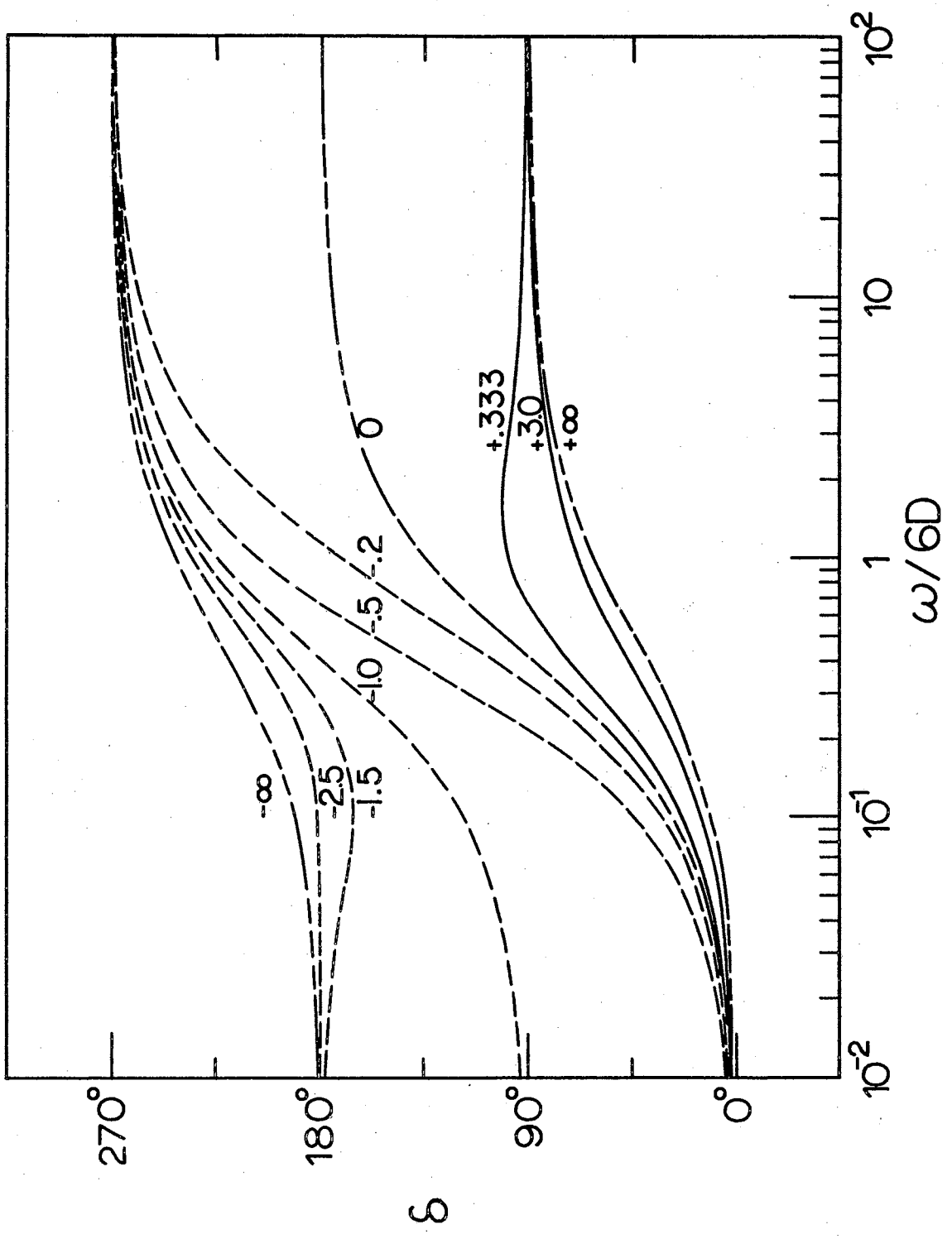
270°
180°
90°
0°
θ
10^{-2}
10^{-1}
1
10
10^{2}
ω/6D
-∞
-2.5
-1.5
-1.0
-.5
-.2
0
+.333
+3.0
+∞

Other Relaxation Mechanisms

The optical response described above is due to the presence of both a permanent and an induced dipole. The mechanism involved in the response due to a permanent dipole must be orientation, since by its very definition the dipole is permanently attached to the macromolecule. However the induced dipole by its very definition implies something that is transitory.

Mathematically other relaxation mechanisms may be introduced as particular forms of a general scheme in which additional functions specify a variation with frequency of the phase angle. Thus in the first step of the procedure no assumption is made about any mechanism in the induction of the dipole.

If the variation in magnitude is associated with the term $(g_{1e}-g_{2e})$ and the variation in phase with the electric field then one immediately obtains the term

$$\overline{\gamma^2} = \frac{(g_{1e}-g_{2e})}{kT} f(\omega) E_0^2 \cos^2(\omega t - \phi(\omega)) \quad , \qquad \text{(II-65)}$$

where the $f(\omega)$ and the $\phi(\omega)$ are the functions described. The term $\overline{\gamma^2}$ may be substituted for γ^2 in equation (II-26).

If the substitution described above is made, the effect upon the equations in Appendix A is to alter equation (A-26) such that the $\cos^2 \omega t$ term becomes $\cos^2(\omega t - \phi(\omega))$. The $f(\omega)$ may be carried in the perturbation term γ^2. This produces an equation similar in form to equation (A-51) from which the solution to (A-26) can be deduced. Thus the distribution function ρ is altered only in its last term to become

$$\rho = \frac{1}{4\pi}\left\{ P_0 + P_1\beta \frac{\cos(\omega t - \delta_1)}{1+(\omega/2D)^2} + P_2\beta^2 \frac{1}{6} \right.$$

$$\cdot \left[\frac{1}{1+(\omega/2D)^2} + \frac{\cos(2\omega t - \delta_1 - \delta_2)}{[(1+(\omega/2D)^2)(1+(\omega/3D)^2)]^{1/2}} \right]$$

$$\left. + P_2\gamma^2 f(\omega)\frac{1}{6}\left[1 + \frac{\cos(2\omega t - \delta_2 - 2\phi(\omega))}{[1+(\omega/3D)^2]^{1/2}} \right] \right\}. \qquad \text{(II-66)}$$

The birefringence expression becomes

$$\Delta n = \frac{N}{n}\frac{\pi}{15}(g_1 - g_2)\left\{ \beta^2 \left(\frac{1}{1+(\omega/2D)^2} \right.\right.$$

$$\left. + \frac{\cos(2\omega t - \delta_1 - \delta_2)}{[(1+(\omega/2D)^2)(1+(\omega/3D)^2)]^{1/2}} \right) + \gamma^2 f(\omega)$$

$$\left. \cdot \left(1 + \frac{\cos(2\omega t - \delta_2 - 2\phi(\omega))}{[1+(\omega/3D)^2]^{1/2}} \right) \right\} . \qquad \text{(II-67)}$$

Any theoretical approach to the frequency dependence of the induced moment should now be able to be cast in the form of the last equation.

A number of workers (21,34,39,72) have considered possible polarization mechanisms, but only a few have worked out the time dependency of the mechanisms. O'Konski (44) has done work in which both the Maxwell-Wagner mechanism, which was worked our earlier by Fricke (21), and an addition to this theory of a surface conductivity brought about by the presence of mobile protons, electrons, holes or ions is considered. These surface conductivity contributions are generalized as an effective volume conductivity, which affect the dielectric

increment (which could be related to the magnitude of $(g_{1e}-g_{2e})$) and the relaxation time

$$\tau = \frac{1}{4\pi} \frac{\epsilon + \epsilon_s (1/A - 1)}{\sigma + \sigma_s (1/A - 1)} , \qquad \text{(II-68)}$$

where the A values are the depolarization factors defined by

$$A_j = \frac{1}{2} \int_0^\infty \frac{abc \; ds}{(j+s)[(a^2+s)(b^2+s)(c^2+s)]^{1/2}} . \qquad \text{(II-69)}$$

Here a , b , and c are the principle axes of the equivalent ellipsoid model of the particle and j assumes the values a , b or c . Tables of these values as well as graphs are given by Osborn (55). The relaxation time given is for an expression of the type

$$\epsilon^* = \Delta\epsilon \frac{1}{1+i\omega\tau} + \epsilon_\infty . \qquad \text{(II-70)}$$

For our purposes the $\Delta\epsilon$ may be related to the magnitude of the polarizability $(g_{1e}-g_{2e})$. In the dielectric case, however, the time dependent applied field is implied and in the case of the induced moment it must be stated. Thus the polarization is given by

$$P = Re\{(g_{1e}-g_{2e}) E_0 \frac{1}{1+i\omega\tau} e^{i\omega t}$$

$$= Re \frac{g_{1e}-g_{2e}}{(1+\omega^2\tau^2)^{1/2}} E_0 e^{i(\omega t-\phi)}$$

$$= \frac{(g_{1e}-g_{2e})}{(1+\omega^2\tau^2)^{1/2}} E_0 \cos(\omega t-\phi) , \qquad \text{(II-71)}$$

where

$$\tan \phi = \omega t \quad . \qquad \text{(II-72)}$$

Thus for this model

$$f(\omega) = \frac{1}{(1+(\omega t)^2)^{1/2}} \quad , \qquad \text{(II-73)}$$

and

$$\phi(\omega) = \tan^{-1} \omega t \quad . \qquad \text{(II-74)}$$

It should be noted again that the above describes the Maxwell-Wagner effect and by proper modification of the term σ also includes all effects in which surface conductivity is present. In addition any other mechanism which would present a result of the form of equation (II-70) is immediately applicable.

What has been determined is that a relaxation mechanism of some sort involving the induced moment on the macromolecule would produce a fall off in the alternating and steady component of the electro-optic effect and possibly a dielectric relaxation and loss similar to that expected for orientation of the macromolecules. However unless the two effects are coincident in frequency, they can be separated. This will be considered in more detail in the specific cases where it is useful.

Polydispersity

A brief mention will be made now of the effects of polydispersity. In the theory as developed in this chapter, it has been assumed that the N molecules per unit volume were identical. That is, it was assumed that they had the same μ, g_{1e}, g_{2e}, $(g_1 - g_2)$, and D. This condition is highly improbable in a solution of large molecules. However, if whatever molecules are present do not interact with one another, and this is also an implicit assumption of the theory, then the effect of the different species of molecules present is additive. In this it must be remembered that the alternating component of birefringence has an associated phase angle and the addition for this case must be vectoral addition. The analysis of polydispersity of a solution is possible given a "perfect" set of data. This will be discussed for a particluar case in Chapter IV.

CHAPTER III

EQUIPMENT AND PROCEDURES

The equipment used to measure the electro-optic effect consists of several different equipment combinations which will require separate descriptions. The manner in which basic quantities may be calculated from the measurements will be discussed, so that meaningful comparisons can be made between these measurements and the measurements made by others.

The Electro-Optic Measurement System

The system used to measure the electro-optic effect consists of a series of components that form a narrow beam of right circularly polarized light, a cell containing the macromolecular solution in which birefringence has been induced, and a series of elements for detecting the electro-optic response.

Figure 6 shows a diagram of the optical bench and the equipment which is not directly involved with the signal voltages. The lamp (LA) is powered by a bank of batteries with a storage capacity greatly exceeding the power requirements of the lamp. This prevents excessive change in the light level while measurements are being made. The lamp itself is a Phillips 8 V., 50 watt prefocused projector lamp. The output of the lamp is focused on an aperture (AP) in a plate, thus providing a rough point source of light. Next in place on the optical

Figure 6: The Optical Bench With Associated Equipment. The elements on the bench are the lamp (LA), aperture (AP), photodiode (PD), multiple lens (ML), polarizing prism (P), quarter wave plate (W), electro-optic cell (C), analyzing prism (A), interference filter (F), lens (L) and photomultiplier (PM).

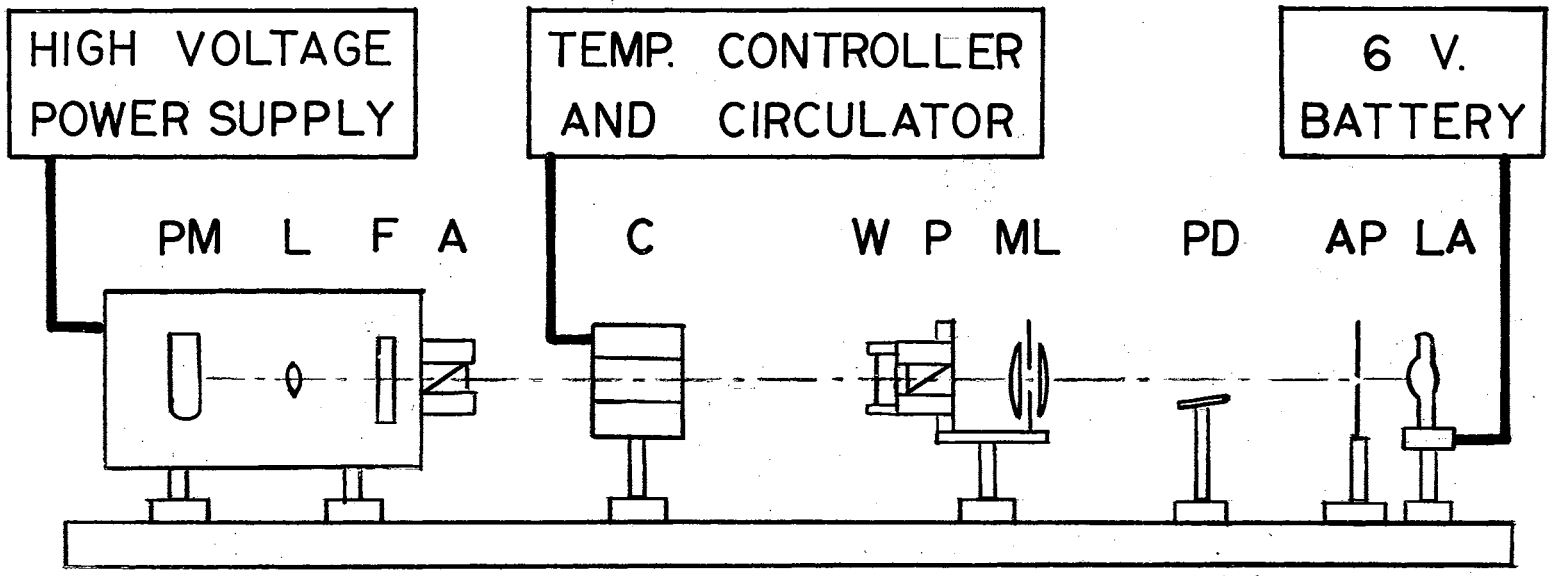
HIGH VOLTAGE
POWER SUPPLY
TEMP. CONTROLLER
AND CIRCULATOR
6 V.
BATTERY
PM
L
F
A
C
W
P
ML
PD
AP
LA

bench but not actually in the optical path is a photodiode (PD), type 1N2175. The function of this photodiode will be described later. The next element is a multiple lens and aperture system (ML) which consists of an f/3.5 100 mm lens system. The image of the aperture formed by this lens system is focused to the left of the cell (C) in Figure 6. Ideally, a collimated beam of nondiverging light focused at infinity is desired. However, because the aperture (AP) is of finite size, as is the aperture in the multiple lens system (ML), focusing the beam to the left of the cell was found to be the best configuration for maintaining a maximum light flux through the system while avoiding a diverging beam with its consequent problems of reflection from the sides of the prisms and the electro-optic cell. Actual distances between elements were determined approximately by calculations in which the major consideration was the maximization of the amount of light striking the photomultiplier. Final fine adjustment was made by trial. The aperture of the lens was adjusted so that a maximum of light would go through the next element of the system without reflecting from any of its sides. The next element is a 5 mm. Glan-Thompson polarizing prism (P). The polarizing direction is at 45° to the horizontal. Following this is a quarter wave plate (W) with its fast axis oriented in the horizontal direction. All of these elements, except the photodiode, produce a right circularly polarized beam of light.

The next element in the system is the cell which contains the material being studied. Two cells were used, and will be described as the large cell and the small cell.

The large cell consists of a brass body and lid, and features a top electrode which is adjustable from the outside so that the distance

between electrodes can be varied. The electrodes are platimum plated brass. They are 8cm. long in the direction of the optical path and 1 cm. wide. The gap can be varied from 0.5 cm. to about 8 cm. There is a provision in the side of the cell for probe electrodes to measure the electric field in the cell itself. There is 1.0 cm. of Teflon between the electrodes and the brass sides of the cell. The electrodes are within 0.004 inches of the glass windows at either end of the cell. A provision for a thermistor is made in the bottom electrode. The circulating water used to maintain the temperature of the cell is in direct contact with the bottom electrode. The bottom electrode is also grounded.

The small cell is made of stainless steel and Teflon. The electrodes are 2.54 cm. square and the bottom electrode may be changed to obtain various spacings. The electrode spacing may be further altered with an additional spacer between the cell cover and the cell body. The total variation in possible gaps is from about 0.05 cm. to 0.35 cm. The side boundaries of the gap are Teflon. At the ends of the cell the glass windows are approximately 0.5 cm. from the electrodes. A provision is made in the cover of the cell for admitting a thermistor probe into the fluid. Another provision is made for circulating a liquid in the cell body to control the temperature.

A Haake temperature controller and circulator is used to maintain the temperature of the cell. Although the controller is capable of control to within 0.01 degrees, the cell is not actually maintained within that range because application of the electric field to the conducting fluids used in all cases causes heating in the cell. This will be considered further under a description of procedures.

All of the remaining elements in the optical system are attached to, or are contained in the photomultiplier housing. The first of these elements is the analyzing prism (A). This is identical to the polarizing prism (P) and is oriented at 90° to the polarizer (P). Next is a 2.0 by 2.0 inch interference filter (F) which passes light at a wavelength of 578 millimicrons. This was placed in the photomultiplier housing because in that position it also filtered stray light entering the photomultiplier housing and reduced the problem created by such light to a negligible level. Next is a small lens (L) used to spread the beam of light slightly so that it strikes the photosensitive surface of the photomultiplier over a larger area. The photomultiplier is an R.C.A. 931A with a piece of plactic placed over its window to furthur diffuse the incoming light over the photosensitive surface. The photomultiplier is powered by a Hamner model 301 high voltage power supply.

An analysis of the function of the optics described above is given by Thurston (77) in a paper describing response of systems of the general nature used in this study. For the specific system described above the photocurrent is given by the expression

$$I = I_0(1+\sin\delta) \quad , \qquad \text{(III-1)}$$

where δ is the phase retardation in the material in the electro-optic cell and I_0 is the photocurrent when $\delta = 0$. If δ is small, this reduces to

$$I \simeq I_0(1+\delta) \quad . \qquad \text{(III-2)}$$

Solving for δ one obtains

$$\delta = \frac{I - I_o}{I_o} = \frac{I}{I_o} - 1 \quad . \qquad \text{(III-3)}$$

This is connected to the theory by the equation

$$\delta = \frac{2\pi L}{\lambda} \Delta n \quad , \qquad \text{(III-4)}$$

where L is the length of the path in the cell, not the optical path length, and λ is the wavelength of the light in air.

Equations (II-58), (II-60) and (II-61) present the form of electro-optic response expected for macromolecular orientation. Even if the theory does not adequately describe what is observed, one can at least measure a steady component of birefringence, an alternating component of birefringence at twice the applied frequency and a phase angle associated with the alternating component. The block diagrams in Figures 7, 8 and 9 show the various equipment configurations used. The different diagrams indicate the differences in the manner of obtaining the reference for phase measurements and the magnitude of the applied voltage for the steady component or alternating component measurements. In general, the probe electrodes and amplifier were used as the voltage reference below 10^3 Hz. in those cases where the sensitivity of the material was great enough that the large cell could be used with at least a 3.5 cm. gap. The voltage across a resistor in series with the cell was used with the small cell at low frequencies and the voltage applied to the cell was used in both the small cell and large cell at frequencies above 10^3 Hz.

Figure 7: Block Diagram of the Equipment as Used for Steady Component Measurements. In specific applications the elements in the dashed lines may be replaced by one of the two systems in Figure 9.

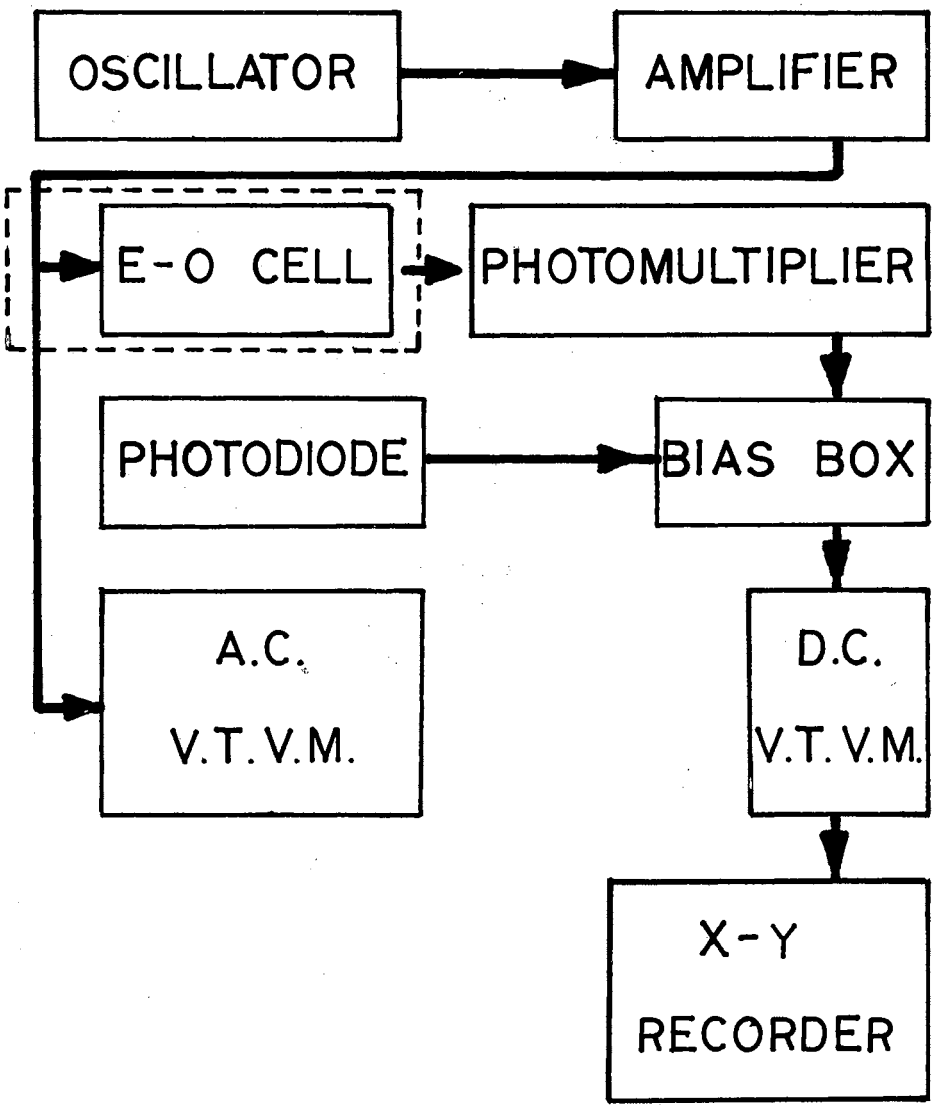
OSCILLATOR
AMPLIFIER
E-O CELL
PHOTOMULTIPLIER
PHOTODIODE
BIAS BOX
A.C.
V.T.V.M.
D.C.
V.T.V.M.
X-Y
RECORDER

Figure 8: Block Diagram of the Equipment as Used for Alternating Component Measurements. In specific applications the elements in the dashed lines may be replaced by one of the two systems in Figure 9.

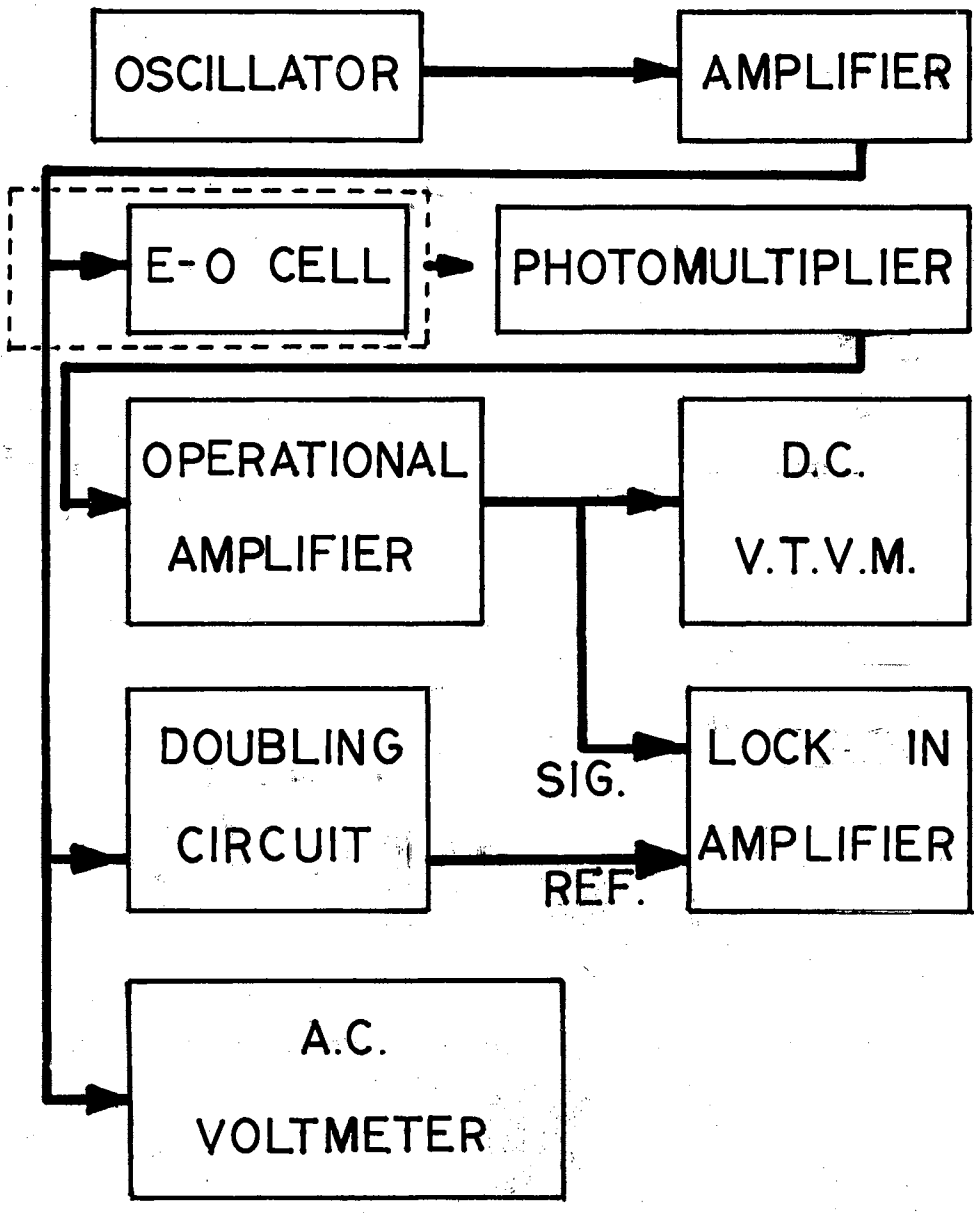
OSCILLATOR
AMPLIFIER
E-O CELL
PHOTOMULTIPLIER
OPERATIONAL AMPLIFIER
D.C. V.T.V.M.
DOUBLING CIRCUIT
SIG.
REF.
LOCK IN AMPLIFIER
A.C. VOLTMETER

Figure 9: Block Diagrams of Alternate Systems for Reference Voltage Determination.

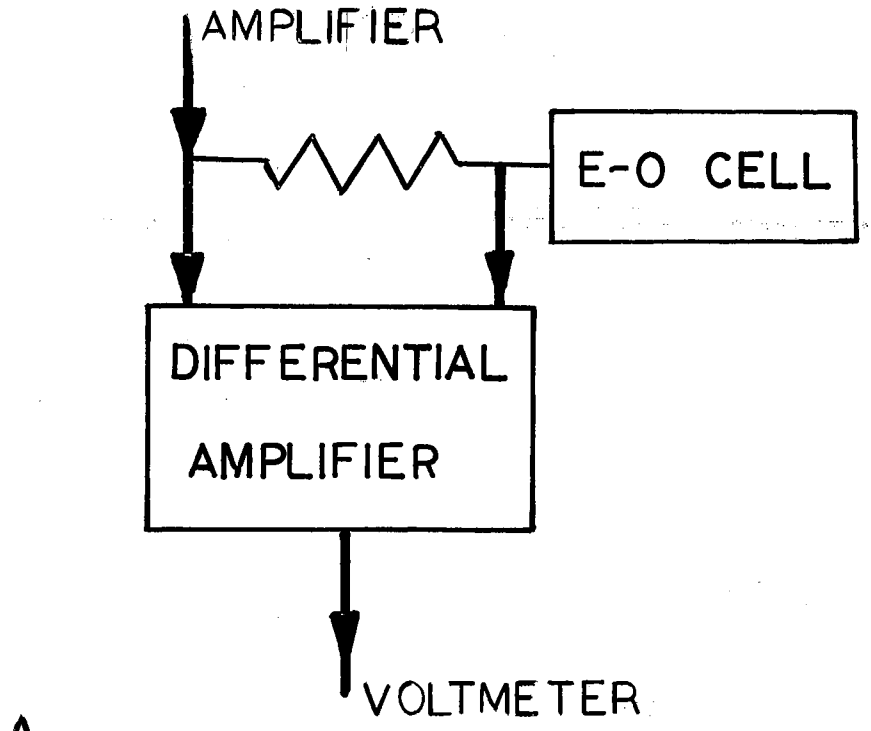
AMPLIFIER
E-O CELL
DIFFERENTIAL
AMPLIFIER
VOLTMETER

A.

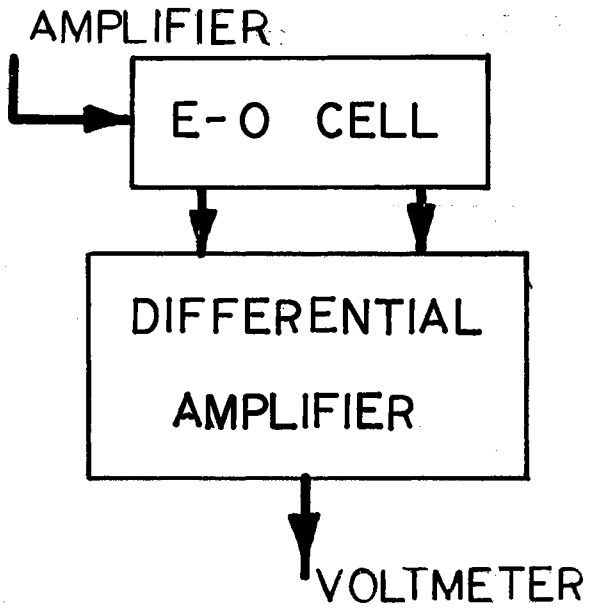
AMPLIFIER
E-O CELL
DIFFERENTIAL
AMPLIFIER
VOLTMETER

B.

The circuit diagrams of the bias box and the frequency doubling circuit are shown in Figure 10. The bias box is designed to compensate for fluctuations in the light level. The circuit involving the photodiode is intended to balance out the voltage that is present even when no birefringence is present, that is, the signal of equation (III-1) when $\delta = 0$. The other bias circuit is present because the photodiode is not linear in its response. Approximate linearity is obtained by inserting a small glass plate in the optical path at the aperture (AP) and varying the voltage in the photodiode and bias circuit until such an insertion produces no change in the output voltage of the bias box. The photomultiplier power supply is adjusted to produce a 1.0 V. output from the photomultiplier (loaded by a 187 K ohm resistor) under the $\delta = 0$ condition mentioned above.

The frequency doubling circuit is a clipping device. That is, one polarity of the sine wave is removed and a zero voltage is substituted. The Fourier analysis of this wave form indicates that the component at twice the sine wave frequency is $\cos 2\omega t$ when the input is $\cos \omega t$. That is, there is no phase shift involved. The D.C. fundamental, and higher harmonic components are filtered out by a Princeton Applied Research Model JB-4 lock-in amplifier. The 15 K ohm resistor is for the protection of the diode.

Figures 7, 8 and 9 illustrate the instrumental configurations used, but a description of this function is still in order. In all cases a sinusoidal signal originates in the oscillator. This is a Hewlett Packard 202C oscillator for the frequency range $1\text{-}10^5$ Hz. and a Hewlett Packard 650A oscillator for frequencies from 10^5 to 10^6 Hz. This signal is amplified by a Kron-Hite D.C.10, 10 watt amplifier

Figure 10: Circuit Diagrams of Frequency Doubler and Bias Box.

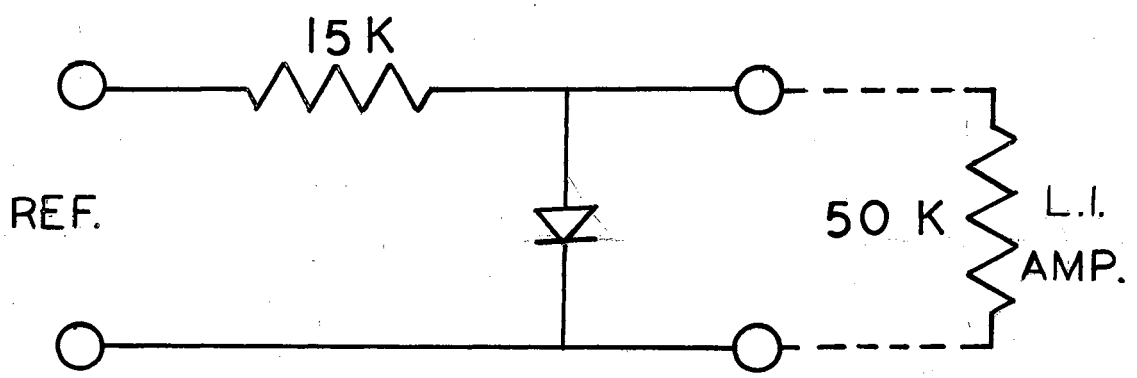
15 K
REF.
50 K
L.I.
AMP.

A.

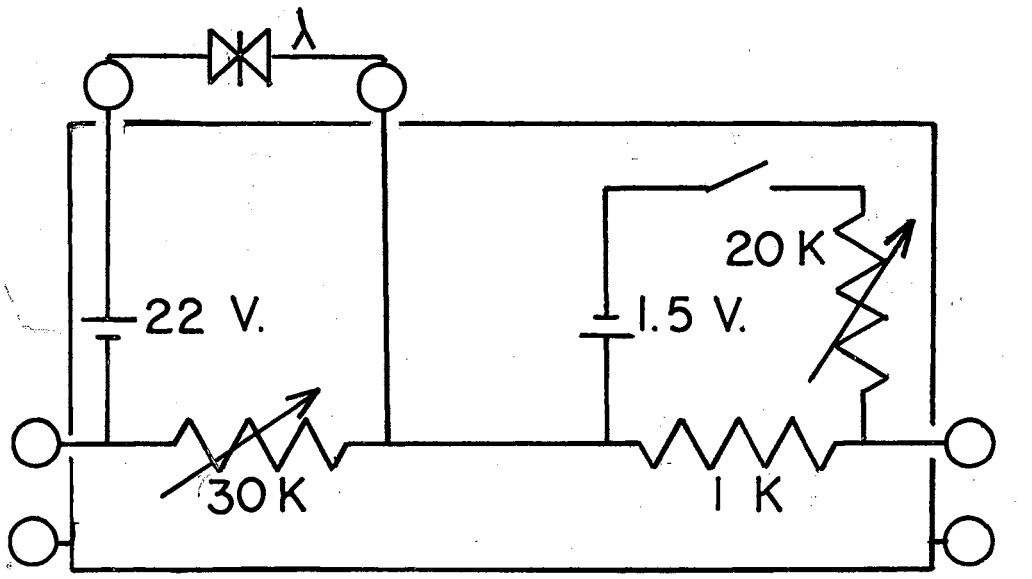
λ
22 V.
20 K
1.5 V.
30 K
1 K
INPUT
(PM)
OUTPUT
VOLTMETER

B.

which has a frequency range of D.C. to 10^6 Hz. If the cell presents a high impedence load to the amplifier, a maximum of about 200 V. r.m.s. can be obtained from the amplifier. The amplified sinusoidal signal is applied to the electrodes of the cell. Depending upon the material in the cell and the frequency of the applied voltage, a reference voltage is taken either from the probe electrodes in the cell as in Figure 9b, the voltage applied to the cell as in Figures 7 and 8, or the voltage across a small resistor placed in series with the cell as in Figure 9a. Further instrumentation depends upon whether the steady component of alternating component of the electro-optic effect is to be measured.

If the steady component is to be measured, the reference voltage goes to a Hewlett Packard 403A A.C. transistor voltmeter. This voltmeter can also operate as a differential voltmeter because it contains its own power supply and is not grounded. If the alternating component is to be measured, the reference voltage goes to both the A.C. voltmeter and to the doubling circuit. From the doubling circuit the signal is fed to the reference channel of the lock-in amplifier.

The voltage applied to the cell produces the electro-optic effect which produces a change in the photocurrent of the photomultiplier. The current from the photomultiplier is directed to ground through a 187 Kohm resistor. The voltage across this resistor is called the photovoltage and it is this that is finally measured using an instrument with a 10 M ohm input resistance.

If the steady component of the response is to be measured, then this voltage is fed into the bias box which adds approximately 1.0 V. and makes minor adjustments for fluctuations in the intensity of the light source. From the bias box the signal is fed to a Hewlett Packard

412A D.C. voltmeter. The voltmeter is used as a visual indicator and as an amplifier to drive one axis of a Moseley 135 x-y recorder. The final data is measured from the plots made by the x-y recorder.

If the alternating component is to be measured, the photovoltage is first fed to an operational amplifier. This is done to provide a proper impedance match. The operational amplifier has a high input impedance while the lock-in amplifier does not. The signal is then directed to the signal channel of the lock-in amplifier. The lock-in amplifier is used to measure both the amplitude and phase angle of the alternating component. The D.C. voltmeter is used to check the no-signal photomultiplier output.

Experimental Procedure

The exact procedures are important as it was found that heating, degradation and electrode effects often produced erroneous results. The procedures used either avoided these problems or checked for their presence. The methods of sample preparation are discussed later.

After preparing the material, the pH and conductivity were measured. The conductivity was measured in the electro-optic cell or in a test cell constructed for that purpose. The filled electro-optic cell was mounted on the bench and the electrical connection, circulating water hoses and thermistor attached. The water circulator was then turned on and everything was allowed to come to thermal equilibrium. The field was then applied for several minutes before measurements were made. This was done because it was observed that if any radical changes occur, they generally occur during the first few minutes of the application of the electric field. The lowest frequency measurements

were taken first because they were usually the most difficult.

When the steady component data was taken the procedure was to (1) adjust the oscillator to the new frequency, (2) adjust the applied voltage, (3) check temperature and photovoltage with no signal applied to cell, (4) start the x-y recorder on a time sweep, (5) apply and remove the voltage at least three times in at least three second intervals while observing the D.C. voltmeter for proper response. The traces on the paper in the x-y recorder then provided a record of the steady component level change which could be averaged to reduce the effect of noise. Between measurements the signal was removed to allow the cell to come to thermal equilibrium again.

When alternating component measurements were made the procedure was to (1) adjust the oscillator to the new frequency, (2) tune the lock-in amplifier to twice the oscillator frequency, (3) adjust the phase angle such that the same signal introduced into both the reference and signal channels produced a null (quadrature condition), (4) adjust the applied voltage, (5) make measurement of quadrature component, (6) readjust phase for in-phase condition, (7) measure the in-phase voltage. Better measurements could often be made if the magnitude were measured by changing the phase to obtain a maximum and then by going back and measuring the phase separately. The lock-in amplifier was uncalibrated so that a separate calibration measurement had to be made to obtain the alternating component in terms of voltages.

After a complete set of data was obtained, a recheck of some of the first data points was made to assure that the material had not changed because of degradation. In a number of the earlier attempts, these rechecks resulted in rejection of the data and repetition of

the measurements.

Another check was made on each of the materials to assure that the measured signal was due to birefringence and not to light intensity variation. This was accomplished by rotating the analyzing prism through 90° and remeasuring the signal. The sign of that part of the signal which was due to birefringence changed, but not that part of the signal which was due to light intensity fluctuations. All of the materials reported in this thesis were found to have negligible light intensity fluctuation contributions. However, in some earlier measurements on TMV taken before final purification, the light intensity fluctuation contribution was as large as 15 per cent of the total signal at low frequencies.

Reduction of Data

A complete reduction of the data to the basic quantities of the theory is not possible without additional measurements of the macromolecular solutions by other methods and additional knowledge about the solvent and its interaction with the macromolecules. Therefore a method of reduction had to be devised which would present results in terms of quantities that others could easily determine from their own measurements and which could be easily related to the basic quantities of the theory if enough information were available. One such scheme can be derived from the constants usually assigned to the Kerr effect.

$$\Delta n = K E^2 = K_{sp} c E^2 \quad , \qquad \text{(III-5)}$$

where K is the Kerr constant, K_{sp} the specific Kerr constant and c the concentration of solute. The specific Kerr constant

has been defined (44) in two ways. The first is the weight specific Kerr constant where C is the weight of solute divided by the weight of solution. The second is the volume specific Kerr constant where C is the volume of solute divided by volume of solution. For the purposes of this thesis the weight specific Kerr constant will be used. Equation (III-5) is applicable in the case of a constant electric field. For the alternating field case a similar form must be adopted which would better fit the theory. Such a form is

$$\Delta n = \left\{ K_{s1} \left[\frac{1}{1+(\omega/2D)^2} + \frac{\cos(2\omega t - \delta_1 - \delta_2)}{((1+(\omega/2D)^2)(1+(\omega/3D)^2)^{1/2}} \right] + K_{s2} \left[1 + \frac{\cos(2\omega t - \delta_2)}{(1+(\omega/3D)^2)^{1/2}} \right] \right\} C E_o^2 \quad , \tag{III-6}$$

where K_{s1} is the specific Kerr constant associated with the permanent moment, K_{s2} is the Kerr constant associated with the induced moment and E is defined by the equation

$$E = E_o \cos(\omega t) \quad , \tag{III-7}$$

where E is the applied field in abvolts per cm. Equation (III-6) describes the response if C, E_o, K_{s1}, K_{s2} and D are known. In terms of theoretical quantities as given in equation (II-56)

$$cK_{s1} = \frac{4\pi^2}{h} N (g_1 - g_2) \frac{1}{15} \beta^2 \quad , \tag{III-8}$$

and

$$cK_{s2} = \frac{4\pi^2}{n} N(g_1 - g_2)\frac{1}{15}\gamma^2 \quad . \tag{III-9}$$

The photoresponse is

$$e = e_0 + e_1 + e_2 \cos(2\omega t - \delta), \tag{III-10}$$

where e is the total voltage appearing at the photomultiplier output, e_0 is the photovoltage when $\Delta n = 0$, e_1 is the D.C. voltage change when a signal is applied to the electro-optic cell and e_2 is the peak value of the alternating component of the photovoltage. Considering equation (III-6), equation (III-3) and equation (III-4) one obtains

$$\frac{e_1}{e_0} = \frac{2\pi L}{\lambda}\left\{K_{s1}\frac{1}{1+(\omega/3D)^2} + K_{s2}\right\} cE_0^2, \tag{III-11}$$

and

$$\frac{e_2\cos(2\omega t-\delta)}{e_0} = \frac{2\pi L}{\lambda}\left\{K_{s1}\frac{\cos(2\omega t-\delta_1-\delta_2)}{[(1+(\omega/2D)^2)(1+(\omega/3D)^2)]^{1/2}}\right.$$

$$\left. + K_{s2}\frac{\cos(2\omega t-\delta_2)}{[1+(\omega/3D)^2]^{1/2}}\right\} cE_0^2 \quad . \tag{III-12}$$

As ω approaches zero, δ, δ_1 and δ_2 approach zero, making the cosine terms approach one. Thus the low frequency limits of equations (III-11) and (III-12) become

$$\left(\frac{e_2}{e_0}\right)_{\omega\to 0} = \left(\frac{e_1}{e_0}\right)_{\omega\to 0} = \frac{2\pi L}{\lambda}\left(K_{s1} + K_{s2}\right) c E_0^2$$

$$= \frac{2\pi L}{\lambda} K_s \, c E_0^2 \quad . \qquad \text{(III-13)}$$

In the high frequency limit they become

$$\left(\frac{e_2}{e_0}\right)_{\omega\to\infty} = 0 \quad , \qquad \text{(III-14)}$$

and

$$\left(\frac{e_1}{e_0}\right)_{\omega\to\infty} = \frac{2\pi L}{\lambda} K_{s2} \, c E_0^2 \quad . \qquad \text{(III-15)}$$

Thus for a given measurement the specific Kerr constants can be determined by

$$K_{s2} = \left(\frac{e_1}{e_0}\right)_{\omega\to\infty} \frac{\lambda}{2\pi L c E^2} \quad , \qquad \text{(III-16)}$$

$$K_s = \left(\frac{e_1}{e_0}\right)_{\omega\to 0} \frac{\lambda}{2\pi L c E^2} \quad , \qquad \text{(III-17)}$$

and

$$K_{s1} = K_s - K_{s2} \quad . \qquad \text{(III-18)}$$

For a monodisperse medium the D value may be obtained by finding the point halfway between the high frequency limit and the low

frequency limit (f_o). That is, if

$$\frac{1}{1 + (\omega_o / 2D_o)^2} = \frac{1}{2} \quad , \tag{III-19}$$

then

$$2D_o = \omega_o \quad , \tag{III-20}$$

or

$$D_o = \pi f_o \quad . \tag{III-21}$$

Even if the material is polydisperse such a method is a consistent way of determining an average D value.

In addition, a rough measure of polydispersity can be obtained by making determinations of D at two other points. If these points are arbitrarily taken to be 1/5 and 4/5 of the values between the high and low frequency limits of the steady component data, then at these points

$$\frac{1}{1 + (\omega_o / 2D_1)^2} = \frac{1}{5} \quad , \tag{III-22}$$

or

$$D_1 = 2\pi f_1 \quad , \tag{III-23}$$

and

$$\frac{1}{1 + (\omega/2D_2)^2} = \frac{4}{5} \quad , \tag{III-24}$$

or

$$D_2 = \frac{1}{2}\pi f_2 \quad . \tag{III-25}$$

In the next chapter this rough determination will be compared to an actual polydispersity of one case.

The formalism for determining the values of K_{s1}, K_{s2} and K_s should not be affected by polydispersity since only the high and low frequency limits of the data are used. Further reduction could occur only if the values N and $(g_1 - g_2)$ were known. These could be determined by flow birefringence measurements.

For convenience in presenting the frequency dependent part of the data, the steady component and the alternating component will be normalized by dividing by the low frequency limit of the steady component. Such a procedure puts the data in a form that is easily compared with the theoretical curves in Figures 2, 3 and 4. This normalization in no way affects the phase angle which is already in a convenient form for comparison with theory.

CHAPTER IV

EFFECTS OF POLYDISPERSITY

The effect of polydispersity in a sample is easy to determine only if the polydispersity is known. In this chapter an example of a polydispersity analysis will be given and a synthesis of the results expected for the determined polydispersity will be made to check the results. The material used for the example is Baymal. The analysis will be divided into sections on the determination of polydispersity from the steady component of birefringency, a synthesis of the expected results of that polydispersity and a discussion of possible variations of other parameters.

Preparation of Baymal

Baymal is the trade name of a colloidal alumina produced by the E.I. DuPont de Nemours Company and is supplied in the form of a dry powder. A further description of the material is given in Chapter V.

The sample was prepared as follows: (1) a slurry of the Baymal powder was made at a concentration of 20 per cent in 2 per cent nitric acid and was allowed to stand for 24 hours; (2) the resulting sol was then diluted to 4 per cent and blended in a Waring blender for 15 minutes; (3) the solution was then dialyzed against deionized water for 19 days and filtered through a 3 micron millipore filter to remove dust particles; (4) concentration was determined by drying a weighed

sample of the solution in an 80° oven for approximately 4 hours and weighing the residue; (5) the solution concentration was then lowered to 0.3 per cent by adding deionized water.

The resistivity of the solution was approximately 1.8×10^4 ohm-cm. and the pH was 5.5. The conductivity is approximate because at the time the data was taken silicone rubber was used to attach the windows to the cell and this was a source of ionic contamination.

The data was taken as described in Chapter III, and is shown in Figure 11. The steady component was analyzed for polydispersity as described below.

Polydispersity Analysis

The steady component data was chosen as the basis for the polydispersity analysis because the form of the theoretical equations for the steady state is the same for all values of P. The frequency variable part of that equation can be analyzed for polydispersity with respect to D independently of any polydispersity of P.

The method employed to make this analysis is a specialization of the method described by Barlow and Lamb (1). The method consists of approximating the polydispersity by the slope of the birefringence. The theoretical form of this method will be developed and then related to the electro-optic response.

Suppose that an equation

$$I(\ln \omega) = \int_{-\infty}^{\infty} W(\ln \tau) \frac{1}{1+(\omega\tau)^2} \, d(\ln \tau) \qquad \text{(IV-1)}$$

is to be analyzed for $W(\ln \tau)$ given $I(\ln \omega)$. The term

Figure 11: Electro-Optic Response of 0.3 Per Cent Baymal No.1. The best monodisperse fit is represented by dashed lines and the polydisperse fit for constant P is represented by the solid lines. The dimensions of D and frequency are both $sec.^{-1}$.

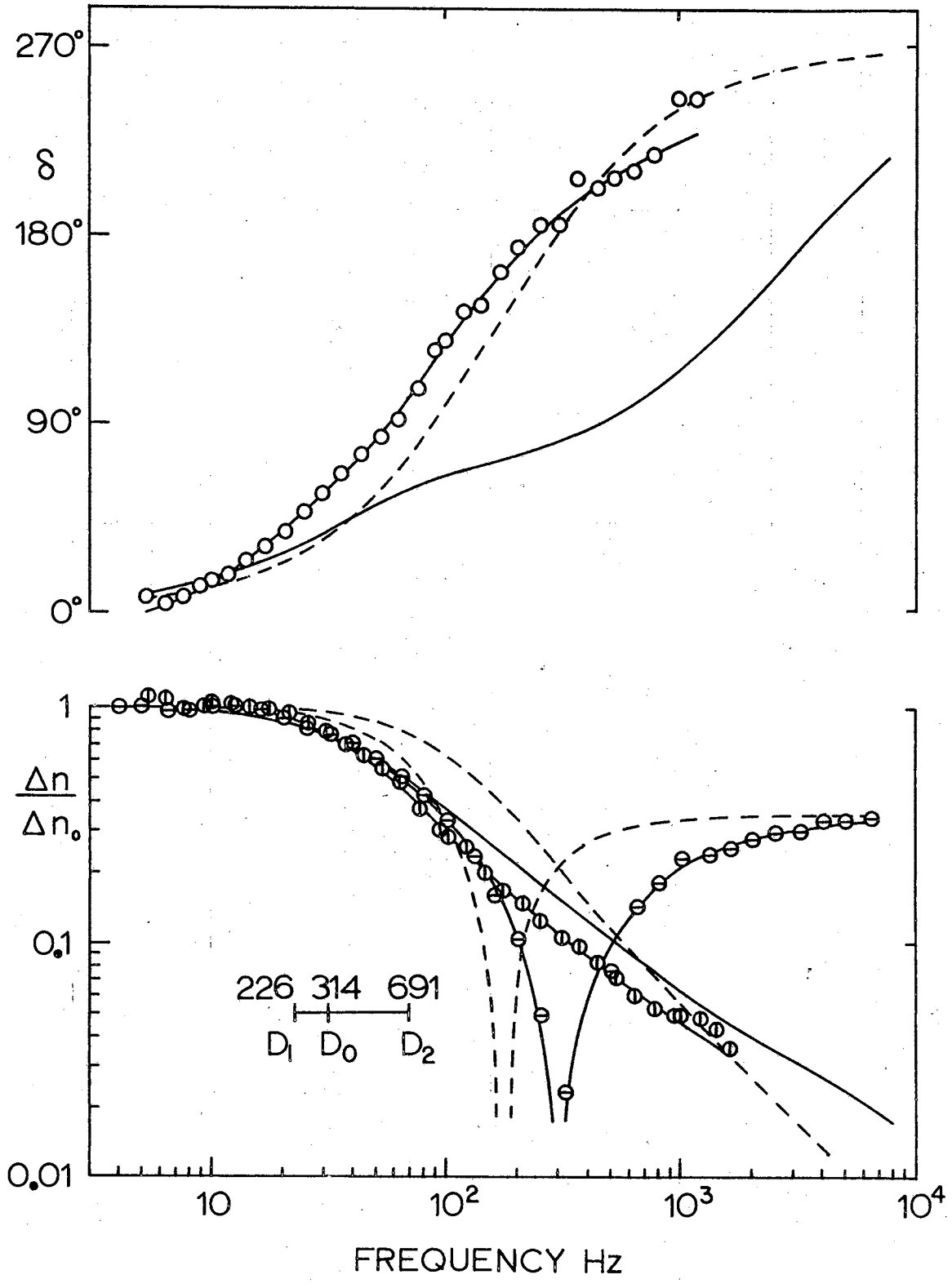
270°
δ
180°
90°
0°
1
Δn
Δn₀
0.1
0.01
226 314 691
D1 D0 D2
10
10²
10³
10⁴
FREQUENCY Hz

$W(\ln\tau)$ can be described as a distribution function over $\ln\tau$ of the expression $\frac{1}{1+(\omega\tau)^2}$. An approximate solution may be obtained by substituting a step function for $\frac{1}{1+(\omega\tau)^2}$. That is, if $\omega\tau<1$ then $\frac{1}{1+(\omega\tau)^2}$ will be approximated by 1 and if $\omega\tau>1$, by 0. Thus equation (IV-1) becomes

$$I(\ln\omega) \simeq \int_{-\infty}^{\ln\tau'} W(\ln\tau)\, d(\ln\tau) \quad . \qquad \text{(IV-2)}$$

$\ln\tau'$ is determined by $\omega\tau'=1$. Differentiation with respect to $\ln\tau'$ produces

$$\frac{dI(\ln\omega)}{d(\ln\omega)} = \frac{dI(\ln\omega)}{d(\ln\tau')}\,\frac{d(\ln\tau')}{d(\ln\omega)} = -W(\ln\tau'). \qquad \text{(IV-3)}$$

Thus the result obtained is that a first approximation to the distribution function is the negative of the slope of the function $I(\ln\omega)$. From equation (IV-1) it can be determined that the effect of $W(\ln\tau)$ on $I(\ln\omega)$ is additive. The second approximation may be made by recalculating a function I' using equation (IV-1) and using the procedure outlined above for finding the distribution function of the difference between the original function and the recalculated function. The second approximation to the distribution function is then the sum of the two distribution functions obtained. This procedure may be repeated as many times as desired. However the procedure does not quickly converge to the desired answer.

The form of the steady component of the electro-optic effect is given by

$$\Delta n = \Delta n_o \left(P + \frac{1}{1+(\omega\tau)^2} \right) , \qquad \text{(IV-4)}$$

where

$$\tau = 1/2D . \qquad \text{(IV-5)}$$

If there are m discrete species of molecules then

$$\Delta n = \sum_{i=1}^{m} \Delta n_o W_i \left(P_i + \frac{1}{1+(\omega\tau_i)^2} \right) . \qquad \text{(IV-6)}$$

If a continuous spectrum of such species is present then

$$\Delta n = \sum_{i=1}^{m} \Delta n_o W(\tau_i) \left(P(\tau_i) + \frac{1}{1+(\omega\tau_i)^2} \right) d\tau_i , \qquad \text{(IV-7)}$$

where the intervals $d\tau_i$ neither overlap nor leave gaps in the values of τ .

The data was taken in approximately equal logrithmic steps. The values τ_i and $d\tau_i$ are completely general in equation (IV-7) and could easily represent logrithmic steps in τ . However, it is convenient to rewrite the equation in terms of $\ln \tau_i$ instead of τ_i .

$$\Delta n = \sum_{i=1}^{m} \Delta n_o W(\ln\tau_i) \left(P(\ln\tau_i) + \frac{1}{1+(\omega\tau_i)^2} \right) d(\ln\tau_i) . \qquad \text{(IV-8)}$$

The equation is still completely general, but the functions W and P are redefined to give the same values for the argument $\ln\tau_i$

as for τ_i in equation (IV-7). In the limit as m becomes very large and $d(\ln \tau_i)$ very small equation (IV-8) becomes

$$\Delta n = \int_{-\infty}^{\infty} \Delta n_o W(\ln \tau) \left[P(\ln \tau) + \frac{1}{1+(\omega\tau)^2} \right] d(\ln \tau) . \quad \text{(IV-9)}$$

The two terms in brackets may be separated to give

$$\Delta n = \int_{-\infty}^{\infty} \Delta n_o W(\ln \tau)\, P(\ln \tau)\, d(\ln \tau) + \int_{-\infty}^{\infty} \Delta n_o W(\ln \tau) \frac{1}{1+(\omega\tau)^2}\, d(\ln \tau) . \quad \text{(IV-10)}$$

The first integral is a constant with respect to ω, and is $\Delta n_o P$. Thus

$$\Delta n - \Delta n_o P = \int_{-\infty}^{\infty} \Delta n_o W(\ln \tau) \frac{1}{1+(\omega\tau)^2} d(\ln \tau) \quad \text{(IV-11)}$$

which is an equation of the form of equation (IV-1).

The program "PLYDIX", found in Appendix B, was used to calculate the distribution function as described above. Using this program, the calculated distribution function for a set of "perfect" data did not change significantly after the eighth approximation. The half width resolution of the distribution function was about one-sixth of a decade after eight approximations.

Data obtained by measuring the Baymal sample was plotted and a smooth line drawn through the plotted points. Points were taken from this line at one twenty-fifth decade intervals. These points were then

the input to the program "PLYDIX". The results of the calculations using this program are shown in Figure 12. The results are plotted as a function of D rather than as a function of τ because it is then possible to compare the polydispersity directly with the data. This was helpful in visualizing the effect of the polydispersity on the sample. The one to one functional relationship between τ and D necessary for the transformation is given in equation (IV-5). A recalculation of the electro-optic response using these points did not produce an accurate retrace on any of the response curves. Several similar distribution functions were tried. The one which eventually was most successful in fitting the steady component is shown in Figure 11 as the solid line.

The values of D_1, D_0 and D_2 for this sample are also plotted on the same graph. The spacing of these values is very much less than the actual spread in the values of the polydispersity, but these three values do illustrate the approximate D value and the skewness of the polydispersity.

Figure 10 shows the data and recalculated curves with the value of P assumed to be constant for all the species of particles present. The fit of the data to the steady component curve is very good. However, the alternating component and phase angle data fit the monodisperse curves better than the polydisperse curves.

Polydispersity of P

The poor fit of the alternating component and phase angle may be due to the use of a constant P rather than one which varies with D. That is, it is probable that the P_i of equation (IV-6) would vary

Figure 12: The Calculated Polydispersity and a Polydispersity Producing a Better Fit Between the Steady Component Theory and Data. The points connected by dashed lines and having vertical bars are the calculated points and those connected by the solid line and having horizontal bars are the polydispersity values producing the best fit.

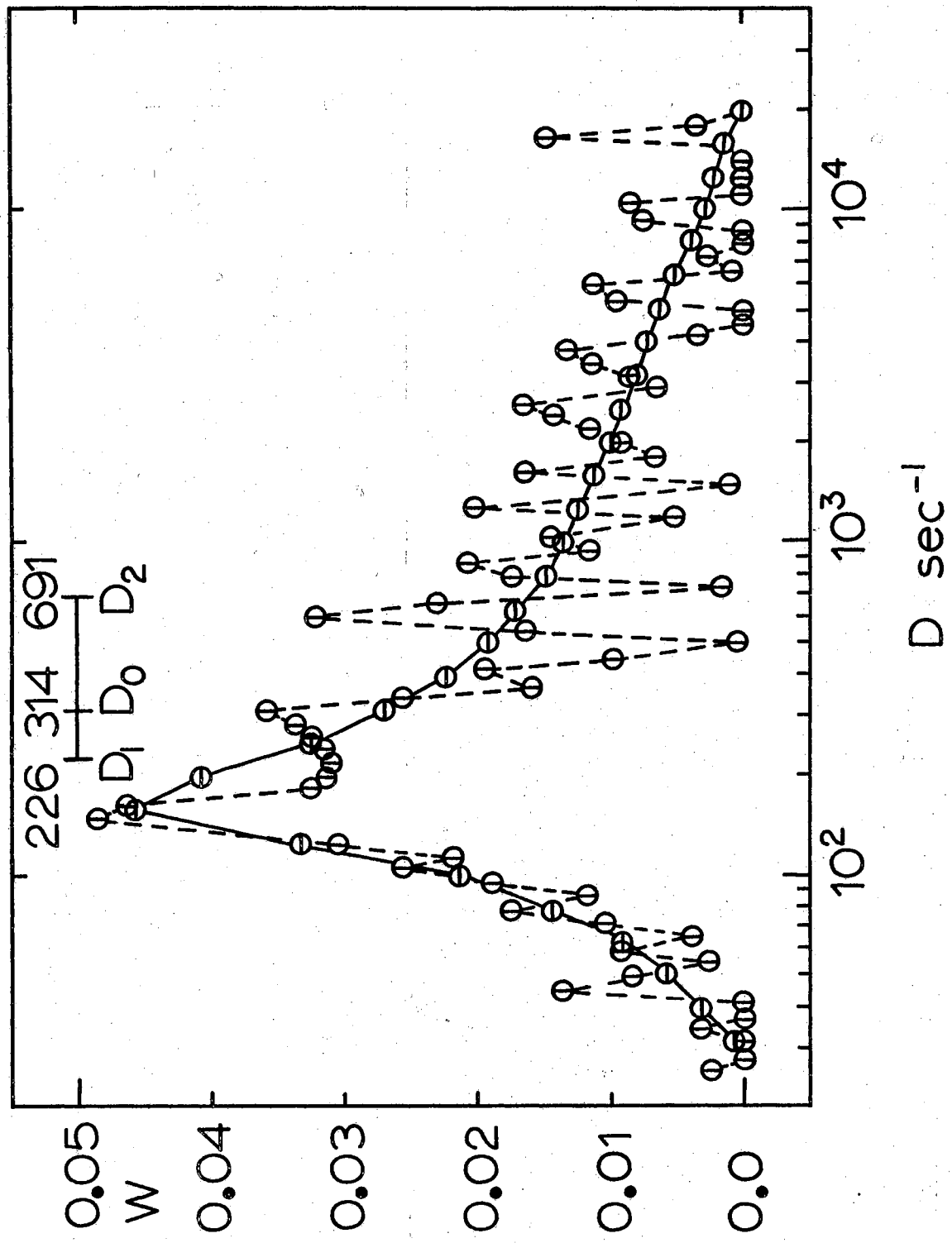
0.05
W
0.04
0.03
0.02
0.01
0.0
10^2
10^3
10^4
D sec^{-1}
226 314 691
D_1 D_0 D_2

as some function of D or τ . A method of analyzing the data for such a variation in P may be possible, but it would be quite involved since two functions would have to be determined simultaneously. However, a synthesis of a curve given a polydispersity of D and a variation of P as a function of D as in equation (IV-10) is possible. The program "POLYP" was written to do this. Using this program, reasonable approximations may be made of variations of P with D and the resultant curves may be calculated. The equations used to perform this calculation are for the steady component

$$\frac{\Delta n_{st}}{\Delta n_0} = \sum_{i=1}^{m} W_i \left(P_i + \frac{i}{1+(\omega/2D_i)^2} \right) , \qquad \text{(IV-12)}$$

for the out of phase component

$$\frac{\Delta n''_{alt}}{\Delta n_0} = \sum_{i=1}^{m} W_i \left[\frac{-\omega/2D_i - \omega/3D_i}{(1+(\omega/2D_i)^2)(1+(\omega/3D_i)^2} \right. \qquad \text{(IV-13)}$$

$$\left. - P_i \frac{\omega/3D_i}{1+(\omega/3D_i)^2} \right] ,$$

and for the in phase components

$$\frac{\Delta n'_{alt}}{\Delta n_0} = \sum W_i \left[\frac{1 - \omega^2/6 D_i^2}{(1+(\omega/2D_i)^2)(1+(\omega/3D_i)^2)} \right.$$

$$\left. + P_i \frac{1}{1+(\omega/3D_i)^2} \right] . \qquad \text{(IV-14)}$$

The alternating component and phase angle were calculated from the in

and out of phase components by

$$\frac{\Delta n_{alt}}{\Delta n_0} = \left[\left(\frac{\Delta n'_{alt}}{\Delta n_0} \right)^2 + \left(\frac{\Delta n''_{alt}}{\Delta n_0} \right)^2 \right]^{1/2} , \qquad \text{(IV-15)}$$

and

$$\delta = \tan^{-1} \left(\frac{\Delta n''}{\Delta n_0} \Big/ \frac{\Delta n'}{\Delta n_0} \right) . \qquad \text{(IV-16)}$$

Figure 13 illustrates the variations that may be possible in the alternating component and phase angle with variations in the value of P as a function of D. In these cases the average value of P as defined by (IV-10) and (IV-11) is held constant even though P is a function of D. The cases selected show that such variation produces a better fit to the data. In one case the phase angle fit is very much closer at the expense of the alternating component fit. In another case both components are closer. These are compared with the constant P case and the data.

Frequency Dependence of P

The possibility that the poor fit between the data and the phase angle and alternating component was due to a frequency dependence in P was considered. Two computer programs, "SEP" and "ALL" were written to analyze the data for the functions $f(\omega)$ and $\phi(\omega)$ as in equation (II-67) and to then synthesize the magnitude, phase angle, and steady component from known polydispersity and P functions. That is, functions were calculated which would force the alternating component and phase angle to fit the data. This was done for the case

Figure 13: The Effect of Variation of P Upon the Phase Angle and Alternating Components of the Electro-Optic Response as Calculated for a Case Having the Steady Component of Baymal No.1. Curve 1 is an approximation of the data for Baymal No.1, curve 2 is a special case of a P variation which brings the phase angle in sharply, curve 3 is a special case of P variation which brings both phase angle and alternating component nearer to the data and curve 4 is the case of no variation in the P value.

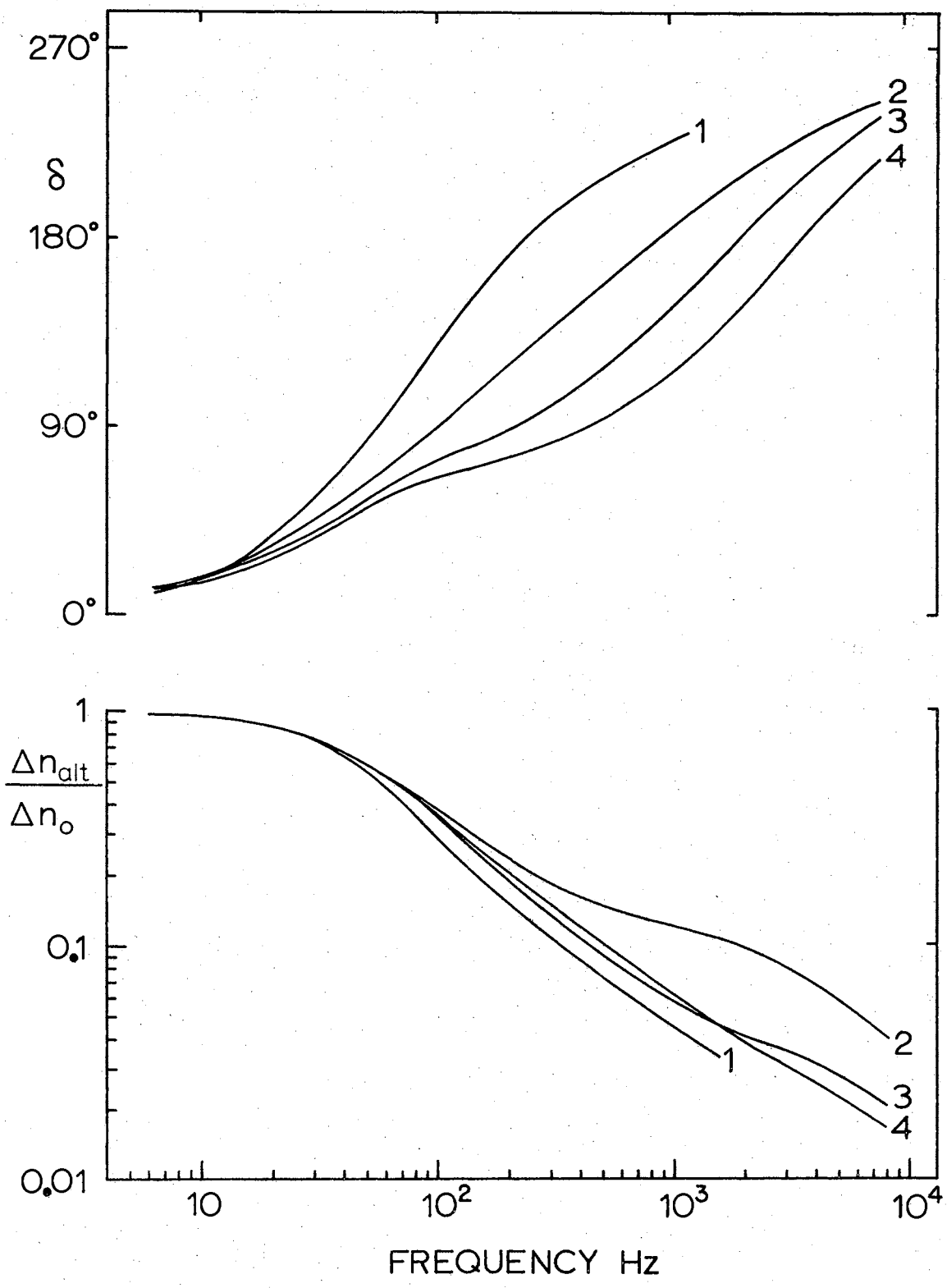
270°
δ
180°
90°
0°
1
2
3
4
1
$\frac{\Delta n_{alt}}{\Delta n_o}$
0,1
0,01
10
10^2
10^3
10^4
FREQUENCY Hz

of the polydispersity as determined from the steady component and for several examples with a single value of D. In all examples the functions $f(\omega)$ had values of greater than one over much of the frequency range. The $\phi(\omega)$ functions had both positive and negative values. In all cases a recalculation of the steady component produced a curve that was not significantly related to the data. That is, the general character of the curve was destroyed.

It was therefore concluded that a frequency dependence was probably not the reason for the discrepancy and this approach was abandoned.

Discussion

By using the procedure outlined earlier in this chapter, a dispersity function can be determined which produces a very good fit of the steady component data. This fit, however, is independent of variations in the value of P with D. Functional variations of P were found which produced a closer fit to the alternating component and phase angle of the data, but because this was not an exact procedure, a good fit was not obtained.

For the case presented the steady component approached a finite value in the high frequency limit, while the alternating component became very small with increasing frequency. Thus, changes in the polydispersity function, expecially in the higher values of D, had relatively little effect upon the steady component compared to the effect they had upon the alternating component and the phase angle, especially at the higher frequencies.

Since the discrepancy was greatest at higher frequencies, and because of the relatively greater sensitivity of the alternating

component to changes in polydispersity and variation in P, there may exist a combination of a slightly different polydispersity function and a variation in P with D (not necessarily a unique combination) that would provide a very good fit of all three of the response curves.

The attempt to produce a better fit by considering the possibility of a frequency dependent P was not successful. The other approaches attempted appeared to be more promising for the data examined in this case. There is no other evidence to support the idea that there is a frequency dependence in the low frequency range. However, the results do not conclusively indicate that the frequency dependence is trivial (that is, $f(\omega)=1$ and $\phi(\omega)=0$ for all ω). Also, because of the strong evidence of frequency dependence at higher frequencies presented in Chapter VI, this approach may well be fruitful for materials not considered in this thesis.

CHAPTER V

COMPARISON OF THE GENERAL CHARACTER OF DATA WITH THEORY FOR FOUR MATERIALS

In this chapter four materials will be compared to the theory for the electro-optic effect to demonstrate the agreement in general character between data for a variety of materials and the theory. In addition, the physical constants of the materials will be calculated for these materials as discussed in Chapter III.

Each of the materials will be discussed in turn as to the preparation procedure, details of the measurement and results of frequency dependent measurements. The results of field and concentration dependency tests will be discussed, and finally, the constants which can be calculated from the data will be presented in tabular form and general conclusions will be drawn.

Tobacco Mosaic Virus

Tobacco mosaic virus (TMV) is a plant virus which may be grown on the leaf of the tobacco plant. The TMV particle is a rod about 3000 Å long and 149 Å in diameter with a molecular weight of 39×10^6 (7). The sample of TMV was supplied by Dr. E. Basler in the form of a crude sap in a phosphate buffer. It had been grown on the tobacco leaves followed by crushing the infected leaves in a 0.5M phosphate buffer. A single low speed centrifugation had been used to separate the fibrous mass of the plant leaf from the sap.

The sample was further processed after receipt according to the method of Boedtker and Simmons (7). The concentration of the sample was determined by drying a portion of TMV in an oven at 40°C and weighing the residue. The sample was then diluted to 0.1% by weight.

Measurements were made on the TMV sample in the large electro-optic cell according to the procedure outlined in Chapter III. The conditions of measurement are listed in Table I along with the conditions of measurement for the other materials. The data is presented in Figure 14 along with the monodisperse fit. This particular case will require some further explanation.

In Chapter III a method of determining an average value of D was presented, based on the use of the frequency dependence of the steady component. In TMV the steady component is almost non-varying with frequency over the low frequency range. There is a very small rise as the frequency is increased, but it is not enough to accurately determine a center frequency. Therefore the alternating component was used to determine the average value of D assuming a value of $P = \infty$. This value of D was then used to recalculate a curve but with a P value of -8. The resulting fit is rather good. The general character of the data fits the theory in that the high frequency and low frequency behavior of all components is correct. The data falls at or near the theoretically expected values just about everywhere and the general character of deviation from the theoretical curve is a dispersion of the response over a wider frequency range. This is the type of variation expected to be produced by a slight polydispersity of the sample.

One important disparity between the theory and the data is the difference in frequency between the expected rise in the steady

Figure 14: The Electro-Optic Response of 0.1 Per Cent TMV. The dashed curves represent the best monodisperse fit, the data with the horizontal bars represents the steady component, the data with the vertical bar, the alternating component and the open data circles, the phase angle.

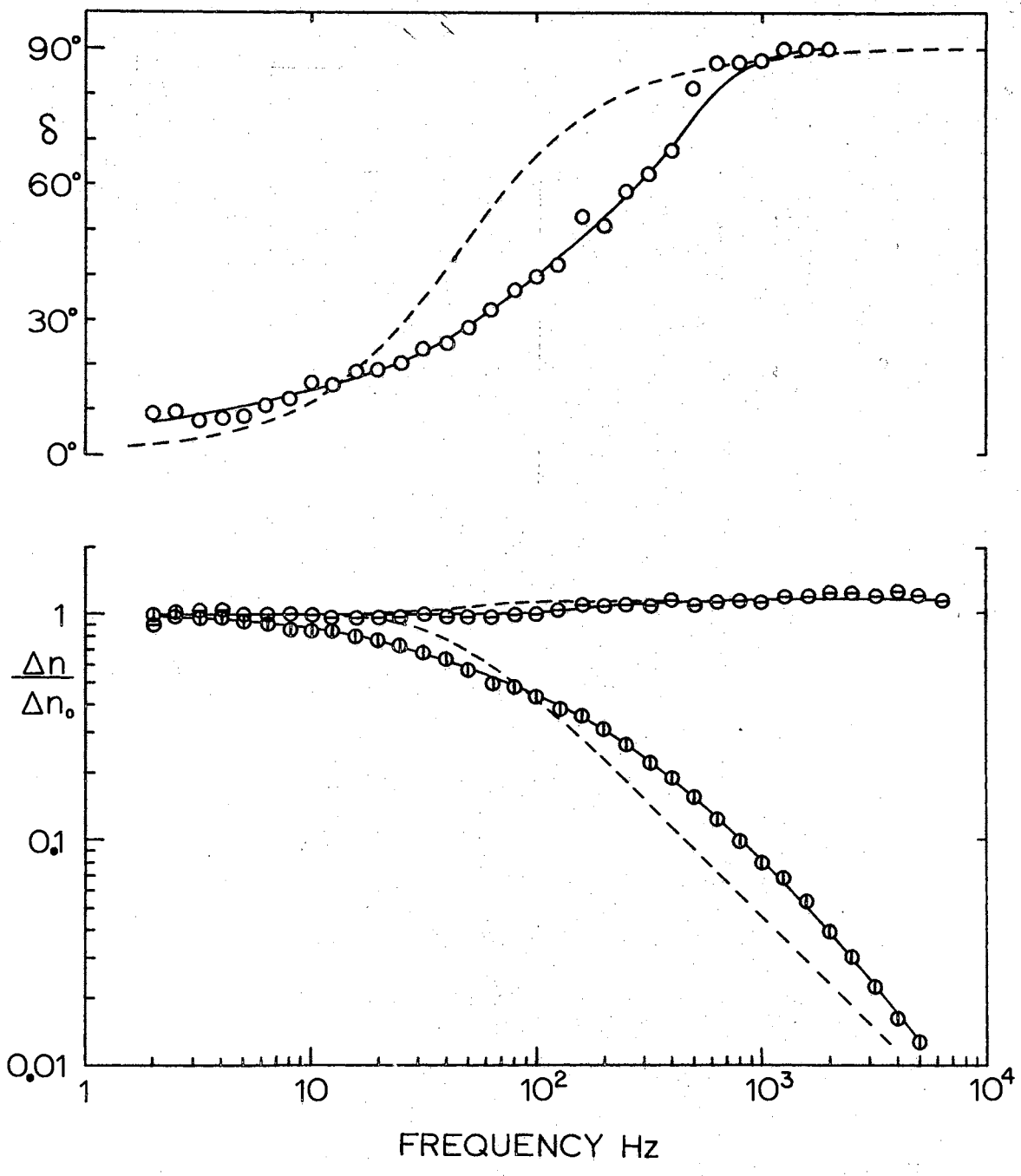
90°
δ
60°
30°
0°
1
Δn/Δn₀
0.1
0.01
1
10
10²
10³
10⁴
FREQUENCY Hz

component and the place where it actually occurs.

The rise in the steady component was consistent in all the TMV samples tested (these cases will be presented in Chapter VI). Careful tests using varying polarization conditions on the optical bench indicated that the rise was not attributable to any other electro-optic effect. The rise would normally be attributed to the presence of a permanent moment on the TMV molecule. However, since the rise is not correctly placed in frequency such a conclusion would have to be qualified.

Bentonite

The sample of Wyoming bentonite clay used was obtained from Central Scientific Company in 1945. Bentonite consists mostly of montmorellonite in a layered structure much like mica (66, 69). The sample was prepared from wet bentonite which had been in the laboratory for an undetermined length of time. The clay was placed in a Waring blender for 15 minutes. After blending the bentonite solution was placed in a jar and allowed to settle overnight. Most of the clay settled out at this stage. The remaining fluid was then centrifuged at 1500 times gravity for 45 minutes. The supernatant solution was then dialyzed in cellulose tubing against deionized water for 24 hours. The dialyzing water was agitated gently by placing the beaker in which dialysis was occuring on a rocking table assembly. The solution was placed in the large electro-optic cell and was measured under the conditions listed in Table I.

A graphical presentation of the data for this material is given in Figure 15 along with the curve for the best monodisperse fit as

TABLE I

SUMMARY OF EXPERIMENTAL CONDITIONS

Material	% Concentration By Weight	Resistivity ohm-cm	pH	E-O Cell	Field Strength (E_o) RMA V/cm	Field Measurement Method	
						Low Freq.	High Freq.
Baymal #1	0.3	18,700	5.50	S	26.3	Voltage* Across Cell	Voltage Across Cell
Baymal #2	0.2	3,753	5.05	L	9.5	Probes	"
Bentonite	0.331	1,813	7.05	L	4.0	Probes	"
Avicel	0.1	48,500	6.60	S	61.7	Current	"
TMV	0.1	16,250	6.50	L	39.12	Probes	"

All experiments were done at a temperature of 25°C.
* Checked by current through cell immediately after measurements.

Figure 15: The Electro-Optic Response of 0.331 Per Cent Bentonite. The dashed curves represent the best monodisperse fit, the data with the horizontal bars represents the steady component, the data with the vertical bar, the alternating component and the open data circles, the phase angle. The dimensions of D and frequency are both $sec.^{-1}$.

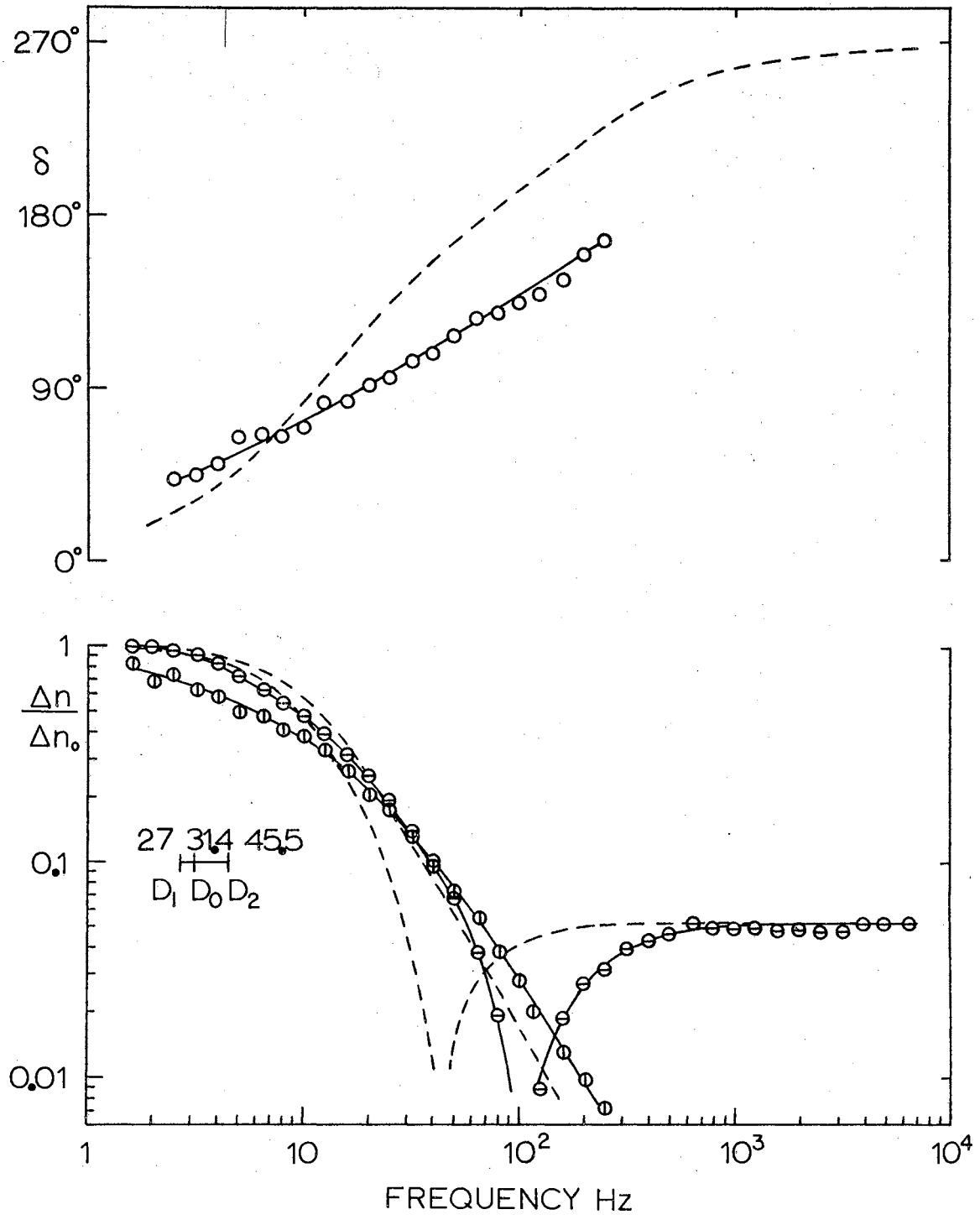
270°
δ
180°
90°
0°
1
Δn/Δn₀
0.1
0.01
27 314 455
D₁ D₀ D₂
1
10
10²
10³
10⁴
FREQUENCY Hz

determined from the average D value. Again the high and low frequency values show good agreement in character with the data and the difference in exactness of the fit could be attributed to polydispersity. The values of D_1, D_0, and D_2 indicate that the polydispersity is probably skewed with the greatest spread of D values to the right of the average value of D_0.

The largest spread of values of D, that is, the greatest polydispersity, is expected for this sample. According to Shaw and Hart (69) particle sizes in bentonite range from less than 0.5 microns to more than 50 microns. Apparently the preparation procedure was successful in separating out the largest particles. If the particles are discs, the diameter of the particles which have the value D_0 is 0.5 microns.

Baymal

Two samples of Baymal were prepared and data taken for both. The preparation procedures for the first sample (Baymal No. 1) is described in Chapter IV. The preparation procedure for Baymal No. 2 will be described in this section.

Baymal is the trade name for DuPont's colloidal alumina. The material consists of fibrils of boehmite alumina (AlOOH). The material comes in the form of a dry powder containing approximately 13 per cent acetic acid plus smaller amounts of other ionic materials (14). The powder readily disperses into water. The initial laboratory method of manufacturing the Baymal is described by Bugosh (9). The sample used was from lot 64-7.

The No. 1 sample of Baymal was prepared as described in DuPont's Product Bulletin (14) under "Sols of Maximum Clarity". The exact

procedure is described in Chapter IV.

Sample No. 2 was prepared by soaking a 20 per cent slurry of Baymal powder in 2 per cent nitric acid for about 40 hours, diluting and then mixing the Baymal into water using a low speed stirrer. The solution was then brought to a concentration of 4 per cent. The material was centrifuged for 2 hours at 2000 times gravity. The retained supernatant solution was then centrifuged for 15 minutes at 20,000 times gravity. The concentration of the resulting supernatant solution was .639 per cent, indicating that less than one-fifth of the Baymal solids remained. The solution was then diluted to 0.2 per cent.

Data was taken on both of the Baymal samples as described in Chapter III. The calculated physical constants of both samples are presented in Table I. Data for Baymal sample No. 1 is found in Figure 11 and for sample No. 2 in Figure 16 along with the monodisperse value fit for the D_o value.

Again in both of these samples the high and low frequency response shows good agreement in general character with the theoretical curves. The data also shows the greater frequency dispersion expected of a polydisperse sample. However, in the phase angle the fit is expected to spread out more to the right in cases where the total angular excursion is 270°. In the case of sample No. 1 the monodisperse fit is very much better than the polydisperse fit and the fit is similarly good in the case of sample No. 2.

The values of P and D_o are different for the two samples and the direction in which P is changing with D is the same as the direction assumed for the variation of P with D to obtain a better fit of theory and data for sample No. 1. This supports the

Figure 16: The Electro-Optic Response of 0.2 Per Cent Baymal No.2. The dashed curves represent the best monodisperse fit, the data with the horizontal bars represents the steady component, the data with the vertical bar, the alternating component and the open data circles, the phase angle. The dimensions of D and frequency are both $sec.^{-1}$.

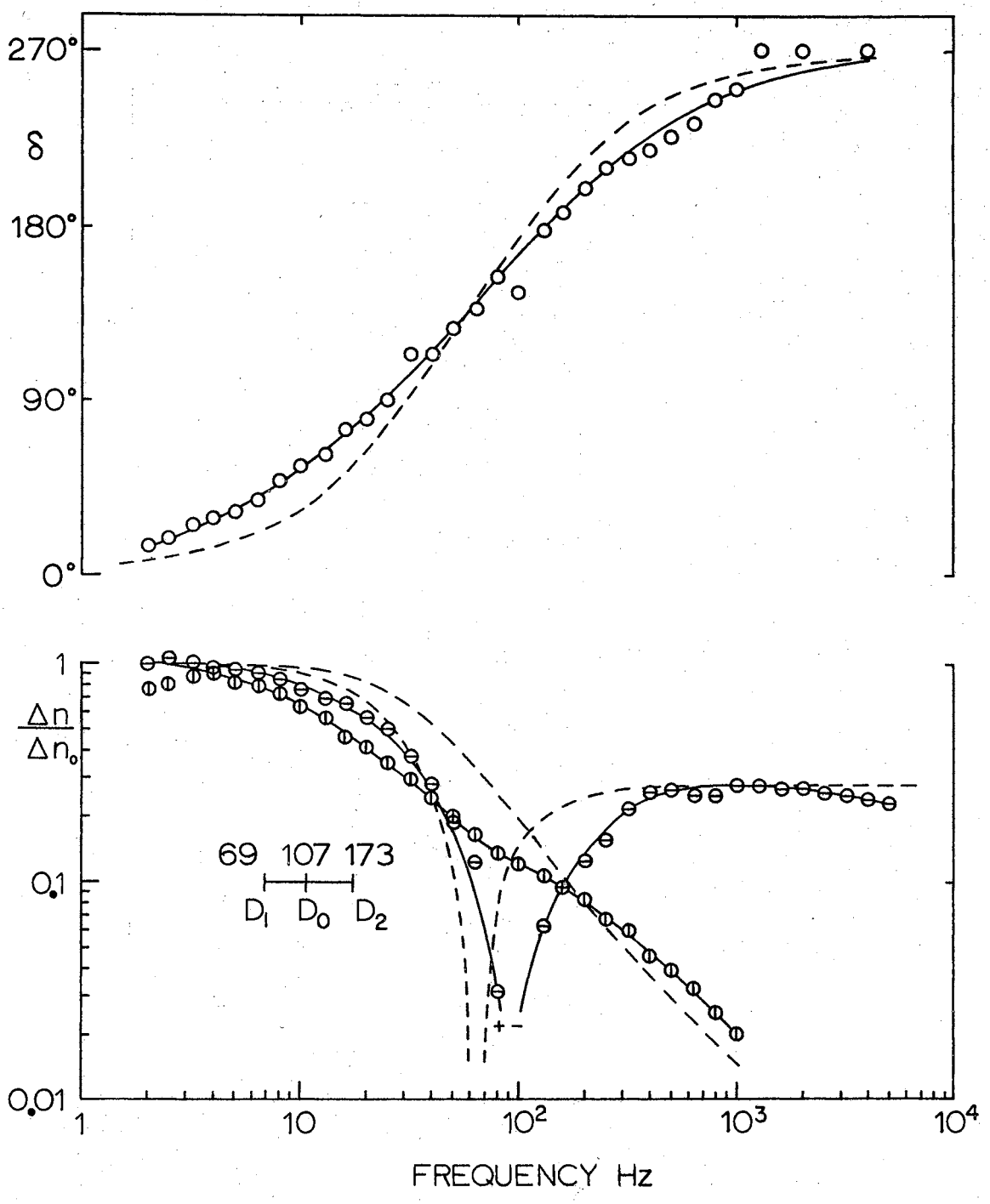
270°
δ
180°
90°
0°
1
Δn/Δn₀
0.1
0.01
69 107 173
D₁ D₀ D₂
1
10
10²
10³
10⁴
FREQUENCY Hz

idea that a properly chosen variation of P with D and a slightly altered polydispersity distribution function might provide a better fit to the data in case No. 1.

Avicel

Avicel is described (16) as a modified microcrystaline cellulose. It is a product of the FMC Corporation. A laboratory sample was supplied by the FMC Corporation and was designated by the company as Avicel-CM Technical grade. A product bulletin states that the Avicel powder supplied contains 11 per cent Sodium Carboxymethyl-cellulose to aid in dispersion and suspension.

A sample was prepared by blending the powder at 4 per cent by weight in a Waring blender in deionized water for 15 minutes. The material was then allowed to settle overnight. This removed very little of the material. The solution was lowered to a concentration of 1 per cent. At this stage the material was so turbid that a pencil could barely be seen through 3 cm. of fluid. The sample was centrifuged at 10,000 times gravity for 20 minutes. This seemed to remove very little material but did clear the solution considerably. The sample was then diluted to 0.1 per cent.

Data was taken as described in Chapter III under conditions described in Table I. The data is presented in Figure 17 along with the monodisperse curve for a particular D and P value chosen. The low frequency limiting values are off the graph somewhere to the left. The D value used for the recalculation of a monodisperse case was determined by estimating where the alternating and steady component curves might go and then determining the D value on the basis

Figure 17: The Electro-Optic Response of 0.1% Per Cent Avicell. The dashed curves representing the best monodisperse fit, the data with the horizontal bars represents the steady component, the data with the vertical bar, the alternating component and the open data circles, the phase angle.

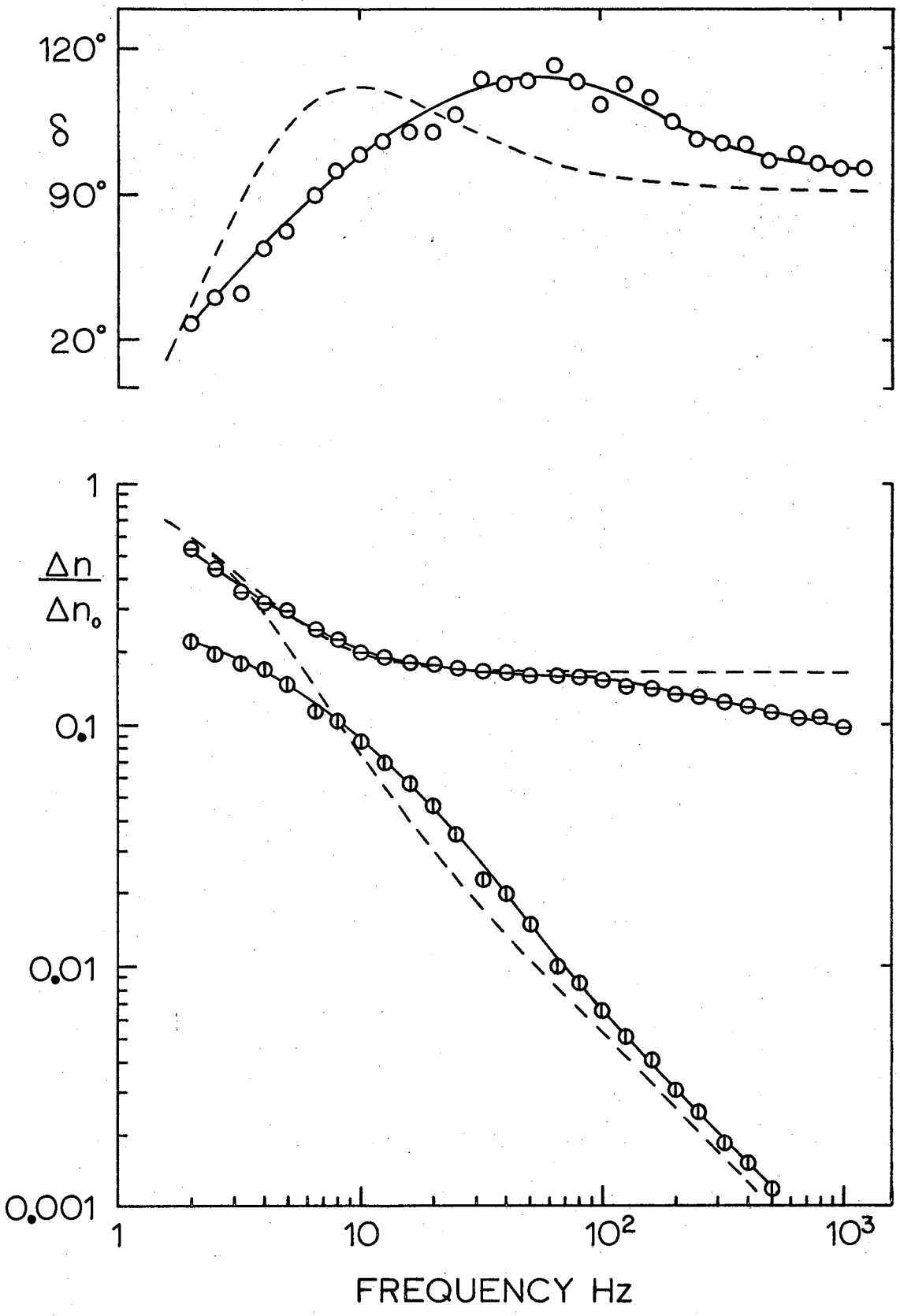
120°
δ
90°
20°
1
Δn
Δn₀
0.1
0.01
0.001
1
10
10²
10³
FREQUENCY Hz

TABLE II

EXPERIMENTAL ELECTRO-OPTIC FACTORS

Material	D_1 Sec. $^{-1}$	D_o Sec. $^{-1}$	D_2 Sec. $^{-1}$	$K_s \times 10^9$ cm^2/V^2	$K_{s1} \times 10^9$ cm^2/V^2	$K_{s2} \times 10^9$ cm^2/V^2	P
Baymal #1	226.0	314.00	691.0	1.222	1.606	-0.384	-0.260
Baymal #2	69.0	106.80	172.7	0.4205	0.5275	-0.1070	-0.219
Bentonite	27.0	31.40	45.5	46.36	48.54	-2.179	-0.0499
Avicel	-	6.54	-	-5.518	-4.595	-0.9228	+0.200
TMV	-	84.60	-	-1.530	0.263	-1.766	-8.00

of that. The P value then had to be chosen so that the curve fitted the steady component data at the higher frequencies. The phase angle data was valuable in this case for making estimates of the P and D values and extrapolating the curve to low frequency values.

The electro-optic response is of the general character expected for the P and D values chosen. The data in the case of the phase angle is to the right of the best fit monodisperse curve, but again for this value of P this is expected if the sample is polydisperse. As mentioned earlier, the phase angle is the most sensitive to changes in the value of P with D and to changes in polydispersity.

The greatest discrepancy between theory and data occurs at the low frequency end of the alternating component. No explanation is given to account for this, although it could be due to polydispersity.

This is an example of a case where the electro-optic effect can clearly determine that the relaxation mechanism is particle orientation-reorientation, even though the frequency dispersion cannot be measured in detail. Some discussion is found in the literature (76,60,44) concerning the interpretation of dielectric relaxation phenomena in which there is no positive means of separating particle relaxation mechanisms from purely electronic or ionic relaxation mechanisms.

Field and Concentration Dependence

The theory of the electro-optic effect predicts that the birefringence increases with the square of the electric field and directly with the concentration of the material. As a test of the theory an attempt was made to verify these predictions.

Each of the materials used was tested for dependency of the electro-optic effect on the field strength. The steady component was tested near the low frequency limit (except for Avicel), at some point in the frequency dispersion region and at some point in the high frequency limit. The alternating component was tested only at a point near the lower end of the frequency range. In all cases an E^2 dependence was found. That is, when the data was plotted on a logarithmic scale, a second power slope represented a best fit. For most materials the range of E over which measurements could be made was rather limited and few points were actually obtained. For Avicel, the possible range of measurement was the widest of any of the materials tested. Avicel could be measured over a range of E of about one and one-half decades on a logarithmic scale. In this case a large number of points were obtained. Unlike the other materials, the field for Avicel had to be kept below a certain value. In order that the birefringence be proportional to E^2, β^2 and γ^2 must be $<<$ 1. There is sufficient data in the literature to make a determination of these values only for the case of TMV. Using Jennings and Jerrard's data for TMV (29), the calculated value for β^2 is .014, and the value for γ^2, .025. Measurements made on TMV indicated that at a field strength of 79 V./cm., the response was still proportional to E^2. In Baymal No. 2 the response was still proportional to E^2 at 185 V./cm. and in bentonite at 10 V./cm. All of these values represent the highest field at which measurements could be made. In Avicel, measurements were made at field strengths up to 125 V./cm. but linearity was present only to about 65 V./cm.

Similar tests were conducted to determine the concentration

dependence, but these tests failed to produce the predicted results. Each sample was diluted with deionized water to produce several samples of different concentrations. Measurements were then made on these samples at the same frequency and voltage. This produced a different conductivity in each of the samples. In general, the optical retardation as a function of concentration was found to be less than first power. Apparently an increase in ionic concentration caused a decrease in Kerr constant. This was also noticed in the measurements of TMV shown in the next chapter, except for the case where the ions were removed from the atmosphere by exhaustive dialysis. No way was found to control precisely the conductivity of the solutions so that accurate measurements could be made of concentration dependence.

The birefringence is probably directly proportional to the concentration, but this cannot be accurately measured without very precise control of the ionic atmosphere of the macromolecules. Also, the birefringence is quite sensitive to changes in ionic atmosphere. The explanation for this can be found theoretically in O'Konski's treatment of induced moment mechanisms and also in the fact that the ions may mask permanent moments of the particles, reducing their role in the total Kerr constant.

Discussion

The general character of the electro-optic response agrees with the theory as developed in Chapter II. The four samples represent a considerable range in the values of P and the rather dramatic differences in the electro-optic response with varying values of P has been demonstrated (see Table II). A more precise fit between data and

theoretical curves could be obtained if a method of determining both the polydispersity and P as a function of rotary diffusion constant were available.

Of the four materials measured only two have been previously measured by the use of the electro-optic effect. O'Konski and Haltner (47) measured TMV and obtained values of D from about 80 sec.$^{-1}$ to 310 sec.$^{-1}$. The value obtained in this study and tabulated in Table II is 84.6 sec.$^{-1}$. This indicates possible dimerization of the TMV. The specific Kerr constant of -1.53×10^{-9} cm^2/V^2 obtained in this study compares with the value -6.9×10^{-9} cm^2/V^2 obtained by O'Konski and Haltner. This is due partly to a difference in the frequency of the light used in the study. The entire discrepancy between the two figures could be accounted for by the wide variation in Kerr constant with ionic strength which is demonstrated in Chapter VI.

The other sample which has been previously measured is bentonite. Using the measurements of Shah (66) a specific Kerr constant of 36.5×10^{-9} cm^2/V^2 is obtained, while in this study a constant of 46.36×10^{-9} cm^2/V^2 was obtained. The agreement here is very good, considering the differences in preparation procedure.

CHAPTER VI

POLARIZATION MECHANISMS AND HIGH FREQUENCY RESPONSE

In this chapter the approach to the problem of a frequency dependent induced moment contribution to the steady component of the electro-optic effect is discussed. First, the theoretical approach to this problem in the high frequency region is examined in general terms and in terms of a theory developed by O'Konski (44). Secondly, the four materials examined in the previous chapter are again examined with special emphasis placed on the high frequency steady component. The O'Konski approach to non-orientation polarization mechanisms will be considered along with the special case of the Maxwell-Wagner mechanism and compared to the data. Finally, the TMV will be considered as a special case and the temperature and conductivity dependence of the high frequency steady component will be explored.

A great deal of useful information could be derived if it were possible to make both the electro-optic measurements and dielectric measurements on the same material over the same frequency range. The theory developed by O'Konski to explain non-orientation polarization mechanisms is presented as a theory of dielectric effects and has been adapted to the electro-optic effect since polarizability terms occur in both the dielectric and electro-optic equations.

General Considerations

In Chapter IV the possibility of a frequency dependent variation in P, based upon a frequency dependency in the polarizability was briefly considered. In the low frequency range there was apparently no contribution from such a source. However, if the frequency range is extended to 10^6 Hz., a falling off of the steady component of the electro-optic effect is observed in all but one of the four materials described in Chapter V.

For the four materials investigated, the frequency range in which the particle actually moved in response to the variation of the electric field was exceeded. This was demonstrated by the decrease of the alternating component of the electro-optic effect to levels so low that they could not be measured with the available equipment. Thus at high frequencies orientation was due to the induced moment of the particle. The particle tended to stay relatively orientated (except for Brownian motion) while the moment changed sign with the field.

The addition to the theory described in the last part of Chapter II was presented to explain this high frequency behavior. The equations can be simplified because for all practical purposes the alternating component and the permanent moment contribution to the steady component of birefringence is no longer present. With the alternating component absent there is no longer a means of measuring $\phi(\omega)$. Thus, there remains only an equation which includes $f(\omega)$.

$$\Delta n = \frac{N}{n}\frac{\pi}{15}(g_1 - g_2)\gamma^2 f(\omega) . \qquad \text{(VI-1)}$$

If the special case of a mechanism such as the Maxwell-Wagner effect or

the combined effects described by O'Konski is adopted, the equation becomes

$$\Delta n = \frac{N}{n}\frac{\pi}{15}(g_1-g_2)\gamma^2\frac{1}{(1+(\omega\tau)^2)^{1/2}}, \quad \text{(VI-2)}$$

where the value τ is that described by equation (II-68). According to equation (VI-2) the rate at which the steady component of birefringence can decrease has a maximum limit of $1/\omega$.

The polarization mechanisms which are mentioned by O'Konski include the mobility of ions in the diffuse double layer surrounding the molecule, an idea introduced by Smoluchowski (72), and the mobile proton of Kirkwood and Shumaker (34), in addition to the Maxwell-Wagner effect as presented by Fricke (21). However, any mechanism which produces a conductivity very near the surface of the molecule, and is different from the conductivity of the surrounding medium, is accounted for in this theory. Such a surface conductivity is demonstrated by O'Konski to be equivalent to a volume conductivity of the molecule.

High Frequency Steady Component Data

The high frequency steady component values of electro-optic effect for the four materials discussed in the previous chapter are shown in Figure 18. The data is shown for the frequency range of 1 Hz. to 10^6 Hz. and is normalized to the low frequency values. These cases will be discussed briefly before they are considered in more detail.

The bentonite data illustrates the result expected for a case where there is no non-orientation relaxation mechanism. With increasing frequency the particle goes through the orientation-reorientation

Figure 18: The High Frequency Steady Component of 0.1 Per Cent TMV, 0.2 Per Cent Baymal No.2, 0.331 Per Cent Bentonite and 0.1 Per Cent Avicel.

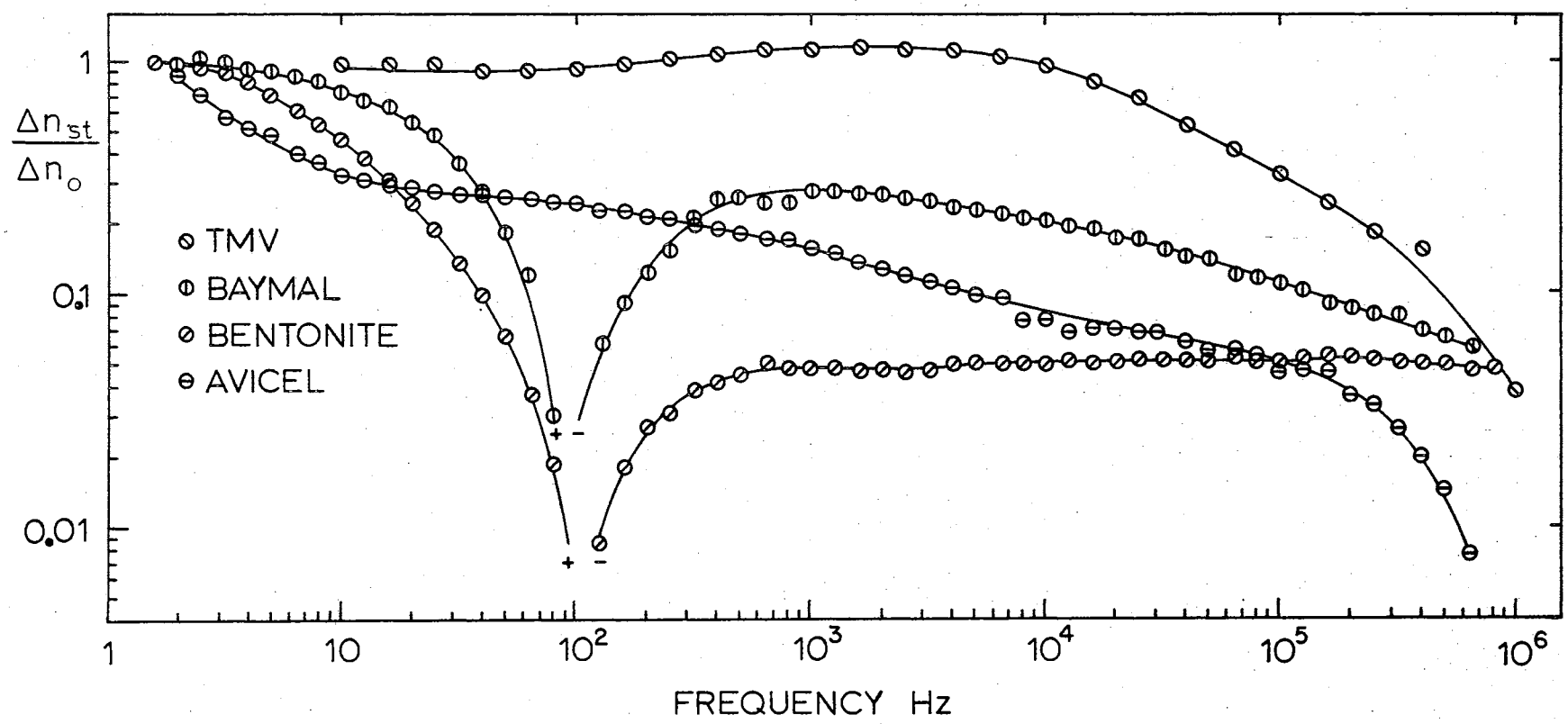
1
$\frac{\Delta n_{st}}{\Delta n_o}$
0.1
0.01
TMV
BAYMAL
BENTONITE
AVICEL
+
−
+
−
1
10
10^2
10^3
10^4
10^5
10^6
FREQUENCY Hz

region and then the steady component remains constant as frequency is further increased. Thus over the frequency range of 1 to 10^6 Hz. the function is $f(\omega) = 1$ for bentonite.

With increasing frequency the plot of the Baymal data shows the particle orientation-reorientation region and then between 300 and 1200 Hz. flattens out. Beyond this frequency the curve slowly falls off. The rate of the decrease does increase as the frequency increases, but does not appear to approach the $1/\omega$ rate expected at high frequencies if the response is to be explained by equation (VI-2).

With increasing frequency the TMV steady component shows only a slight rise before leveling off at 10^3 Hz. Thereafter it decreases with the decrease becoming sharper at the higher frequencies. The slope of this data exceeds the $1/\omega$ slope expected. This is shown more clearly with the data presented in Figure 19.

In the case of Avicel, there is not a true leveling off of the steady component with increasing frequency. However, on the basis of the alternating component data, one can conclude that the orientation-reorientation region has been passed at about 40 or 50 Hz. Between 10^5 and 10^6 Hz. the steady component does decrease sharply and exceeds the $1/\omega$ slope of equation (VI-2).

The interpretation of this data will now be considered. The function $f(\omega)$ could be determined, but this would do little more than repeat the data as presented. In the case of bentonite, there is no problem because the frequency dependence of the induced moment is trivial ($f(\omega) = 1$). For the Baymal it is possible to calculate an average relaxation time in much the same way as the value D_o was determined in the previous chapter. The behavior could be explained

Figure 19: Frequency Dependence of the Steady Component of the Electro-Optic Effect of 0.1 Per Cent TMV in Water of Varying Conductivity.

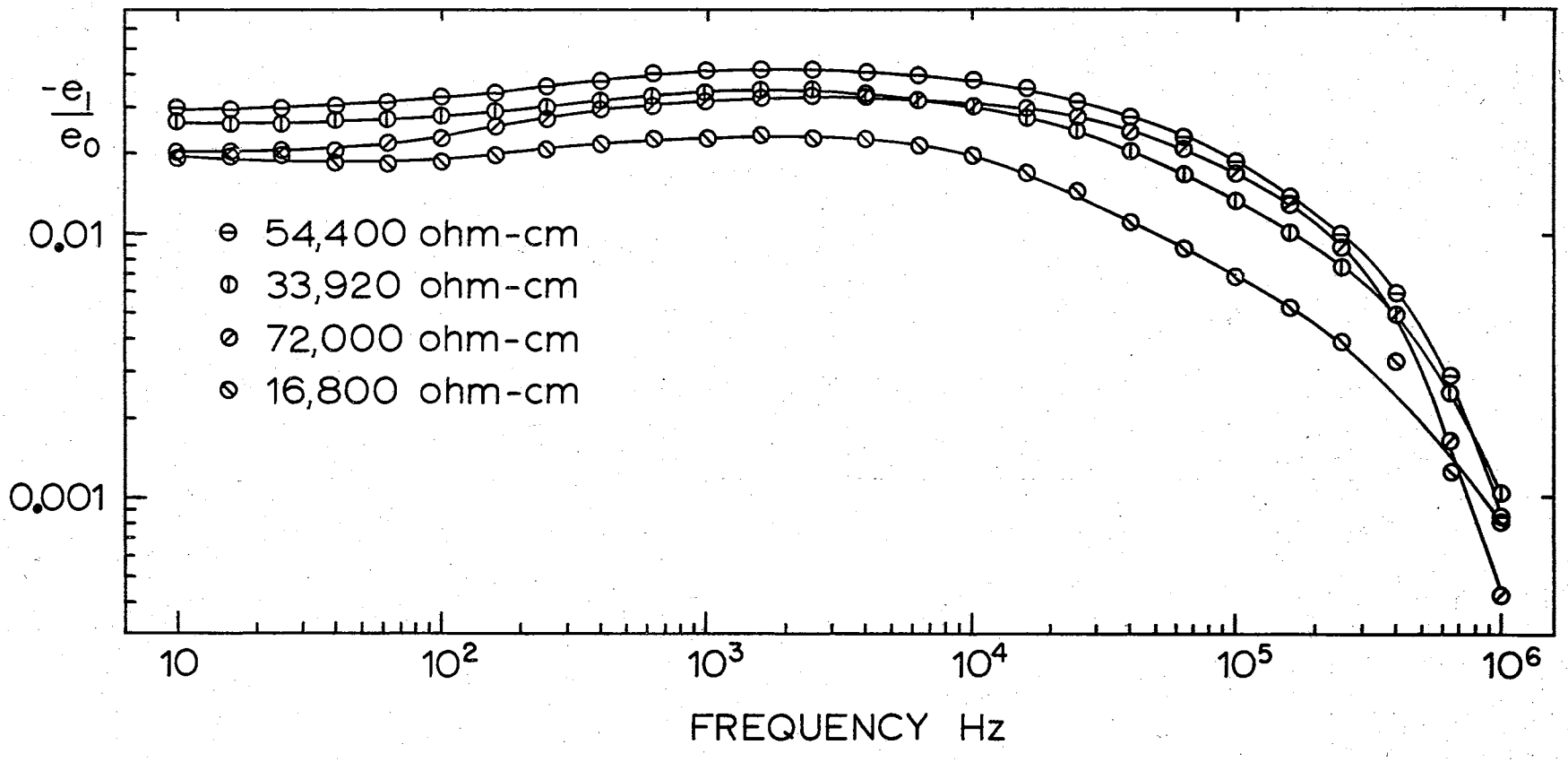
$\frac{-e_1}{e_0}$
0.01
0.001
54,400 ohm-cm
33,920 ohm-cm
72,000 ohm-cm
16,800 ohm-cm
10
10^2
10^3
10^4
10^5
10^6
FREQUENCY Hz

as a polydispersity in values of τ . In the Maxwell-Wagner effect such a variation could be explained on the basis of differences in axial ratios of the various particles in the solution. If the surface conductivity, as introduced by O'Konski, is also considered, then such a polydispersity could be accounted for by differences in axial ratios of the particles or by a variation in the sizes of the particles.

In the Avicel and TMV a complete explanation of the response is not possible on the basis of the O'Konski theory because of the sharp decline in the steady component at the highest frequencies which exceeds the $1/\omega$ slope predicted by the theory. It is clear that something is happening that is not described by O'Konski's theory. Two or more sequential processes may be involved, the first of which requires some time for action. Beyond a certain frequency there may not be enough time in a single cycle for the first process to occur; therefore, the subsequent processes cannot occur. About all that can be done is to note the frequency at which the slope exceeds the expected according to O'Konski's theory.

The relaxation times determined from the data along with the calculated relaxation times for a Maxwell-Wagner mechanism are listed in Table III. For the Maxwell-Wagner calculation the solvent conductivity was assumed to be the conductivity of the materials as shown in Table I. The dielectric constant was assumed to be 80 since the solvent was water in all cases. The particle dielectric constant and conductivity were assumed to be 1.0 and zero respectively. This was a convenience since it is known that for all the materials used both the dielectric constant and conductivity should be low compared to those of water. The values of A defined by equation (II-68) were approximated

TABLE III

RELAXATION TIMES OF POLARIZATION MECHANISMS

Material	Relaxation Times Derived From Data		Maxwell-Wagner	Values Assumed For Maxwell-Wagner Calculation				
	τ_a sec.	τ_b sec.	τ sec.	ϵ_s	σ_s mho/cm	ϵ	σ mho/cm	A
Bentonite	-	-	4.04×10^{-8}	80	551.6	1	0	.01
Baymal	1.33×10^{-5}	-	2.67×10^{-8}	80	266.4	1	0	.10
Avicel	2.65×10^{-4}	5.2×10^{-6}	3.44×10^{-7}	80	20.61	1	0	.10
TMV	7.96×10^{-6}	2.3×10^{-7}	1.152×10^{-7}	80	61.53	1	0	.01

τ_a is the apparent relaxation time calculated by equation (VI-4).
τ_b is the apparent relaxation time at the frequency at which the response curves exceeds slope of -1

from graphs of a related value given by Fricke (21). A variation of A about these values would cause only a minor change in the calculated value of τ. Also slight variations in σ and ϵ would change the calculated τ insignificantly.

O'Konski's theory and the Maxwell-Wagner specialization of that theory made allowances for three polarizations and three polarization times corresponding to the three principle axis directions of the equivalent ellipsoid considered. The one value considered in this section is the one which produced the longest relaxation time. In the case of elongated particles such as Avicel, TMV and Baymal, this is in the axis of symmetry. In the case of flattened particles such as bentonite, this corresponds to one of the transverse axes.

The τ_a value in Table III is calculated in much the same way that the D_o value was calculated in Chapter V. The equation in this case is

$$\Delta n = \Delta n_o \frac{1}{(1+(\omega\tau)^2)^{1/2}} \quad , \qquad \text{(VI-3)}$$

so that if the τ_a value is to be obtained from the frequency at which $\omega\tau_a = 1$, then

$$\frac{\Delta n}{\Delta n_o} = \frac{1}{\sqrt{2}} \simeq .707 \quad . \qquad \text{(VI-4)}$$

That is, instead of using the frequency at which the steady component falls off to 0.5 of its maximum value, one uses the frequency at which the steady component decreases to 0.707 of its maximum value. The value of τ_b represents the time, again calculated by equation (VI-3),

where the slope begins to exceed the $1/\omega$ slope of the O'Konski theory.

When the values of τ in Table III are compared, one consistency appears. The Maxwell-Wagner relaxation times are very much shorter than the observed relaxation times. If a surface mobility of any type is ass med, the relaxation times become shorter than the Maxwell-Wagner relaxation time making the discrepancy between experiment and theory greater. Thus O'Konski's theory is inadequate to explain the relaxation of the steady component of birefringency at high frequencies.

Conductivity Dependence

A portion of the TMV solution was dialyzed for 48 hours against deionized water. The steady component of the electro-optic effect was then measured over the frequency range 10 to 10^6 Hz. at 25°C. The conductivity of the sample was increased by the addition of a drop of very dilute phosphate buffer and was measured again over the same frequency range. This process was repeated two more times with the concentration of the drop of buffer gradually raised. The data obtained from these measurements is shown in Figure 19. Two observations may be made about the outcome of these measurements. The first is that the Kerr constant varied with increasing conductivity. At first it increased rather sharply and then decreased with the further addition of ions. The second observation is that the high frequency decrease in the electro-optic effect was more abrupt in the case of the deionized sample, and with the addition of ions the decrease shifted to a lower frequency. However, the apparent frequency change could be attributed

to a greater dispersion of relaxation times. For the ion free solutions the electro-optic effect decreased at the high frequency end more rapidly than predicted by O'Konski but for the most conductive solution this was not observed. The addition of ions apparently shifted this sharp decrease above 10^6 Hz. This shift is in the direction predicted by O'Konski's theory, but the frequency is much lower than that predicted by the theory.

Temperature Dependence

The sample of TMV described in the previous section was used to make similar measurements at different temperatures. Figure 20 illustrates the data obtained in this measurement. The temperature range was limited to 10°C to 50°C by experimental difficulties rather than by physical limitations of the material, which were 0°C, the freezing point of the solvent, and approximately 70°C, the degradation point of the material.

The data indicates that only the sensitivity, that is, the Kerr constant of the material, is changed by the variation in temperature. However, small changes in relaxation time, such as might be expected with comparable temperature changes in the particle orientation-reorientation region, could not easily be detected.

The change in sensitivity was larger than the $1/T$ variation expected. Thus, a second set of measurements was made to determine this variation more exactly. Measurements were taken at 10^3 Hz. at approximately 5 C° intervals from 10°C to 45°C, and then measurements were made at approximately 35°C, 26°C and 16°C in that order. The measurements were made again at the lower temperatures to assure that

Figure 20: Frequency Dependence of the Steady Component of the Electro-Optic Effect in 0.1 Per Cent TMV at Different Temperatures.

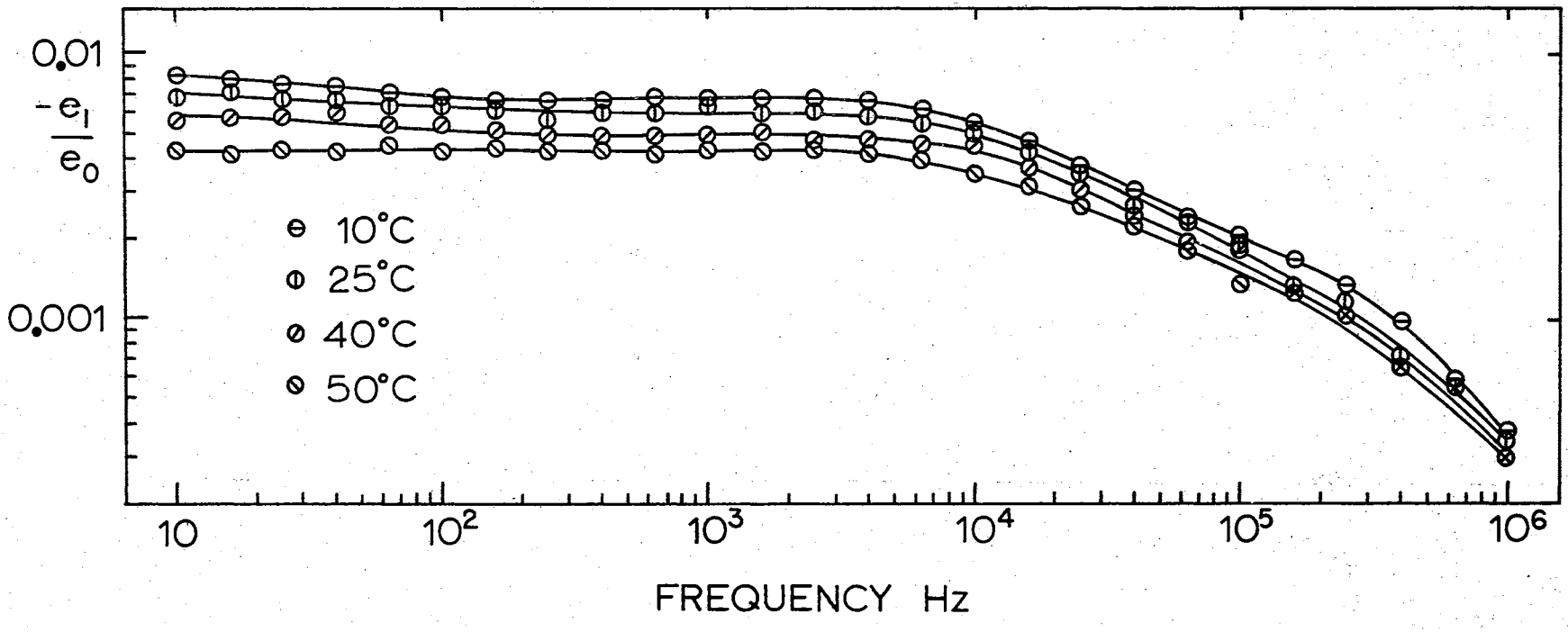
0.01
$-\frac{e_1}{e_0}$
0.001
10°C
25°C
40°C
50°C
10
10^2
10^3
10^4
10^5
10^6
FREQUENCY Hz

the observed change was not due to some progressive degradation of the TMV and to make sure that degradation did not occur at the highest temperatures attained. Figure 21 illustrates the data. An estimation of the temperature dependence was obtained by taking the values of the extremes of a line drawn through these points. The variation thus calculated was $(1/T)^{3.27}$. Thus the temperature is involved in more than the disorienting effects of Brownian motion. That is, in equation (VI-1) either (g_1-g_2) or γ^2 or both are temperature dependent.

Using values for the index of refraction of TMV given by Donnet (13) and assuming that this index of refraction remains constant while the index of refraction of the water changes with temperature, one obtains the result that (g_1-g_2) varies as $(1/T)^{-0.328}$. Actually, the indices of refraction of both the water and the TMV should change at about the same rate such that the change in (g_1-g_2) is small and can be neglected.

Thus a variation of $(1/T)^{2.27}$ must be present in the term $(g_1-g_2)\,\gamma^2$. The Maxwell-Wagner mechanism cannot explain such a variation except to the extent that the conductivity and dielectric constants of the TMV solvent may change with temperature. As an example, using Fricke's (21) equations for the dielectric constant of a suspension, and assuming a large axial ratio for the suspended particle, the dielectric increment is

$$\Delta\epsilon \propto \frac{\epsilon_s\sigma + 1}{\sigma_s} - \epsilon \quad , \qquad \text{(VI-5)}$$

where ϵ_s is the dielectric constant of the solvent, ϵ is the dielectric constant of the suspended particle, σ_s is the permittivity

Figure 21: Temperature Dependence of the Steady Component of the Electro-Optic Effect for 0.1 Per Cent TMV at a Frequency of 10^3 Hz. Points with horizontal bars represent data taken as temperature is lowered. The temperature is in degrees Kelvin.

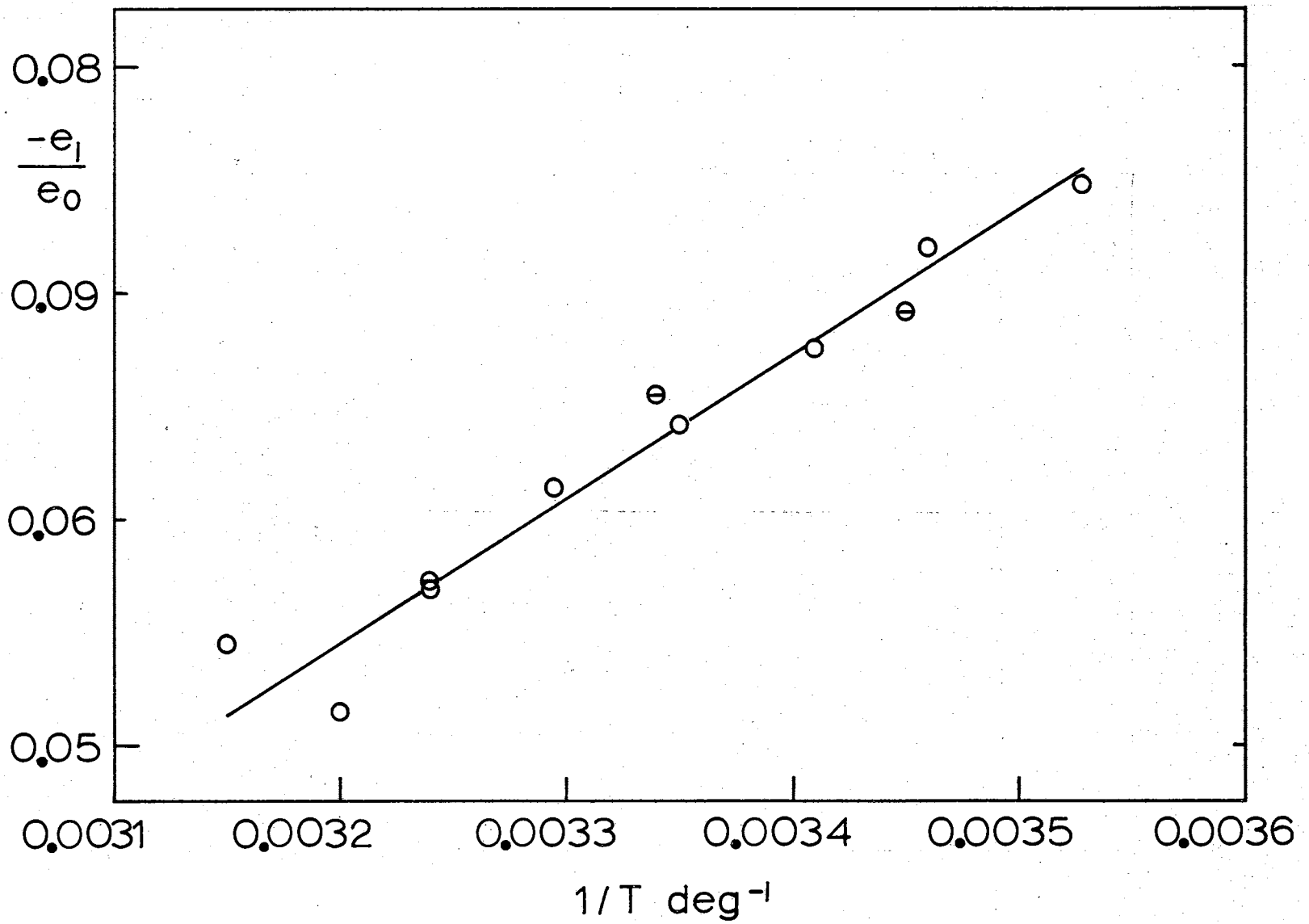
0.08
$\frac{-e_1}{e_0}$
0.09
0.06
0.05
0.0031
0.0032
0.0033
0.0034
0.0035
0.0036
1/T deg^{-1}

of the solvent and σ is the permittivity of the suspended particle. If the permittivity of the solute particle is very low, as it should be with TMV, then the dielectric increment, and thus the polarization of the suspension will vary inversely as the conductivity of the solution. It is known that the conductivity of dilute solutions of simple salts may vary by factors of 4 or 5 over the temperature range of 10°C to 50°C so that a large temperature dependence in the electro-optic effect could be explained by the Maxwell-Wagner mechanism.

If O'Konski's extension of this theory is used, the change is not as rapid since it is assumed that the effect of greater ionic strength in the solution is to increase the surface conductivity and thus the effective conductivity of the particle. This would cause an increase in the polarization. However, the change in conductivity with temperature could still explain the variation observed.

Conclusion

Some relaxation mechanism other than particle orientation-reorientation is occuring at the higher frequencies. The most reasonable explanation is that this mechanism is related to a time dependent polarization of the molecule. A simple framework can be provided to describe such a mechanism, but existing theories as generalized by O'Konski do not adequately describe the experimental observations.

CHAPTER VII

SUMMARY AND CONCLUSIONS

This chapter will be divided into a section on the findings of this study and a section containing suggestions for further study. A great deal of the time involved in this study was devoted to attempting to obtain data in the face of such problems as electrode polarization, heating in the solutions during measurement, parasitic effects which could produce systematic errors, variations in light source level, measurement and birefringence in the windows of the electro-optic cells. This chapter will present suggestions which might be of help in avoiding similar problems in other studies.

Conclusions

The conclusions to be drawn from this study may be divided into three parts. The first is the general adequacy of the theory as developed to describe the general character of the electro-optic response. The second is the ability of the theory, modified by considerations of polydispersity in the sample, to describe the electro-optic response exactly. The third is the adequacy of the theory of O'Konski to describe the frequency dependent behavior of that part of the electro-optic response which depends upon the presence of an induced moment on the particle.

The adequacy of the theory in the description of the general

character of the expected response has been demonstrated quite well. In the four materials and give cases examined, (1) the range of phase angle excursion agreed with the theoretical expectation, (2) the high frequency slope and low frequency limit of the alternating component agreed with theory, and (3) the high and low frequency limits of the steady component agreed with theory. The actual data had a greater dispersion over the frequency range than the best monodisperse fit, as would be expected for a sample that was not monodisperse. The field dependence of the data also agreed with theory in every case. The concentration dependence of the effect was not verified, but the fact that the verification could not be made was reasonably explained on the basis of the dependence of the Kerr constant on the ionic concentration of the solvent. However, the theory does not adequately explain the character of the high frequency steady component electro-optic response.

A method of analyzing the steady component data of the electro-optic effect for polydispersity was developed. The formal procedure for obtaining the polydispersity was not exact, but provided a basis for making estimates of the actual polydispersity. Unfortunately, the steady component was the least sensitive of the three measurable components to slight changes in the polydispersity, and the polydispersity was determined from this component alone. Thus for the case which was used as an example, this polydispersity failed to give an adequate fit of the data to theory for the alternating component and phase angle. A variation in the value of P along with the polydispersity might possibly reconcile the discrepancy.

The difficulty of determining both a P and polydispersity function of approximately 20 to 30 points and obtaining an adequate

fit of all the components was not overcome. Some means of doing this will be necessary before a completely adequate fit between data and theory can be obtained. The necessity of a P variation is demonstrated by the difference in the P values of the two Baymal samples. Theoretically, the polydispersity and P functions would include all other variations in the basic parameters of the theory. Thus one concludes that with an adequate knowledge of both the polydispersity and variation in P of a particular solution, agreement could be obtained between experiment and theory.

At high frequencies the steady component of the electro-optic effect decreased for three of the four materials measured. A general theoretical framework for such a variation was developed and a specific example was used in this framework. This example was the theory of O'Konski which included the Maxwell-Wagner effect and additional effects that would contribute to a surface conductivity. This theory incorporates many previous theories used to explain induced polarization. It was not possible to compare magnitudes of induced moments because the complete determination of the theoretical constants of the electro-optic theory is not possible without some auxiliary measurements such as flow birefringence being made on the same materials. However, a relaxation time was specified by the theory which could be compared to relaxation times determined from the data.

Comparison was made between the experimentally determined relaxation time and the Maxwell-Wagner relaxation time. In all cases the measured relaxation time was longer than the Maxwell-Wagner relaxation time. The effect of the other mechanisms included in O'Konski's theory was to make the theoretical relaxation time shorter still. The ratio

between the measured and theoretical relaxation times ranged from about 70 to over 1000. In addition, in TMV and Avicel a frequency was reached at which the decrease in the steady component exceeded that predicted by O'Konski's theory. The frequency at which this occured was more closely related to the Maxwell-Wagner relaxation time than to the relaxation time determined by equation (IV-4). Therefore, one concludes that there is some relaxation mechanism probably associated with the induced moment, which cannot be adequately explained by O'Konski's theory and for which there is apparently no other adequate theory. More will be said about this later in the chapter.

Improvements and Variations in Procedure

A review of the manner in which data was analyzed for this thesis indicates that a great deal of reliance was placed on the information which could be obtained from the steady component of the electro-optic effect alone. For example, the average D value was obtained from the frequency of the point midway between the high and low frequency limit of the steady component and the P value was calculated from the high and low frequency limit values of the steady component. A recalculation of all components then provided the first opportunity to actually use the alternating component and phase angle measurements. A similar reliance on the steady component is found in the polydispersity analysis. The principal reason for this is that the mathematical form of the steady component is very much simpler than the form of the alternating component and phase angle.

Information about the variation of P with D was also needed to adequately provide a description of what was taking place in

a polydisperse sample. This information could not be obtained from the steady component alone. On the other hand, the alternating component and phase angle information taken together could possibly be used to determine both the polydispersity and the variation of P with D.

Even if the theoretical problem of the analysis of the alternating component and phase angle were solved, the problem of making accurate measurements to use the method would remain. In this study the measurement of the phase angle was the least reliable of all the measurements made. The problem was one of obtaining a signal that is accurately in phase with the electric field inside the electro-optic cell, doubling the frequency in such a way that the phase accuracy is not lost and then comparing this to the optical signal to obtain the phase difference between the two signals. In this study it was estimated that an accuracy of not better than $\pm 5^{\circ}$ was obtained on any single measurement. In many cases the accuracy could have been less, but no method was available for checking the accuracy of the system.

The problem in accuracy of measurement was multiple. It was not always possible to obtain an accurate signal in phase with the electric field in the fluid. Also, the accuracy of the frequency doubler could only be checked to within 5° under ideal conditions. The signal that was supposed to be in phase with the field was taken either from a resistor in series with the cell or from probe electrodes in the cell. In the first case, the method depended upon the assumption that the solution was predominately resistive rather than reactive and that there were no current leaks or sources anywhere. The voltage at the probe electrodes, measured by a high impedance device, made possible a direct measurement of the field in the fluid, but was dependent upon

a low current through the probes to avoid polarization problems at the probes. An assumption was made that there was no other time dependent mechanism. The frequency doubler presented no theoretical problem, but again its accuracy was in doubt. All that could be done was to make sure that the proper output waveform was being produced and that, as far as could be detected with an oscilloscope, there was no waveform distortion or phase shift.

Finally, at high frequencies the accuracy of the phase angle measurement deteriorated because the angle to be measured was usually near 90° or 270° and it was necessary to measure the in- and out-of-phase components accurately at very low signal levels. The in-phase component near those angles was so small that detection was difficult.

To use the alternating component and phase angle as bases for analysis, all of the above problems would have to be overcome or circumvented. The magnitude of the alternating component should present no problem. If adequate measuring equipment can be obtained, then the alternating component should be the most accurate of the three components.

The alternating component is considered more accurate than the steady component because of the problem of variation in the intensity of the light source. For example, a 1 per cent change in light level would show up as a 1 per cent change in the steady background voltage. This would change the measured steady component voltage by 100 per cent while changing the alternating component voltage by only 1 per cent.

Thus, a further study of the electro-optic effect might be directed towards solving the above problems and then making use of the alternating component and phase angle in the analysis of polydispersity

and P variation rather that using the steady component.

Other problems encountered in the measurements were noise, beam spreading between narrowly spaced electrodes and abrupt changes in the light source level. The noise was mainly due to the small amount of light which was ultimately measured. Only a small fraction of the lamp's energy was used and then this was filtered by a narrow band pass filter to obtain monochromatic light, further reducing the intensity. Beam spreading could be reduced, but only at the expense of intensity. Abrupt changes in light level of as much as 10 per cent were common when the incandescent lamp was warming up or underwent a temperature change due to cooling by convection currents. All of these problems could be overcome by using a stable laser as a light source. This would also simplify the optical system. The emphasis here is on a stable laser. Lasers available in this laboratory were found to provide a greater variation in output than the incandescent bulb.

Suggestions for Further Study

The electro-optic effect, while useful by itself for measuring rotary diffusion constants and determining whether or not a molecule has an induced or permanent moment, would be most effective if used with flow birefringence measurements. If measurements of both the electro-optic effect and of flow birefringence were made on the same material, it would be possible to determine every quantity in the theory of the electro-optic effect including values for the permanent moment and the electrical polarizability. This and dielectric measurements would provide independent methods of determining these important quantities. When used with dielectric measurements, the

electro-optic effect provides a means of identifying different polarization mechanisms which are indistinguishable by dielectric measurements alone. This separation could be important in mixed biological systems, that is, in systems where more than one molecule may be contributing to both the dielectric and electro-optic effects.

Studies should be made on materials, such as DNA, which are known to exhibit all three of the effects mentioned above. Similarly, any other material might be studied in this way if both the electrical and optical constants of the material are considered important.

In a previous section of this chapter it was suggested that methods of analyzing the alternating component and phase angle measurements of any material be developed. If this were done, it would be possible, with a single set of measurements, to determine both the size distribution and physical property variation with size of materials such as clays.

Finally, the existing theories for the polarization mechanisms of the molecules do not adequately account for the relaxation times observed at the higher frequencies in the steady component of the electro-optic effect. Since O'Kronski presented his theory for the combined effects suggested by others, McTague and Gibbs (39) have suggested that the macroscopic considerations of the O'Konski theory are inappropriate to the case of macromolecules and have worked out an approximate theory based on microscopic considerations. Unfortunately, their approach did not account for the frequency dependence of the effect. Theoretical work to explain the polarization mechanisms of macromolecules needs to be undertaken.

BIBLIOGRAPHY

(1) A. J. Barlow and J. Lamb, Proc. Roy. Soc. (London), A., 253, 52 (1959).

(2) O. A. Battista, N. Z. Erdi, C. F. Ferraro and F. J. Karasinski, J. Appl. Polymer Sci. 11, 481 (1967).

(3) R. E. Bellman, Perturbation Techniques in Mathematics, Holt, Rinehart and Winston, New York (1964).

(4) H. Benoit, J. Chim. Phys. 49, 58 (1952).

(5) E. R. Blout and R. H. Karlson, J. Am. Chem. Soc. 78, 941 (1956).

(6) G. Boeckel, J. Genzling, G. Weill and H. Benoit, J. Chim. Phys. 59, 999 (1962).

(7) H. Boedtker and N. S. Simmons, J. Am. Chem. Soc. 80, 2050 (1958).

(8) W. F. Brown, Encyclopedia of Physics, XVII, edited by S. Fluegge, Springer-Verlag, Berlin (1956).

(9) J. Bugosh, J. Phys. Chem. 65, 1789 (1961).

(10) Burr-Brown Research Corporation, Handbook of Operational Amplifier Applications (1963).

(11) R. Cerf and H. A. Scheraga, Chem. Rev. 51, 185 (1952).

(12) P. A. Debye, Polar Molecules, Dover, New York (1947).

(13) J. B. Donnet, J. Polymer Sci. 12, 53 (1954).

(14) E. I. DuPont de Nemours and Co., Industrial and Biochemicals Department, Dupont Baymal Colloidal Alumina.

(15) A. Einstein, Investigation of the Theory of Browian Motion, Dover, New York (1956).

(16) FMC Corporation, Avicel Applications Bulletin A CM-3-467 (1967).

(17) I. L. Fabelinskii, Soviet Phys. JETP 45, 822 (1963).

(18) W. A. Farry, Phys. Rev. 107, 7 (1957).

(19) J. D. Ferry and J. L. Oncley, J. Am. Chem. Soc. 60, 1123, (1938).

(20) J. D. Ferry and J. L. Oncley, J. Am Chem. Soc. 63, 272, (1941).

(21) H. Fricke, J. Phys. Chem. 57, 934 (1953).

(22) E. I. Golub and V. G. Nazerenko, Biophys. J. 7, 13 (1967).

(23) W. Heller, Rev. Mod. Phys. 14, 390 (1942).

(24) L. N. Huller and D. Robson, J. Sci. Instr. 43, 728 (1966).

(25) S. Ikeda, J. Chem. Phys. 38, 2839 (1963).

(26) P. Ingram and H. G. Jerrard, Nature 196, 57 (1962).

(27) P. Ingram and H. G. Jerrard, Brit. J. Appl. Phys. 14, 572 (1963).

(28) J. D. Jackson, Classical Electrodynamics, John Wiley and Sons, New York (1962).

(29) B. R. Jennings and H. G. Jerrard, J. Chem. Phys. 44, 1219 (1966).

(30) H. G. Jerrard, Chem. Rev. 59, 345 (1959).

(31) H. G. Jerrard and B. A. W. Simmoms, Nature 184, 1715 (1959).

(32) J. Kerr, Phil. Mag. 50, 337 (1875).

(33) J. Kerr, Phil. Mag. 50, 446 (1875).

(34) J. G. Kirkwood and J. B. Schumaker, Proc. Nat. Acad. Sci. 38, 855 (1952).

(35) H. Labhart, Tetrahedron 19, 223 (1963).

(36) M. A. Lauffer, J. Am. Chem. Soc. 66, 1188 (1944).

(37) M. A. Lauffer, J. Am. Chem. Soc. 66, 1195 (1944).

(38) R. J. W. LeFevre, Dipole Moments - Their Measurement and Application in Chemistry, Methuen and Co., London (1948).

(39) J. P. McTague and J. H. Gibbs, J. Chem. Phys. 44, 4295 (1966).

(40) P. Moser, P.G. Squire and C. T. O'Konski, J. Phys. Chem. 70, 744 (1966).

(41) Y. Mukohata, J. Mol. Biol. 1, 442 (1963).

(42) K. J. Mysels, J. Chem. Phys. 21, 201 (1953).

(43) C. T. O'Konski, J. Chem. Phys. 23, 1559 (1955).

(44) C. T. O'Konski, J. Phys. Chem. 64, 605 (1960).

(45) C. T. O'Konski and K. Bergmann, J. Chem. Phys. 37, 1573 (1962).

(46) C. T. O'Konski and A. J. Haltner, J. Am. Chem. Soc. 78, 3604 (1956).

(47) C. T. O'Konski and A. J. Haltner, J. Am. Chem. Soc. 79, 5634 (1957).

(48) C. T. O'Konski and R. M. Pytkowicz, J. Am. Chem. Soc. 79, 4815 (1957).

(49) C. T. O'Konski and N. C. Stellwagen, Biophys. J. 5, 607 (1965).

(50) C. T. O'Konski, K.Yoshioka and W. H. Ortung, J. Phys. Chem. 63, 1558 (1959).

(51) C. T. O'Konski and B. H. Zimm, Science 111, 113 (1950).

(52) F. Ollendorff, Potentialfelder, J. Springer, Berlin (1932).

(53) J. L. Oncley, J. Am. Chem. Soc. 60, 1115 (1938).

(54) L. Onsager, J. Am. Chem. Soc. 58, 1486 (1936).

(55) J. A. Osborn, Phys. Rev. 67, 351 (1945).

(56) F. Perrin, J. Phys. Radium 5, 497 (1934).

(57) A. Peterlin and H. A. Stuart, Hand und Jahrbuch der Chem. Physik 8, 1B (1930).

(58) A. Peterlin and H. A. Stuart, Z. Physik 112, 1 (1939).

(59) A. Peterlin and H. A. Stuart, Z. Physik 112, 129 (1939).

(60) M. Pollak, J. Chem. Phys. 43, 908 (1965).

(61) R. M. Pytkowicz, Characterization of Some Biological Macromolecules by Transient Electric Birefringence, Thesis, University of California, Berkley (1957).

(62) Y. Rozart, J. Phys. Radium 4, 247 (1933).

(63) W. Scheider, Biophys. J. 5, 617 (1965).

(64) H. P. Schwan, Physical Techniques in Biological Research 6, W. L. Nastuk, editor, Academic Press, New York, 323 (1963).

(65) H. P. Schwan and K. Sittel, A.I.E.E. Trans. 72, 114 (1953).

(66) M. J. Shah and C. M. Hart, IBM J. Res. Develop. 7, 44 (1963).

(67) M. J. Shah, J. Phys. Chem. 67, 225 (1963).

(68) M. J. Shah, D. C. Thompson and C. M. Hart, J. Phys. Chem. 67, 1170 (1963).

(69) M. J. Shah, J. Phys. Chem. 68, 2215 (1964).

(70) T. M. Shaw, J. Chem. Phys. 10, 609 (1942).

(71) J. W. Smith, Sci. Prog. 48, 684 (1960).

(72) M. von Smoluchowski, Two Monographs on Electro Kinetics, trans. by P. E. Bocquet, Univ. of Mich., 51 (1959).

(73) J. A. Stratton, Electromagnetic Theory, McGraw-Hill, New York, 211 (1941).

(74) S. Takashima, J. Mol. Biol. 7, 455 (1963).

(75) S. Takashima, J. Phys. Chem. 70, 1372 (1966).

(76) S. Takashima, Advan. Chem. Ser. 63, 232 (1967).

(77) C. Tanford, Physical Chemistry of Macromolecules, John Wiley and Sons, New York (1961).

(78) G. B. Thurston, Appl. Op. 3, 755 (1964).

(79) G. B. Thurston, Seminars given at Oklahoma State University in June 1965.

(80) I. Tinoco, J. Am. Chem. Soc. 77, 3476 (1955).

(81) I. Tinoco, J. Am. Chem. Soc. 77, 4486 (1955).

(82) I. Tinoco and W. G. Hammerle, J. Chem. Phys. 60, 1619 (1956).

(83) I. Tinoco and K. Yamoka, J. Phys. Chem. 63, 423 (1959).

(84) NA. A. Tolstoi, A. A. Spartakov and A. A. Trusov, Opt. i Spectroskopya, 19, 826 (1955).

(85) V. N. Tsvetkov, Yu. V. Mitin, V. R. Glushenkova, A. Ye Grishchenko, N. N. Biotsova and S. Ya. Lyubina, Vysokomolekul. Soedin. 5, 453 (1963).

(86) V. N. Tsvetkov, Polymer Reviews 6, edited by Bacon Ke, Interscience, New York, 563 (1964).

(87) V. N. Tsvetkov, I. N. Shtennikova, Ye. I. Ryumtsev and V. S. Skazka, Vysokomolekul. Soedin. 7, 1111 (1965).

(88) M. L. Wallach and H. Benoit, J. Polymer Sci. 57, 41 (1962).

(89) C. Wippler, J. Chim. Phys. 51, 122 (1954).

(90) C. Wippler and H. Benoit, Macromol. Chem. 13, 7 (1954).

(91) B. H. Zimm, J. Chem. Phys. 24, 269 (1956).

APPENDIX A

SOLUTION TO THE DIFFERENTIAL EQUATION

FOR ELECTRIC FIELD ORIENTATION

The differential equation developed in the text which describes the orientation of macromolecules in a liquid under the influence of an oscillating electric field is

$$\frac{\partial^2 \rho}{\partial \sigma} + \frac{\cos\sigma}{\sin\sigma}\frac{\partial \rho}{\partial \sigma} + \beta\left(\sin\sigma \frac{\partial \rho}{\partial \sigma} + 2\cos\sigma\,\rho\right) \cdot \cos\omega t + \gamma^2\left[\sin\sigma\cos\sigma\frac{\partial \rho}{\partial \sigma} + (3\cos^2\sigma - 1)\right] \cdot \cos^2\omega t = \frac{1}{D}\frac{\partial \rho}{\partial t} \cdot \tag{A-1}$$

In this section ρ is the distribution function, σ is the polar angle, ω the angular frequency, t the time variable, D the rotary diffusion constant, E the electric field, k Boltzman's constant, T the temperature, μ the permanent moment, N the number of molecules per unit volume, and g_{1e} and g_{2e} the electrical polarizabilities of a particle in the longitudinal and transverse directions. In addition the ρ , γ^2 and β are defined by

$$\rho = \underset{\Delta\Omega \to 0}{\text{Limit}} \frac{1}{N}\frac{\Delta N}{\Delta \Omega} \quad , \tag{A-2}$$

$$\gamma^2 = \frac{(g_{1e} - g_{2e})E^2}{kT} \qquad \text{(A-3)}$$

and

$$\beta = \frac{\mu E}{kT} \qquad \text{(A-4)}$$

If the substitutions $\cos\sigma = u$ and $\frac{\partial}{\partial\sigma} = -\sin\sigma\frac{\partial}{\partial u}$ are made, the equation becomes

$$(1-u^2)\frac{\partial^2\rho}{\partial u^2} - 2u\frac{\partial\rho}{\partial u} + \beta\left[-(1-u^2)\frac{\partial\rho}{\partial u} + 2u\rho\right]$$

$$\cdot\cos\omega t + \gamma^2\left[-u(1-u^2)\frac{\partial\rho}{\partial u} + (3u^2-1)\rho\right]\cos^2\omega t \qquad \text{(A-5)}$$

$$= \frac{1}{D}\frac{\partial\rho}{\partial t} \quad .$$

This equation can be solved by perturbation techniques as described below.

If one encounters an equation of the form

$$F(\rho) + \alpha F_1(\rho) + \epsilon F_2(\rho) + a = 0 \quad , \qquad \text{(A-6)}$$

where F , F_1 and F_2 are linear operators, ρ and a are functions and α and ϵ are parameters with values less than one and are known as perturbation parameters, then a solution exists of

the form

$$\rho = \sum_{n=0}^{\infty} \sum_{m=0}^{\infty} \alpha^n \epsilon^m \rho_{mn} \quad . \tag{A-7}$$

The functions ρ_{nm} are determined by the individual solutions to the equations listed below. For $n=0$, $m=0$

$$F(\rho_{00}) + a = 0 \quad , \tag{A-8}$$

for $m=0$, $n=1$

$$F(\rho_{01}) + F_1(\rho_{00}) = 0 \quad , \tag{A-9}$$

for $m=0$, $n=n$

$$F(\rho_{0n}) + F_1(\rho_{0\,n-1}) = 0 \quad , \tag{A-10}$$

for $m=1$, $n=0$

$$F(\rho_{10}) + F_2(\rho_{00}) = 0 \quad , \tag{A-11}$$

for $m=1$, $n=1$

$$F(\rho_{11}) + F_2(\rho_{01}) + F_1(\rho_{10}) = 0 \quad , \tag{A-12}$$

for $m=1$, $n=n$

$$F(\rho_{1n}) + F_2(\rho_{on}) + F_1(\rho_{1\,n-1}) = 0 \quad , \tag{A-13}$$

for $m = m$, $n = 0$

$$F(\rho_{mo}) + F_2(\rho_{m-1\,o}) = 0 \quad , \tag{A-14}$$

for $m = m$, $n = 1$

$$F(\rho_{m1}) + F_2(\rho_{m-1\,1}) + F_1(\rho_{mo}) = 0 \quad , \tag{A-15}$$

for $m = m$, $n = n$

$$F(\rho_{mn}) + F_2(\rho_{m-1\,n}) + F_1(\rho_{m\,n-1}) = 0 \quad . \tag{A-16}$$

Equation (A-5) is an equation of the form of (A-6) where

$$F = (1-u^2)\frac{\partial^2}{\partial u^2} - 2\frac{\partial}{\partial u} - \frac{1}{D}\frac{\partial}{\partial t} \quad , \tag{A-17}$$

$$F_1 = \cos \omega t \left[-(1-u^2)\frac{\partial}{\partial u} + 2u\right] \quad , \tag{A-18}$$

$$F_2 = \cos^2 \omega t \left[-u(1-u^2) \frac{\partial}{\partial u} + (3u^2 - 1) \right] , \tag{A-19}$$

$$\alpha = \beta , \tag{A-20}$$

$$\epsilon = \gamma^2 , \tag{A-21}$$

and

$$a = 0 . \tag{A-22}$$

As will be shown later, only solutions for ρ_{00}, ρ_{10}, ρ_{20} and ρ_{01} need be sought. Refering to equations (A-9) through (A-16) the set of equations requiring solution are

$$(1-u^2) \frac{\partial^2 \rho_{00}}{\partial u^2} - 2u \frac{\partial \rho_{00}}{\partial u} = \frac{1}{D} \frac{\partial \rho_{00}}{\partial t} , \tag{A-23}$$

$$(1-u^2) \frac{\partial^2 \rho_{10}}{\partial u^2} - 2u \frac{\partial \rho_{10}}{\partial u} + \left[-(1-u^2) \frac{\partial \rho_{00}}{\partial u} + 2u \rho_{00} \right] \cdot \cos \omega t = \frac{1}{D} \frac{\partial \rho_{10}}{\partial t} , \tag{A-24}$$

$$(1-u^2)\frac{\partial^2 \rho_{20}}{\partial u^2} - 2u\frac{\partial \rho_{20}}{\partial u} + \left[-(1-u^2)\frac{\partial \rho_{10}}{\partial u} + 2u\rho_{10}\right] \cdot \cos \omega t = \frac{1}{D}\frac{\partial \rho_{20}}{\partial t} \tag{A-25}$$

and

$$(1-u^2)\frac{\partial^2 \rho_{01}}{\partial u^2} + 2u\frac{\partial \rho_{01}}{\partial u} + \left[-u(1-u^2)\frac{\partial \rho_{00}}{\partial u} + (3u^2-1)\rho_{00}\right]\cos^2 \omega t = \frac{1}{D}\frac{\partial \rho_{01}}{\partial t} \; . \tag{A-26}$$

These four equations will now be solved in order.

Equation (A-23) is separable. $\rho_{00} = U T$, where U is a function of u only, and T is a function of time only. Thus

$$\frac{1}{U}(1-u^2)\frac{\partial^2 U}{\partial u^2} - \frac{1}{U}2u\frac{\partial U}{\partial u} = \frac{1}{D}\frac{1}{T}\frac{\partial T}{\partial t} = -n(n+1), \tag{A-27}$$

where $-n(n+1)$ is the separation constant. The two resulting differential equations are

$$(1-u^2)\frac{\partial^2 U}{\partial u^2} - 2u\frac{\partial U}{\partial u} + n(n+1)U = 0 \; , \tag{A-28}$$

and

$$\frac{1}{D}\frac{\partial T}{\partial t} + n(n+1)T = 0 \quad . \tag{A-29}$$

(A-28) is just Legendres differential equation with solutions $P_n(u)$ where n is a positive integer. Equation (A-29) can be written

$$\frac{1}{T}\partial T = -n(n+1)D\,\partial t \quad , \tag{A-30}$$

which upon integration becomes

$$\ln T = -n(n+1)Dt + \text{const.} \quad , \tag{A-31}$$

or

$$T = \text{const.}\ e^{-n(n+1)Dt} \quad . \tag{A-32}$$

Thus the solution to equation (A-23) is

$$\rho_{oo} = \sum_{n=0}^{\infty} C_n P_n(u)\, e^{-n(n+1)Dt} \quad . \tag{A-33}$$

If only the steady state solution is desired then the solution is

$$\rho_{oo} = C_o \quad . \tag{A-34}$$

If the solution (A-34) is placed in the appropriate place in equation (A-24), one obtains

$$(1-u^2)\frac{\partial^2 \rho_{10}}{\partial u^2} - 2u\frac{\partial \rho_{10}}{\partial u} + 2u C_0 \cos \omega t = \frac{1}{D}\frac{\partial \rho_{10}}{\partial t} . \quad \text{(A-35)}$$

Since each term of the equation contains either ρ_{10} or $\cos \omega t$ it is obvious that one solution to the equation is on the form

$$\rho_{10} = U \cos \omega t = U \, \mathrm{Re}\, e^{i\omega t} . \quad \text{(A-36)}$$

The exponential form will be used with the understanding that the real part of the complex quantity is intended. If (A-36) is substituted into (A-35) one obtains

$$(1-u^2)\frac{\partial^2 U}{\partial u^2} - 2u\frac{\partial U}{\partial u} + 2u C_0 = \frac{1}{D} i\omega U . \quad \text{(A-37)}$$

The solution to (A-37) is

$$U = \sum_{n=0}^{\infty} b_n u^n . \quad \text{(A-38)}$$

When this is substituted into (A-37) one obtains

$$\sum_{n=0}^{\infty} \Big\{ (1-u^2) b_n n(n-1) u^{n-2} + b_n 2n u^n + 2u C_0 - \frac{i\omega}{D} b_n u^n \Big\} = 0 . \quad \text{(A-39)}$$

In terms of powers of u this may be rewritten as

$$\sum_{n=0}^{\infty} \left\{ (n+2)(n+1)\, b_{n+2} - n(n+1)\, b_n - \frac{i\omega}{D} b_n \right\} u^n$$

$$+ 2u C_0 = 0 \qquad (A\text{-}40)$$

If each power of u is individually equated to zero one obtains the equations

$$(n+2)(n+1)\, b_{n+2} - \left[(n+1)n + \frac{i\omega}{D} \right] b_n = 0 \,, \qquad (A\text{-}41)$$

where there is one equation for each positive integer and zero, except for the case of $n=1$ for which

$$6 b_3 - \left(2 + \frac{i\omega}{D}\right) b_1 + 2 C_0 = 0 \,. \qquad (A\text{-}42)$$

These equations can be solved in the ordinary manner or one can merely recognize that a solution to the equations is $b_n = 0$ for each n except for

$$b_1 = \frac{2 C_0}{2 + i\omega/D} \,. \qquad (A\text{-}43)$$

Thus the solution to (A-37) is

$$U = \frac{1}{1 + i\omega/2D}\, u \,. \qquad (A\text{-}44)$$

The solution to the homogeneous part of the equation (A-35) must be added to this solution to obtain a complete solution. The homogeneous equation is the same as equation (A-28). Thus the solution for the steady state is

$$\rho_{10} = Re\left[\frac{C_0}{1+i\omega/2D}\ e^{i\omega t}\right]u + C_{10}\ , \tag{A-45}$$

where C_{10} is a constant which depends upon initial or boundary conditions.

To obtain an alternate form of this solution, consider the identities

$$\frac{C_0}{1+i\omega/2D} = \frac{C_0(1-i\omega/2D)}{1+(\omega/2D)^2} = A\,e^{-i\delta} = A\cos\delta - iA\sin\delta \tag{A-46}$$

From the real and imaginary parts of the equation one can obtain the relations

$$\tan\delta = \omega/2D \tag{A-47}$$

and

$$A = \frac{C_0}{[1+(\omega/2D)^2]^{1/2}} \tag{A-48}$$

Equation (A-45) can then be rewritten

$$\rho_{10} = \frac{C_0}{[1+(\omega/2D)^2]^{1/2}}\ u\cos(\omega t - \delta) + C_{10}\ . \tag{A-49}$$

Next, equation (A-25) will be solved. If the solution (A-49) is placed in equation (A-25) one obtains the equation

$$(1-u^2)\frac{\partial^2 \rho_{20}}{\partial u^2} - 2u\frac{\partial \rho_{20}}{\partial u} + \left[-(1-u^2)\frac{C_0}{[1+(\omega/2D)^2]^{1/2}}\right.$$

$$\cdot \cos(\omega t - \delta) + 2u^2\frac{C_0}{[1+(\omega/2D)^2]^{1/2}}\cos(\omega t-\delta) \qquad \text{(A-50)}$$

$$\left. + 2u\,C_{10}\right]\cos\omega t = \frac{1}{D}\frac{\partial \rho_{20}}{\partial t} \,.$$

The solution to this equation is the sum of the solutions to the equation

$$(1-u^2)\frac{\partial^2 \rho'_{20}}{\partial u^2} - 2u\frac{\partial \rho'_{20}}{\partial u} + (3u^2-1)\frac{C_0}{[1+(\omega/2D)^2]^{1/2}} \qquad \text{(A-51)}$$

$$\cdot \cos(\omega t-\delta)\cos\omega t = \frac{1}{D}\frac{\partial \rho'_{20}}{\partial t}$$

and

$$(1-u^2)\frac{\partial^2 \rho''_{20}}{\partial u^2} - 2u\frac{\partial \rho''_{20}}{\partial u} + 2u\,C_{10}\cos\omega t = \frac{1}{D}\frac{\partial \rho''_{20}}{\partial t} \qquad \text{(A-52)}$$

Equation (A-52) is identical in form to equation (A-35), so that the result may be written out as

$$\rho''_{20} = \frac{C_{10}}{[1+(\omega/2D)^2]^{1/2}}u\cos(\omega t-\delta) + C''_{20} \,, \qquad \text{(A-53)}$$

where δ is the same as in equation (A-47).

In complex notation

$$\frac{1}{[1+(\omega/2D)^2]^{1/2}}\cos(\omega t-\delta)\cos\omega t = \cos\omega t$$

$$\cdot[\cos\omega t\cos\delta + \sin\omega t\sin\delta]\frac{1}{[1+(\omega/2D)^2]^{1/2}} \qquad \text{(A-54)}$$

$$= \frac{1}{2}\frac{1}{[1+(\omega/2D)^2]^{1/2}} + \frac{1}{2}\mathrm{Re}\left[\frac{1}{1+i\omega/2D}\, e^{i2\omega t}\right].$$

So equation (A-51) becomes

$$(1-u^2)\frac{\partial^2\rho_{20}}{\partial u^2} - 2u\frac{\partial\rho'_{20}}{\partial u} + (3u^2-1)\left[\frac{1}{2}\frac{C_0}{[1+(\omega/2D)^2]^{1/2}}\right. \qquad \text{(A-55)}$$

$$\left. + \frac{1}{2}\frac{1}{1+i\omega/2D}e^{i2\omega t}\right] = \frac{1}{D}\frac{\partial\rho'_{20}}{\partial t}.$$

Again this can be broken into two equations. The sum of the solutions to these two equations is the solution to equation (A-55). These equations are

$$(1-u^2)\frac{\partial^2\rho'''_{20}}{\partial u^2} - 2u\frac{\partial\rho'''_{20}}{\partial u} + (3u^2-1)\frac{1}{2}\frac{C_0}{1+(\omega/2D)^2} = \frac{1}{D}\frac{\partial\rho'''_{20}}{\partial t} \qquad \text{(A-56)}$$

and

$$(1-u^2)\frac{\partial^2\rho''''_{20}}{\partial u^2} - 2u\frac{\partial\rho''''_{20}}{\partial u} + (3u^2-1)\frac{1}{2}\frac{1}{1+i\omega/2D}e^{i2\omega t} = \frac{1}{D}\frac{\partial\rho''''_{20}}{\partial t} \qquad \text{(A-57)}$$

By the same reasoning as used earlier, it is evident that one solution to equation (A-56) is of the form

$$\rho_{20}''' = U \quad . \tag{A-58}$$

If this is substituted into equation (A-56) one obtains

$$(1-u^2)\frac{\partial^2 U}{\partial u^2} - 2u\frac{\partial U}{\partial u} + (3u^2-1)\frac{1}{2}\frac{C_0}{1+(\omega/2D)^2} = 0 \quad . \tag{A-59}$$

The term which makes this equation inhomogeneous is a multiple of $P_2(u)$, so a solution to this equation is

$$B\,P_2(u) = U \quad , \tag{A-60}$$

where B is a constant. Thus

$$-B\,2(3)\,P_2(u) + \frac{C_0}{1+(\omega/2D)^2}P_2(u) = 0 \tag{A-61}$$

or

$$-B = \frac{1}{6}\,\frac{C_0}{1+(\omega/2D)^2} \quad , \tag{A-62}$$

so

$$\rho_{20}''' = \frac{1}{6}\,\frac{C_0}{1+(\omega/6D)^2}\,P_2(u) \quad . \tag{A-63}$$

Equation (A-57) can be solved in a similar manner. A solution to this is

$$\rho_{20}'''' = e^{i2\omega t} U \quad . \tag{A-64}$$

Substituting this into equation (A-57) yields the equation

$$(1-u^2)\frac{\partial^2 U}{\partial u^2} - 2u\frac{\partial U}{\partial u} + (3u^2-1)\frac{1}{2}\frac{C_0}{1+i\omega/2D} = \frac{1}{D} i2\omega U \quad . \tag{A-65}$$

This equation has a solution of the form

$$U = \sum_{n=0}^{\infty} b_n u^n \quad . \tag{A-66}$$

When this is substituted into equation (A-65) one obtains, in a manner similar to that for equations (A-37), (A-38) and (A-39), the equation

$$\sum_{n=0}^{\infty} \left\{(n+2)(n+1)b_{n+2} - (n+1)n b_n - \frac{1}{D} i2\omega b_n\right\} \tag{A-67}$$

$$\cdot u^n + (3u^2-1)\frac{1}{2}\frac{C_0}{1+i\omega/2D} = 0 \quad ,$$

and the system of equations

$$b_{n+2}(n+2)(n+1) - \left[(n+1)n + \frac{1}{D} i2\omega\right] b_n = 0 \quad , \tag{A-68}$$

where there is one equation for each n equal to a positive integer, except that for $n=0$ and $n=2$ the applicable equations are

$$12\,b_4-\left(6+\frac{1}{D}i2\omega\right)b_2+\frac{3}{2}\,\frac{C_0}{1+i\omega/2D}=0 \qquad \text{(A-69)}$$

and

$$2\,b_2-\frac{1}{D}i2\omega b_0-\frac{1}{2}\,\frac{C_0}{1+i\omega/2D}=0\ . \qquad \text{(A-70)}$$

As before a solution can be found to be $b_n=0$ for all n except $n=0$ and $n=2$ where

$$b_2=\frac{1}{4}\,\frac{C_0}{(1+i\omega/2D)(1+i\omega/3D)} \qquad \text{(A-71)}$$

and

$$b_0=\frac{1}{12}\,\frac{C_0}{(1+i\omega/2D)(1+i\omega/3D)}\ . \qquad \text{(A-72)}$$

Thus a solution to equation (A-57) is

$$\rho_{20}^{\prime\prime\prime\prime}=C_0(3u^2-1)\frac{1}{12}\,\frac{1}{(1+i\omega/2D)(1+i\omega/3D)}\,e^{i2\omega\tau}+C_{20}^{\prime\prime\prime\prime}\ . \qquad \text{(A-73)}$$

Now combining the solutions (A-53), (A-63) and (A-73) with the homogeneous solution, the solution to equation (A-25) is

$$\rho_{20}=C_0(3u^2-1)\frac{1}{12}\left[\frac{1}{1+(\omega/2D)^2}+\frac{1}{(1+i\omega/2D)(1+i\omega/3D)}\right.$$

$$\left.\cdot\,e^{i2\omega t}\right]+\frac{C_{10}}{[1+(\omega/2D)^2]^{1/2}}\,e^{i(\omega t-\delta)}+C_{20}\ . \qquad \text{(A-74)}$$

It is known that

$$\frac{1}{1+i\omega/2D} = \frac{1}{[1+(\omega/2D)^2]^{1/2}} e^{-i\delta_1} , \tag{A-75}$$

where

$$\tan \delta_1 = \omega/2D , \tag{A-76}$$

and that

$$\frac{1}{1+i\omega/3D} = \frac{1}{[1+(\omega/2D)^2]^{1/2}} e^{-i\delta_2} , \tag{A-77}$$

where

$$\tan \delta_2 = \omega/3D . \tag{A-78}$$

Therefore equation (A-74) can be rewritten in the form

$$\rho_{20} = C_0 (3u^2-1)\frac{1}{12}\left[\frac{1}{1+(\omega/2D)^2} + \frac{1}{[(1+(\omega/2D)^2)(1+(\omega/3D)^2]^{1/2}} \cdot e^{i(\omega t-\delta_1-\delta_2)}\right] + \frac{C_{10}}{[1+(\omega/2D)^2]^{1/2}} e^{i(\omega t-\delta_1)} + C_{20} . \tag{A-79}$$

Finally, equation (A-27) must be solved. When the steady state solution for (A-34) is substituted into (A-27) one obtains

$$(1-u^2)\frac{\partial^2 \rho_{01}}{\partial u^2} - 2u\frac{\partial \rho_{01}}{\partial u}(3u^2-1)C_0 \cos^2\omega t = \frac{1}{D}\frac{\partial \rho_{01}}{\partial t} . \tag{A-80}$$

Except for the constant factor C_o in the third term, this equation is the same as equation (A-51) with δ set equal to zero. Thus by similarity the solution to (A-80) is deduced to be

$$\rho_{01} = C_o(3u^2-1)\frac{1}{12}\left(1 + \frac{1}{[1+(\omega/3D)^2]^{1/2}} e^{i(2\omega t-\delta)}\right) + C_{01}, \quad \text{(A-81)}$$

As before this may be transformed into the more convenient form

$$\rho_{01} = C_o(3u^2-1)\frac{1}{12}\left(1 + \frac{1}{[1+(\omega/3D)^2]^{1/2}} \cos(2\omega t-\delta)\right) + C_{01}, \quad \text{(A-82)}$$

where as before δ_2 is given by equation (A-78).

All equations derived from the perturbation procedure which were to be solved have now been solved. It remains to combine them to obtain the solution to the original equation (A-1). Recall that in the perturbation procedure it was specified that the α and ϵ were to be less that one. These quanities are now related (by equations (A-20) and (A-21) to the β and γ^2 respectively. Practical experience with various materials used in this study indicate that it may be expected that both are quite a bit smaller than one for the field strengths being used. Therefore in any expansion of the solution to equation (A-1) in terms β and γ^2 only the first few terms will make significant contributions. Accordingly equation (A-1) has the solution

$$\rho = [\rho_{00} + \beta\rho_{10} + \beta^2\rho_{20} + \gamma^2\rho_{01} + \dots], \quad \text{(A-83)}$$

$$\rho = \{C_0 + \beta\left[\frac{C_0}{[1+(\omega/2D)^2]^{1/2}} u\cos(\omega t - \delta_1) + C_{10}\right]$$

$$+ \beta^2\left[C_0(3u^2-1)\frac{1}{12}\left(\frac{1}{1+(\omega/2D)^2} + \frac{1}{[(1+(\omega/2D)^2)(1+(\omega/3D)^2]^{1/2}}\right.\right.$$

$$\left.\left.\cdot\cos(2\omega t - \delta_1 - \delta_2)\right) + \frac{C_{10}}{[1+(\omega/2D)^2]^{1/2}} u\cos(\omega t - \delta_1) + C_{20}\right] \qquad \text{(A-84)}$$

$$+ \gamma^2\left[C_0(3u^2-1)\frac{1}{12}\left(1 + \frac{1}{[1+(\omega/3D)^2]^{1/2}} u\cos(2\omega t - \delta_2)\right) + C_{02}\right] + \ldots\}.$$

If the function ρ is considered to be a probability density, then the total probability of an axis pointing somewhere on the unit sphere must be one, or

$$\int_\Omega \rho \, d\Omega = 1 \qquad \text{(A-85)}$$

In terms of equation (A-83) this becomes

$$\int_\Omega \rho \, d\Omega = 1 = \int_\Omega \rho_{00} \, d\Omega + \beta \int_\Omega \rho_{10} \, d\Omega + \beta^2 \int_\Omega \rho_{20} \, d\Omega \qquad \text{(A-86)}$$

$$+ \gamma^2 \int_\Omega \rho_{01} \, d\Omega + \ldots$$

This equation must hold for any values of β and γ^2. This can only occur if

$$\int_{\Omega} \rho_{mn} = \begin{cases} 0 \text{ for } m \text{ or } n \neq 0 \\ 1 \text{ for } m = n = 0 \end{cases} \quad \text{(A-87)}$$

The following terms occur in the expression for ρ and upon integration give the following equations. For $m=n=0$

$$\int_0^{\pi} \int_0^{2\pi} C_0 \sin\sigma \, d\sigma \, dv = 4\pi C_0 = 1 \quad \text{(A-88)}$$

Therefore

$$C_0 = \frac{1}{4\pi} \quad \text{(A-89)}$$

For $m=1$, $n=0$

$$\int_0^{\pi} \int_0^{2\pi} C_0 \cos\sigma \sin\sigma \, d\sigma \, dv = 0 \quad , \quad \text{(A-90)}$$

which means that

$$\iint_{\Omega} C_{10} \, d\Omega = 0 \quad \text{(A-91)}$$

or

$$C_{10} = 0 \quad \text{(A-92)}$$

For $m=2$, $n=0$

$$\int_0^{\pi}\int_0^{2\pi} C_0 3 P_2(\cos\sigma)\sin\sigma\, d\sigma\, d\nu = 0, \quad \text{(A-93)}$$

which means that

$$\int\int_{\Omega} C_{20}\, d\Omega = 0 \quad \text{(A-94)}$$

or

$$C_{20} = 0 \quad . \quad \text{(A-95)}$$

Similarly

$$C_{01} = 0 \quad . \quad \text{(A-96)}$$

Thus the function ρ can be written

$$\rho = \frac{1}{4\pi}\left\{1 + \beta u \frac{\cos(\omega t - \delta_1)}{1+(\omega/2D)^2} + \beta^2(3u^2-1)\right.$$

$$\cdot\frac{1}{12}\left[\frac{1}{1+(\omega/2D)^2} + \frac{\cos(2\omega t - \delta_1 - \delta_2)}{[(1+(\omega/2D)^2)(1+(\omega/3D)^2)]^{1/2}}\right] \quad \text{(A-97)}$$

$$\left. + \gamma^2(3u^2-1)\frac{1}{12}\left[1 + \frac{\cos(2\omega t - \delta_2)}{[1+(\omega/3D)^2]^{1/2}}\right] + \ldots\right\},$$

where

$$\tan \delta_1 = \omega/2D \qquad \text{(A-76)}$$

and

$$\tan \delta_2 = \omega/3D \qquad \text{(A-78)}$$

Equations (A-97), (A-76) and (A-78) represent the most significant part of the solution to equation (A-1). The practical accuracy of this solution depends upon the extent to which the factors β and γ^2 are less than one.

APPENDIX B

COMPUTER PROGRAMS

A number of computer programs were used to calculate various curves and to reduce data. Each of the programs carries a brief description of its function as comments preceeding the program. In some cases a more detailed description is given in the text of the thesis. The programs are written in the Fortran IV language as used in the IBM 7040. The control cards for the PR 150 system used at Oklahoma State University have been omitted so that the program may be used with other operating systems by the addition of the proper control cards.

```
C PROGRAM EOEFF
C THIS PROGRAM CALCULATES THE E-O EFFECT CURVES FOR UP TO 10 VALUES OF P.
C B REPRESENTS THE P VALUES.  OM/6D ARE THE VALUES OF TAU= OMEGA/6D.
      DIMENSION  B(10), OM6D(40), ACAMP(40),DCAMP(40),TAND(40),DELTA(40)
      READ(5,40) (B(I),I=1,10),(OM6D(J),J=1,40)
   40 FORMAT (10F8.0)
   42 FORMAT (1PE10.2,1P3E20.5,0PF20.2 )
      DO 10 I=1,10
      WRITE(6,41) B(I)
   41 FORMAT(1H1,26H  CURVES FOR VALUE OF P=  1PE10.3 ///90H  OMEGA/6D
     1          AC VALUE             DC VALUE        TANGENT DELTA
     2       DELTA/)
      DO 11 J=1,40
      ACAMP(J)=(((B(I)*B(I)+(1.0+2.0*B(I))/(1.0+9.0*OM6D(J)**2.0))/(1.0+
     14.0*OM6D(J)**2.0))**.5)/(1.0+B(I))
      DCAMP(J)=(B(I)+1.0/(1.0+9.0*OM6D(J)**2.0))/(B(I)+1.0)
      TAND(J)=3.0*OM6D(J)*(2.0*B(I)+5.0+18.0*B(I)*OM6D(J)**2.0)/(3.0*(1.
     10+B(I))+(3.0*B(I)-2.0)*9.0*OM6D(J)**2.0)
      DELTA(J)=ATAN(TAND(J)) *180.0/3.14159
   11 WRITE (6,42) OM6D(J), ACAMP(J), DCAMP(J),TAND(J), DELTA(J)
      IF (B(I)) 10, 12, 10
   10 CONTINUE
   12 STOP
      END
```

```
C PROGRAM PLYDIX
C THIS PROGRAM CALCULATES THE POLYDISPERSITY WITH RESPECT TO TAU= 1/3D.  DN
C VALUES ARE THE VALUES OF THE STEADY COMPONENT CURVE9  OM ARE THE CORRESPONDING
C VALUES OF OMEGA.  L IS THE NUMBER OF VALUES OF DATA AND OF OMEGA.  N IS THE
C NUMBER OF POINTS OVER WHICH THE CALCULATION IS MADE.  M IS THE NUMBER OF
SUCCESSIVE APPROXIMATIONS MADE TO OBTAIN THE DISTRIBUTION FUNCTION.
      DIMENSION OM(50), DF(50), DNC(50), DN(50), DFC(50), REL(50), OMI(5
     10), ENT(50)
      READ (5,50) L, N, M, (DN(I),I=1,L), (OM(I), I=1,L)
   50 FORMAT (3I2/(5E16.0))
      WRITE (6,51)
   51 FORMAT ( 35H1  DISTRIBUTION OF POLYDISPERSITY     //// 62H   REL.
     1TIME  DIST. FCN.      | OMEGA         DATA     RESULTS          )
      ENT(1)= 0.0
      ENT(N)= 0.0
      NM1=N-1
      DO 10 I=2,NM1
   10 ENT(I)= ALOG(OM(I+1))- ALOG(OM(I-1))
      DO 1 I=1,N
      DNC(I)=DN(I)
    1 DF(I)=0.0
      DO 6 K=1,M
      DO 2 I=2,NM1
      DFC(I)= (DNC(I-1)-DNC(I+1))/ENT(I)
    2 DF(I)=DF(I)+DFC(I)
      DO 3 I=1,N
      REL(I)=0.0
      DO 4 J=1,N
      TERM=(DF(J)/(1.0+ OM(I)*OM(I)/(OM(J)*OM(J))))*ENT(J)
    4 REL(I)=REL(I)+TERM
    3 CONTINUE
      A= (DN(1)-DN(N))/(REL(1)-REL(N))
      DO 6 I=1,N
    5 DNC(I)=DN(N)+A*REL(I)
    6 DNC(I)= DN(I)-DNC(I)
    9 DO 11 I=1,N
      DNC(I)= DN(I)+ DNC(I)
      OMI(I)= 1.0/OM(I)
      WRITE (6,52) OMI(I), DF(I), OM(I), DN(I), DNC(I)
   52 FORMAT ( 1P5E12.4)
   11 CONTINUE
      WRITE (6,53) M
   53 FORMAT ( 1H0, I4, 42H SUCCESSIVE APPROXIMATIONS HAVE BEEN MADE    )
      STOP
      END
```

```
C PROGRAM CURVE
C THIS PROGRAM IS USED IN CONJUNCTION WITH PLYDIX.  IT CALCULATES ALL OF THE
C ELECTRO-OPTIC EFFECT CURVES FROM A DISTRIBUTION FUNCTION OF TAU VALUES AND A
C P VALUE.  THE Q VALUE IS A NORMALIZATION CONSTANT.
      DIMENSION OM(200), DF(200)
      READ (5,50) N,M, N1,(OM(I), I=1,N)
   50 FORMAT (3I3/(5E16.0))
      READ (5,55) (DF(I), I=1,N), P, Q
   55 FORMAT (5F16.0)
      DO 6 I=1,N                                                          X
    6 OM(I)= 1.0/ OM(I)                                                   X
      WRITE (6,51)
   51 FORMAT ( 50H1  BIREFRINGENCE CURVES FOR GIVEN POLY DISPERSITY
     1 ////130H          1/OMEGA      DIST. FCN.          OMEGA
     2 STEADY             REAL       IMAGINARY     ALTERNATING      PHASE
     3ANGLE               )
      ENT= ALOG(OM(2))- ALOG(OM(1))
      SUM= 0.0
      DO 5 I=1,M
    5 SUM= SUM+ DF(I)*ENT
      RATIO= Q/SUM
      DO 4 I=1,M
    4 DF(I)= DF(I)*RATIO
      DO 1 I=1,M
      STED= 0.0
      REAT= 0.0
      UNREAL= 0.0
      ALT= 0.0
      DELTA = 0.0
      DO 2 J=1,M
      REL1= 1.0/(1.0+ OM(I)*OM(I)/(OM(J)*OM(J)))
      REL2= 1.0/(1.0+ OM(I)*OM(I)*4.0/(OM(J)*OM(J)*9.0))
      STERM= DF(J)*REL1*ENT
      RTERM= DF(J)*((1.0-OM(I)*OM(I)*2.0/(OM(J)*OM(J)*3.0))*REL1*REL2 +
     1P*REL2)*ENT
      UNTERM=DF(J)*((0.0-1.6666667*OM(I)/OM(J))*REL1*REL2-P*REL2*OM(I)*
     1.66666667/OM(J))*ENT
      STED= STED+STERM
      REAT= REAT+ RTERM
    2 UNREAL= UNREAL +UNTERM
      STED= STED+P*Q
      OMIN= 1.0/ OM(I)
      ALT=(REAT*REAT+ UNREAL*UNREAL)**.5
      DELTA = 0.0- ATAN2(UNREAL,REAT) *180.0/3.14159
      WRITE(6,52)  OMIN, DF(I), OM(I), STED, REAT, UNREAL, ALT, DELTA
   52 FORMAT (1P7E16.5, 0PF16.2)
    1 CONTINUE
      STOP
      END
```

```
C PROGRAM POLYP
C THIS PROGRAM IS FOR THE CASE OF A FIRST POWER SLOPE IN THE VARIATION OF P
C THIS PROGRAM COMPUTES POINTS ON THE ELECTRO-OPTIC RESPONSE CURVES FOR A GIVEN
C DISTRIBUTION FUNCTION AND FOR VARIATIONS IN P GIVEN AS A FRACTION OF THE FIRST
C P VALUE.  THE P'S ARE ADJUSTED SUCH THAT THE SUM OF W(I)*P(I) = P.  THE
C DISTRIBUTION FUNCTION MUST BE IN TERMS OF THE D VALUES
      DIMENSION P(50), A(50), W(50), F(50), OM(50), D(50)
      REAL IMAG , MAG
      M= 40
      N= 40
      PP= -.26
      READ (5,50) (F(J), J= 1,N)
      READ (5,50) (D(I), I=1,M)
      READ (5,50) (W(I), I=1,M)
      READ (5,50) (A(I), I= 1,M)
   50 FORMAT (10F8.0)
      PI= 3.1415927
      DO 1 I=1,N
      OM(I)= 2.0*PI*F(I)
    1 CONTINUE
      SUM= 0.0
      DO 2 I=1,M
      SUM= SUM+ W(I)
    2 CONTINUE
      DO 3 I=1,M
      W(I)= W(I)/SUM
    3 CONTINUE
      SUM= 0.0
      DO 4 I=1,M
      SUM= SUM+ A(I)*W(I)
    4 CONTINUE
      PO= PP/SUM
      DO 5 I=1,M
      P(I)= A(I)*PO
      WRITE (6,52) D(I), P(I), W(I), A(I)
   52 FORMAT (1P4E16.7)
    5 CONTINUE
      WRITE (6,53)
   53 FORMAT (1H1)
      DO 7 J= 1,N
      STEADY= 0.0
      IMAG= 0.0
      REAL= 0.0
      DO 6 I=1,M
      STEADY= STEADY+ W(I)*(P(I)+ 1.0/(1.0+OM(J)*OM(J)/(4.0*D(I)*D(I))))
      IMAG= IMAG+W(I)*((-OM(J)/(2.0*D(I))-OM(J)/(3.0*D(I)))/((1.0+OM(J)
     1*OM(J)/(4.0*D(I)*D(I)))*(1.0+OM(J)*OM(J)/(9.0*D(I)*D(I))))-P(I)*
     2OM(J)/(3.0*D(I))/(1.0+OM(J)*OM(J)/(9.0*D(I)*D(I))))
      REAL = REAL+ W(I)*((1.0-OM(J)*OM(J)/(6.0*D(I)*D(I)))/((1.0+ OM(J)*
     1 OM(J)/(4.0*D(I)*D(I)))*(1.0+ OM(J)*OM(J)/(9.0*D(I)*D(I))))+ P(I)/
     2 (1.0+ OM(J)*OM(J)/(9.0*D(I)*D(I))))
    6 CONTINUE
      STEADY= STEADY/(PP+1.0)
      PHASE=ATAN2(IMAG, REAL)*180.0/PI
      ARG= IMAG*IMAG+ REAL* REAL
      MAG= SQRT(ARG)/(PP+1.0)
      WRITE (6,51) F(J), STEADY, MAG, PHASE
   51 FORMAT (1P3E16.7, 0PF12.2)
    7 CONTINUE
      STOP
      END
```

```
C PROGRAM MONO
C THIS PROGRAM CALCULATES THE MONODISPERSE CURVES AS A FUNCTION OF FREQUENCY FOR
C GIVEN VALUES OF P AND D.  ALL DATA IS FOUND IN THE PROGRAM.
      DIMENSION FREQ(50)
      D= 12.5
      P=.586
      NFREQ= 1
      NO= 40
      DATA FREQ/1.,1.25,1.6,2.,2.5,3.2,4.,5.,6.5,8.,10.,12.5,16.,20.,25.
     1,32.,40.,50.,65.,80.,100.,125.,160.,200.,250.,320.,400.,500.,650.,
     2800.,1000.,1250.,1600.,2000.,2500.,3200.,4000.,5000.,6500.,8000.,
     310000.,12500.,16000.,20000.,25000.,32000.,40000.,50000.,65000.,
     480000./
      PI= 3.1415927
      F= FREQ(NFREQ)
      DO 1 I=1,NO
      STED= (P+1.0/(1.0+PI*PI*F*F/(D*D)))/(P+1.0)
      TAND= PI*F/D*(2.0*P+5.0+2.0*P*PI*PI*F*F/(D*D))/(3.0*(1.0+P)+(3.0*P
     1-2.0)     *PI*PI*F*F/(D*D))
      PHASE= ATAN(TAND)*180./PI
      ALT= (((P*P+(1.0+2.0*P)/(1.0+PI*PI*F*F/(D*D)))/(1.0+4.0/9.0*PI*PI*
     1F*F/(D*D)))**.5)/(P+1.0)
      WRITE (6,50) F, STED, ALT, PHASE
   50 FORMAT (1P3E16.7, 0PF10.2)
      N= NFREQ+I
      F= FREQ(N)
    1 CONTINUE
      STOP
      END
```

```
C PROGRAM SEP
C THIS PROGRAM TAKES DATA  OF PHASE ANGLE AND MAGNITUDE AND A GIVEN
C POLYDISPERSITY AND FOR A FIXED P CALCULATES THE MAGNITUDE AND PHASE ANGLE OF
C THE THEORETICAL CONTRIBUTION OF THE INDUCED MOMENT AND THE CONTRIBUTION
C CALCULATED BY SUBTRACTING THE THEORETICAL PERMANENT CONTRIBUTION FROM THE DATA
C AND THEN CALCULATING THE FUNCTIONS F(OM) AND PHI(OM).
      DIMENSION W(50), F(50), OM(50), D(50), PHASE(50), MAG(50)
      REAL MAG, IN, ININ, INOUT, MAGN, MAGIN, MAGDIF
      PI= 3.1415927
      M= 1
      N= 36
      P= -.26
      READ (5,50) (F(J), J= 1,N)
      READ (5,50) (D(I), I= 1,M)
      READ (5,50) (W(I), I= 1,M)
      READ (5,50) (PHASE(J), J= 1,N)
      READ (5,50) (MAG(J), J= 1,N)
   50 FORMAT (10F8.0)
      DO 1 J= 1,N
      OM(J)= 2.0*PI*F(J)
    1 CONTINUE
      SUM= 0.0
      DO 4 I=1,M
      SUM= SUM+ W(I)
    4 CONTINUE
      DO 5 I=1,M
      W(I)= W(I)/SUM
    5 CONTINUE
      DO 3 J= 1,N
      ANGLE=-PHASE(J)
      MAGN= MAG(J)
      CALL PHACOM(ANGLE, MAGN, IN, OUT)
      INOUT= 0.0
      ININ= 0.0
      PERIN= 0.0
      PEROUT= 0.0
      DO 2 I= 1,M
      REL2= 1.0/(1.0+OM(J)*OM(J)/(9.0*D(I)*D(I)))
      REL1= 1.0/(1.0+OM(J)*OM(J)/(4.0*D(I)*D(I)))
      PERIN= PERIN + W(I)*((1.0-OM(J)*OM(J)/(6.0*D(I)*D(I)))*REL1*REL2)
      PEROUT= PEROUT+ W(I)*((-OM(J)/(2.0*D(I))-OM(J)/(3.0*D(I)))*REL1*
     1REL2)
      ININ= ININ+ W(I)*P*REL2
      INOUT= INOUT- W(I)*P*OM(J)/(3.0 *D(I))*REL2
    2 CONTINUE
      DIFIN= IN-PERIN/(P+1.0)
      DIFOUT= OUT-PEROUT/(P+1.0)
      ININ= ININ/(P+1.0)
      INOUT= INOUT/(P+1.0)
      CALL COMPHA( ININ, INOUT, PHAIN, MAGIN)
      CALL COMPHA(DIFIN, DIFOUT, PHADIF, MAGDIF)
      FUN= MAGDIF/MAGIN
      PHI=(PHADIF-PHAIN)/2.0
      WRITE (6,51) F(J)    , MAGIN, PHAIN, MAGDIF, PHADIF, FUN, PHI
   51 FORMAT (1PE16.7, 3(1PE16.7, 0PF12.3))
    3 CONTINUE
      STOP
      END
      SUBROUTINE COMPHA(IN, OUT, ANGLE, MAG)
      REAL MAG, IN
      PI= 3.1415927
      ARG= IN*IN+OUT*OUT
      MAG= SQRT(ARG)
      ANGLE= ATAN2(OUT, IN)*180.0/PI
      IF (ANGLE) 2,2,1
    1 ANGLE = ANGLE- 360.
    2 RETURN
      END
      SUBROUTINE PHACOM(ANGLE, MAG, IN, OUT)
      REAL MAG, IN
      PI= 3.1415927
      ANG= ANGLE*PI/180.0
      IN= COS(ANG)*MAG
      OUT= SIN(ANG)*MAG
      RETURN
      END
```

```
C PROGRAM ALL
C THIS PROGRAM COMPUTES POINTS ON THE ELECTRO-OPTIC RESPONSE CURVES FOR A GIVEN
C DISTRIBUTION FUNCTION AND FOR VARIATIONS IN P GIVEN AS A FRACTION OF THE FIRST
C P VALUE AND FOR ARBITRARY FUNCTIONS OF F AND PHI APPLIED TO THE INDUCED MOMENT
C CONTRIBUTION.  THE P'S ARE ADJUSTED SUCH THAT THE SUM OF W(I)*P(I)=P.  THE
C DISTRIBUTION FUNCTION MUST B IN TERMS OF THE D VALUES.
      DIMENSION P(50), A(50), W(50), F(50), OM(50), D(50), FUN(50),
     1 PHI(50)
      REAL IMAG , MAG
      M=1
      N= 40
      PP= -.26
      READ (5,50) (F(J), J= 1,N)
      READ (5,50) (D(I), I=1,M)
      READ (5,50) (W(I), I=1,M)
      READ (5,50) (A(I), I= 1,M)
      READ (5,50) (FUN(J), J=1,N)
      READ (5,50) (PHI(J), J=1,N)
   50 FORMAT (10F8.0)
      PI= 3.1415927
      DO 1 J=1,N
      OM(J)= 2.0*PI*F(J)
    1 CONTINUE
      SUM= 0.0
      DO 2 I=1,M
      SUM= SUM+ W(I)
    2 CONTINUE
      DO 3 I=1,M
      W(I)= W(I)/SUM
    3 CONTINUE
      SUM= 0.0
      DO 4 I=1,M
      SUM= SUM+ A(I)*W(I)
    4 CONTINUE
      PO= PP/SUM
      DO 5 I=1,M
      P(I)= A(I)*PO
      WRITE (6,52) D(I), P(I), W(I), A(I)
   52 FORMAT (1P4E16.7)
    5 CONTINUE
      WRITE (6,53)
   53 FORMAT (1H1)
      DO 7 J= 1,N
      ANG= 2.0*PHI(J)* PI/180.0
      STEADY= 0.0
      IMAG= 0.0
      REAL= 0.0
      DO 6 I=1,M
      REL2= 1.0/(1.0+OM(J)*OM(J)/(9.0*D(I)*D(I)))
      REL1= 1.0/(1.0+OM(J)*OM(J)/(4.0*D(I)*D(I)))
      STEADY= STEADY+ W(I)*(P(I)*FUN(J)+ REL1)
      IMAG= IMAG- W(I)*((-OM(J)/(2.0*D(I))-OM(J)/(3.0*D(I)))*REL1*REL2-
     1 P(I)*FUN(J)*(OM(J)/(3.0*D(I))*COS(ANG) + SIN(ANG))*REL2)
      REAL= REAL+ W(I)*((1.0-OM(J)*OM(J)/(6.0*D(I)*D(I)))*REL1*REL2+
     1 P(I)*FUN(J)*(COS(ANG)-OM(J)/(3.0*D(I))*SIN(ANG))*REL2)
    6 CONTINUE
      STEADY= STEADY/(PP+1.0)
      PHASE=ATAN2(IMAG, REAL)*180.0/PI
      ARG= IMAG*IMAG+ REAL* REAL
      MAG= SQRT(ARG)/(PP+1.0)
      WRITE (6,51) F(J), STEADY, MAG, PHASE
   51 FORMAT (1P3E16.7, 0PF12.2)
    7 CONTINUE
      STOP
      END
```

VITA

David Ivan Bowling

Candidate for the Degree of

Doctor of Philosophy

Thesis: THE ELECTRO-OPTIC EFFECT IN SOLUTIONS OF RIGID MACROMOLECULES

Major Field: Physics

Biographical:

Personal Data: Born in Los Angeles, California, May 26, 1940, the son of Arthur Ivan and H. Irene Gladden Bowling; married Janice Oehrlein Bowling, August 8, 1964; father of one daughter, Jenelle, born January 25, 1968.

Education: Attended grade school in Los Angeles California, graduated from Fremont High School, Los Angeles, California in January of 1958; recieved a Bachelor of Arts Degree from the University of California, Los Angeles, with a major in physics, in January of 1962; recieved a Master of Science Degree, with a major in physics, from San Diego State College, in May of 1964; Completed requirements for the Doctor of Philosophy Degree in July of 1968.

Professional Experience: Graduate teaching assistant, San Diego State College, September 1962 to January 1964; graduate teaching assistant, Oklahoma State University, 1964; Physicist for Acoustics Section of Naval Electronics Laboratories, summer of 1964; graduate research assistant, Oklahoma State University, 1965-68.

Honorary Organization: Sigma Pi Sigma.